Report of the CIPM Key Comparison CCPR-K1.b

Spectral Irradiance 200 nm to 350 nm

Final Report

September 2008

This document was prepared by
Peter Sperfeld

Physikalisch-Technische Bundesanstalt

1 Introduction **6**

2 Organization of the Key Comparison **7**

2.1 Participants *7*

2.2 Comparison artecfacts *7*

2.3 Comparison philosophy *8*

2.4 Analysis philosophy *8*

2.5 Measurement and analysis schedule *9*

2.6 Acknowledgements *9*

3 BNM-INM **10**

3.1 Overview of UV program at BNM *10*

3.1.1 Traceability 11

3.2 Measurement devices *11*

3.2.1 Absolute irradiance 11

3.2.2 Relative spectral irradiance: Spectral radiance to irradiance comparison 12

3.2.3 Assembly of absolute and relative values 14

3.3 Uncertainty *15*

3.3.1 Lower spectral range measurement uncertainty 15

3.3.2 Higher spectral range measurement uncertainty 16

3.4 Results *17*

3.4.1 Calculation 17

3.4.2 Deuterium Lamp systems used 17

3.4.3 Lamp system electrical stability 17

3.4.4 Numerical results 17

3.4.5 Repeatability between measurement rounds 19

3.4.6 Normalized inner consistency of participants measurements 20

3.4.7 Acceptance of measurements 20

4 NIST **21**

4.1 Make and type of spectroradiometer (or equivalent) *21*

4.2 Laboratory transfer standards used: *21*

4.3 Description of measuring technique (please include a diagram): *22*

4.4 Establishment or traceability route of primary scale including date of last realisation and breakdown of uncertainty: *23*

4.5 Description of calibration laboratory conditions: e.g. temperature, humidity etc. *24*

4.6 References *24*

4.7 Results *25*

4.7.1 Deuterium Lamp systems used 25

4.7.2 Lamp system electrical stability 25

4.7.3 Numerical results 25

4.7.4 Repeatability between measurement rounds 27

4.7.5 Normalized inner consistency of participants measurements 28
4.7.6 Acceptance of measurements 28

5 NPL 29
5.1 Introduction 29
5.2 The Spectral Radiance and Irradiance Primary Scales (SRIPS) Facility 29
5.2.1 The Blackbody Source 30
5.2.2 The Monochromator 30
5.2.3 Detector 31
5.2.4 Filter Radiometers 31
5.2.5 Laboratory Conditions 31
5.3 Scale realisation and traceability 31
5.3.1 Overview 31
5.3.2 Measurement Sequence 31
5.4 Analysis of Measurement Results 33
5.4.1 Measurement Equation — Monochromator 33
5.4.2 Measurement Analysis 34
5.5 Uncertainty Analysis 38
5.5.1 Uncertainty associated with Constants 38
5.5.2 Uncertainty associated with Blackbody Radiance 38
5.5.3 Uncertainty associated with Lamp-Blackbody Signal Ratios 43
5.5.4 Wavelength accuracy 45
5.5.5 Uncertainty associated with the bandwidth correction 45
5.5.6 Uncertainty associated with the overlap correction 47
5.6 Overall Uncertainty associated with Lamp Irradiance 47
5.6.1 Single lamp calibration 47
5.6.2 Increased uncertainty in 270 nm to 310 nm region 48
5.6.3 Multiple calibrations of a lamp 49
5.6.4 Overall uncertainties submitted 50
5.7 References 53
5.8 Results 53
5.8.1 Deuterium Lamp systems used 53
5.8.2 Lamp system electrical stability 54
5.8.3 Numerical results 54
5.8.4 Repeatability between measurement rounds 54
5.8.5 Normalized inner consistency of participants measurements 55
5.8.6 Acceptance of measurements 55

6 NRC 57
6.1 Introduction: 57
6.2 Logistics 57
6.3 NRC Lamp Standards 58

6.4 Measurement Facility *58*
6.4.1 Spectroradiometer: 58
6.4.2 Environmental Conditions: 60
6.5 Measurement Configuration: *60*
6.5.1 Optical Configuration: 60
6.5.2 Lamp Configuration: 62
6.5.3 Measurement Procedure: 63
6.6 Data Analysis: *64*
6.6.1 Calibration of the spectroradiometer: 64
6.6.2 Measurement Results: 65
6.6.3 Uncertainties: 65
6.7 References *68*
6.8 Results *68*
6.8.1 Deuterium Lamp systems used 68
6.8.2 Lamp system electrical stability 68
6.8.3 Numerical results 68
6.8.4 Repeatability between measurement rounds 69
6.8.5 Normalized inner consistency of participants measurements 70
6.8.6 Acceptance of measurements 70

7 PTB 72
7.1 Description of the measurement facility and primary scale *72*
7.1.1 Primary scale realization 72
7.1.2 Measurement facility 72
7.1.3 Calibration procedure 73
7.1.4 Measurement cycle 73
7.2 Working standards used for the intercomparison *74*
7.2.1 Monitor-detector measurements 74
7.2.2 Measurement of electrical parameters 74
7.3 Measurement uncertainties *74*
7.3.1 Blackbody radiator temperature measurements 74
7.3.2 Primary spectral irradiance unit realization 75
7.3.3 Calibration procedure 78
7.4 References *84*
7.5 Results *84*
7.5.1 Deuterium Lamp systems used 84
7.5.2 Lamp system electrical stability 84
7.5.3 Numerical results 85
7.5.4 Repeatability between measurement rounds 85
7.5.5 Acceptance of measurements 85

8 Pilot **87**

8.1 Description of the measurement facility *87*

8.1.1 Measurement cycle and calibration procedure 87

8.2 Reference standards used as pilot's lamps for the intercomparison *87*

8.2.1 Monitor-detector measurements 87

8.2.2 Measurement of electrical parameters 87

8.3 Measurement uncertainties *88*

9 Analysis of data **90**

9.1 Establishing the NMI (National Metrology Institute) representative value *90*

9.1.1 Determination of the mean of each participants lamp systems 91

9.1.2 Establishing the acceptability of a lamp system 91

9.1.3 Establishing the spectral irradiance for the pilot's deuterium lamp systems and the deviation for each participant's lamp 92

9.1.4 Establishing the NMI representative value 93

9.2 Establishing the Key Comparison Reference Value (KCRV) and the deviations of the NMI *93*

10 Results: KCRV and DOE for the CCPR-K1.b intercomparison **96**

10.1 NMIs representative spectral irradiances and the KCRV *96*

10.2 Unilateral DoE *96*

10.2.1 Unilateral DoE for Each participant 97

10.2.2 Unilateral DoE by wavelength – all participants 100

10.3 Bilateral DoE *102*

10.4 Tabulated results *105*

11 Conclusions **112**

Appendix A The Deuterium Lamp System (DLS) **113**

Appendix B List of figures **117**

Appendix C List of tables **119**

1 Introduction

The Mutual Recognition Arrangement (MRA) was signed in 1999 with the objectives of establishing the degree of equivalence of national measurement standards and providing for the mutual recognition of calibration and measurement certificates issued by National Metrology Institutes (NMIs). Under the MRA the equivalence of national measurement standards maintained by the NMIs is determined by a set of key comparisons chosen and organised by the Consultative Committees of the International Committee for Weights and Measures (CIPM), working closely with the Regional Metrology Organisations (RMOs). The Consultative Committee of Photometry and Radiometry (CCPR) identified several key comparisons at its meeting in March 1997. One of these was the CCPR Key Comparison K1.b for Spectral Irradiance in the spectral region 200 nm to 350 nm.

The Physikalisch-Technische Bundesanstalt (PTB), the NMI of Germany, was asked to be the Pilot Laboratory for the CCPR-K1.b Key Comparison and had the responsibility of organising the Key Comparison and to write the Technical Protocol in discussion with a working group comprising representatives of all participating institutes. The Pilot Laboratory was responsible for purchasing and distributing the technical artefacts, for collating the measurement reports from all participants and for analysing the results and preparing the Draft Report.

2 Organization of the Key Comparison

2.1 Participants

Five NMIs (including the pilot) participated in the CCPR-K1.b Key Comparison.

Table 2.1Contact details for the participants of the CCPR-K1.b intercomparison

Contact person	Institute	Contact details	Shortcut
Peter Sperfeld	Physikalisch-Technische Bundesanstalt 4.11 Source-based Spectroradiometry Bundesallee 100 D 38116 Braunschweig Germany	Tel. +49 531 592 4144 Fax +49 531 592 69 4144 Email: Peter.Sperfeld@ptb.de	PTB (pilot)
Nigel Fox	NPL Centre for Optical and Environmental Metrology Teddington Middlesex TW11 OLW United Kingdom	Tel. +44 181 943 6825 Fax +44 181 943 6935 Email: Nigel.Fox@npl.co.uk	NPL
Howard Yoon	NIST Optical Technology Division Building 221/B208 Gaithersburg, MD 20899 USA	Tel. +1 301 975 2482 Fax +1 301 869 5700 Email: hyoon@email.nist.gov	NIST
Bernard Rougie	Institut National de Métrologie Conservatoire National des Arts et Métiers 61 Rue Du Landy 93210 La Plaine Saint Denis France	Tel. +33 1 40 27 20 22 Fax +33 1 58 80 89 00 Email: rougie@cnam.fr	INM
Arnold A. Gaertner	National Research Council of Canada Institute for National Measurement Standards Building M-36 Ottawa, Ontario K1A 0R6 Canada	Tel: +1 613 993-9344 Fax: +1 613 952-1394 Email: arnold.gaertner@nrc.ca	NRC

2.2 Comparison artecfacts

The comparison artifacts for the CCPR-K1.b intercomparison were Deuterium Lamp Systems (DLS) developed by the PTB. The NMIs were required to use a minimum of three (with the option of up to four) DLS for the intercomparison. A DLS consists of a 30 W deuterium lamp mounted and aligned in a protecting housing, an associated power supply and a monitor detector that could be mounted in front of the lamp system before and after each spectral measurement (see alsoAppendix A). The lamps were operated at a constant direct current. The voltage drop across the lamp as well as the signal of the monitor detector was recorded as an indicator of the stability of the DLS.

2.3 Comparison philosophy

Because of the fragile nature of lamps, the comparison was organised as a star comparison. Any individual lamp was measured by the pilot and by one participating NMI, only. Lamps were sent in batches of three or four to each participant. The participants were requested to measure each transfer standard on at least two occasions and the pilot was also asked to make measurements on two occasions to get reliable informations about the lamp stability.

For the intercomparison the measurement sequence NMI – Pilot – NMI was taken to achieve the intercomparison results. Due to multiple measurements with a group of at least three lamps for each participant it was expected that the uncertainties due to the comparison itself could be reduced by averaging.

To provide comparability and equivalence with other participants, the measurements at the PTB were devided into two parts containing two independent sets of deuterium lamp systems. One set of lamps was calibrated as transfer standards by the *participant* PTB similar to the measurements of the other participants of the intercomparison. The other set of lamps was used by the *pilot* PTB as comparison reference standards to compare the calibrations of all participants (including the participant PTB). For this set of lamps it is not essential to have them absolutely calibrated by the pilot. These comparison reference standards, however, were calibrated at the pilot's measurements facility by comparison to the NMI's transfer standards and by using the spectral irradiances as assigned by the participants.

2.4 Analysis philosophy

The group of comparison reference standards was calibrated at the pilot's measurement facility by using the NMI's transfer standards. So for each NMI a spectral irradiance was assigned to the comparison reference standard lamp systems according to the NMI's spectral irradiance calibrations and their assigned measurement uncertainties. This comparison method allows to treat all participants equally and to directly compare the participants' results.

The measurements at each wavelength were treated as an entirely independent comparison for the purposes of the analysis.

The fundamental outcome of a key comparison is the Key Comparison Reference Value (KCRV), the Degrees of Equivalence (DoEs) between each NMI and the KCRV (unilateral DoEs) and between the pairs of NMIs (bilateral DoEs). The determination of the KCRV for this comparison was made according to the guidelines of the CCPR and is based on the weighted mean with "cut-off" of the NMI's calibration of the comparison reference standards established by the pilot. The philosophy of this analysis has been to provide such a KCRV and the corresponding DoEs in a way that ensures that each NMI is treated equitably. The bilateral DoEs between two NMIs, however, rise from the direct intercomparison of two NMIs and are therefore not dependent on the KCRV or the weighted mean.

The KCRV achieved for this intercomparison can be treated as a *virtual* spectral irradiance of a typical deuterium lamp, however, it is assigned to the weighted mean of the spectral irradiances of the group of comparison reference standard lamp systems kept by the pilot.

2.5 Measurement and analysis schedule

The 20 deuterium lamp systems used for this intercomparison have been assembled, aligned and pre-aged at the PTB in the beginning of 2003. After an initial calibration at the PTB in June/July 2003 the DLS had been shipped or hand-carried to the participants for the first measurement rounds. The second measurements at the PTB and the pilot's measurements had been carried out in May 2004. In summer 2004 the transfer standards had been shipped to the participants for their second measurement rounds. The completion of the measurements of the participants was expected for the end of 2004.

The receipt of all participant's measurement results and reports by the pilot was completed at the end of 2006. Pre-Draft A of the intercomparison report was sent in April 2007 to the participants followed by comments and discussions. Detailed informations on the relative stability of the participant's lamps and their inner consistency and redistribution of the irradiance values submitted by the participants for the check of possible copying errors were sent out to each individual participant in June 2007. The detailed analysis method was presented to the participants and discussed in December 2007. Draft A was issued for comments and discussions in January 2008. Draft B was then prepared in April 2008 and approved by the CCPR in September 2008.

2.6 Acknowledgements

The pilot wishes to thank all participants for their support and collaboration of this intercomparison. The cooperation has always been honest and constructive during the duration of CCPR-K1.b. This intercomparison demonstrates clearly the high metrological capabilities of all participating NMIs.

3 BNM-INM

Bureau National de Métrologie BNM

Institut National de Métrologie BNM-INM

CNAM, 292, rue Saint Martin 75003 Paris

Laboratoire National d'Essais BNM-LNE

LNE, ZA de Trappes-Élancourt 29, avenue Roger Hennequin 78197 TRAPPES Cedex

Bernard Rougié	rougie@cnam.fr
Jean Gaudemer	jean.gaudemer@lne.fr
Jean Voyer	jean.voyer@lne.fr
Jean Bastie	bastie@cnam.fr
Jimmy Dubard	jimmy.dubard@lne.fr

3.1 Overview of UV program at BNM

BNM established a first UV reference based on synchrotron radiation in the 1980th . Changes in synchrotron radiation program did not allow to pursue such a reference study. At this time mini argon arcs had been calibrated. Their long term stability has been tested by the comparison of a tenth of devices constructed for a ten years period. All these devices had the same radiance.

BNM decided in 1999 to develop a new UV measurement program. The BNM LNE acquired standard radiance lamps from PTB whilst the BNM INM built UV filter radiometers calibrated against our standard cryogenic radiometer.

Although the UV program has obtained good results the poor long term stability of UV filters makes that our reference cannot be used nowadays with the expected confidence level.

The traceability scheme shown below refers to this situation at present time.

3.1.1 Traceability

The irradiance values of the lamps are issued from two references. The absolute values are derived from our irradiance reference realized by quartz halogen lamps and the spectral relative values are derived from the PTB radiance standard through the comparison of radiance to irradiance carried out on our devoted measurement bench.

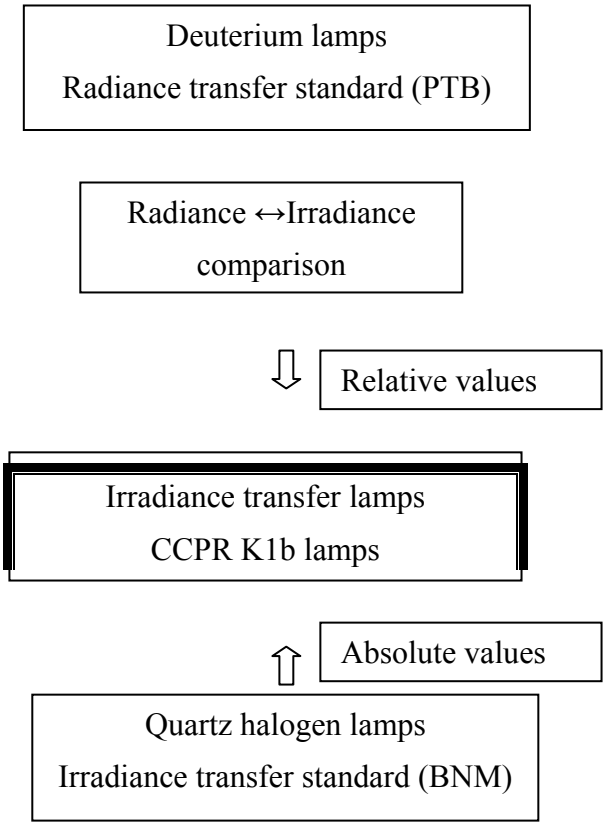

Figure 3.1 Traceability scheme for BNM-INM

3.2 Measurement devices

3.2.1 Absolute irradiance

CCPR-K1.b deuterium lamps have been compared to our irradiance transfer standards (quartz halogen lamps) in the 300-350 nm spectral range at a 10 nm wavelength step.

3.2.1.1 Comparator

The comparator is a spectro radiometer from the MACAM Company, type SR 9910. It is equipped with a double monochromator. The detector is a photomultiplier. The spectral bandwidth is 2.5 nm. The optical head is a plane diffuser. It is connected to the monochromator unit through an optical fibre.

3.2.1.2 Reference lamps

Two FEL lamps are used. They are referenced FEL 914 and FEL 916.

3.2.1.3 Facility

The reference lamp and the deuterium lamp to be calibrated are both set on a translation stage. The lamps are alternately measured at the proper distances from the spectroradiometer optical head (50 cm for FEL reference lamps and 30 cm for DSL lamps).

3.2.1.4 Measurement procedures

- step 1 : 5 spectral scans of the reference 914
- step 2 : 5 spectral scans of the reference 916
- step 3 : 5 spectral scans of DSL1
- step 4 : 5 spectral scans of DSL2
- step 5 : 5 spectral scans of DSL3
- step 6 : 5 spectral scans of the reference 914
- step 7 : 5 spectral scans of the reference 916

Note : For the measurements of the DSL lamps, the distance was taken from the glass plate of the alignment jig, which is 0,7 mm away from the metal ring, Therefore, an additional correction is applied in order to take into account that the distance reference is the metal ring

3.2.2 Relative spectral irradiance: Spectral radiance to irradiance comparison

CCPR-K1.b deuterium lamps have been compared to radiance transfer lamps calibrated at PTB. The comparison has been performed on a special optical bench aimed to compare a radiance source and an irradiance source in relative spectral values.

The device is constituted of an integrating sphere, a monochromator and a detector which measures the photocurrents due to the radiant flux coming from two optical devices. One is proportional to the radiance of a source considered as a reference radiance standard and a second one is proportional to the irradiance of a source to be measured. The two optical devices are designed so as the ratios between the two fluxes radiance (or irradiance respectively) do not depend on wavelength. These optical devices are made of the assembly of two spherical mirrors. They are similar in radiance and irradiance operation but they are placed in optically conjugate positions. In order to avoid a transmittance difference between the two sets of mirrors we make two measurements by exchanging the place of mirrors.

Then we can compute the irradiance of the source by using the measured photocurrents and the calibrated standard radiance. As the dimensions of diaphragm areas and the distance between them cannot be know with the expected accuracy we only compute the irradiance relative values.

3.2.2.1 Details of radiance to irradiance computation

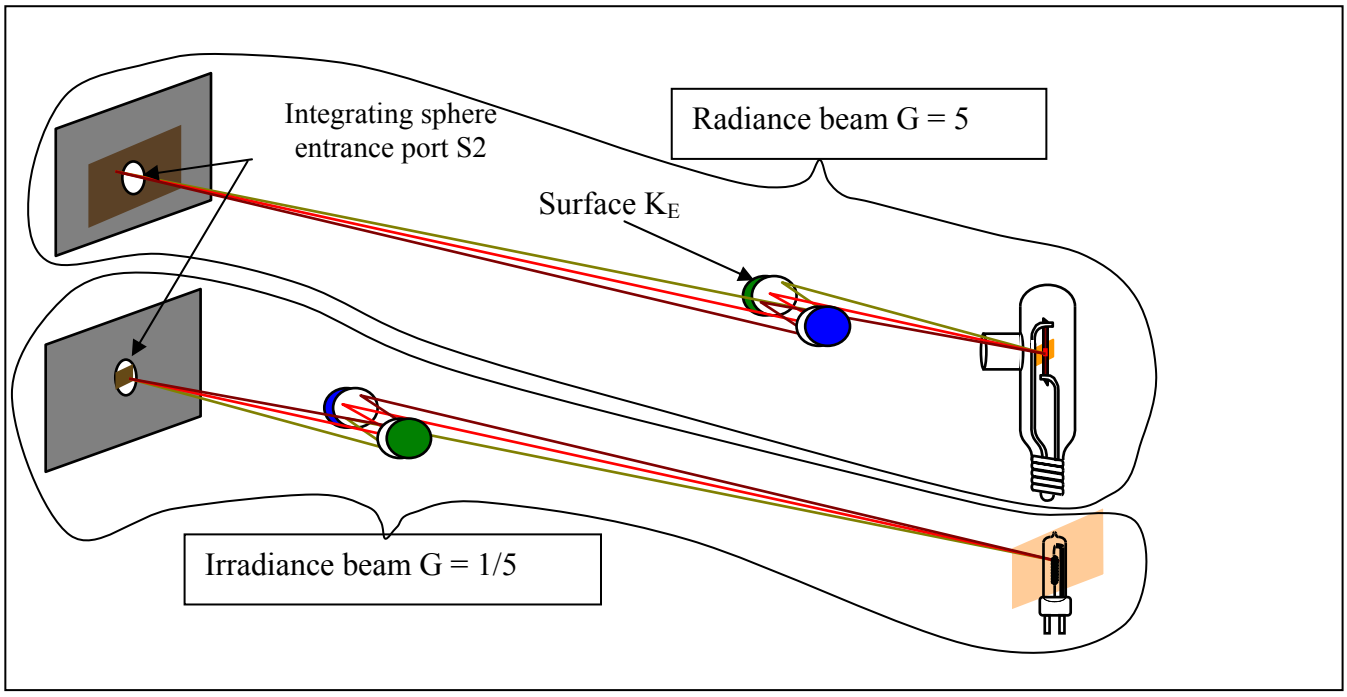

Figure 3.2 Schematic of the entrance optics

For each wavelength we measure the fluxes (photocurrents) in a first mirrors configuration:

-Radiance beam flux $F_{L1}(\lambda)$

-Irradiance beam flux $F_{E2}(\lambda)$

The radiance assembly and irradiance assembly mirrors are inverted and a measurement is performed with the second mirrors configuration (The number 1 or 2 refers to the set of mirrors)

-Radiance beam $F_{L2}(\lambda)$

-Irradiance beam $F_{E1}(\lambda)$

We write:

$L(\lambda)$: Radiance of 'radiance standard source'

$E(\lambda)$: Irradiance of unknown source

$T_1(\lambda)$: Reflectance of first assembly mirrors

$T_2(\lambda)$: Reflectance of second assembly mirrors

$S(\lambda)$: Sensitivity of the whole detector device

K_L : geometrical extension for radiance measurement

K_E : Irradiance diaphragm surface

We have:

First mirror configuration	Second mirror configuration
$F_{L1}(\lambda)=L(\lambda)*T_1(\lambda)*K_L*S(\lambda)$	$F_{L2}(\lambda)=L(\lambda)*T_2(\lambda)*K_L*S(\lambda)$
$F_{E2}(\lambda)=E(\lambda)*T_2(\lambda)*K_E*S(\lambda)$	$F_{E1}(\lambda)=E(\lambda)*T_1(\lambda)*K_E*S(\lambda)$

$$R_1(\lambda) = F_{L1}(\lambda)/F_{E2}(\lambda) = (L(\lambda)/E(\lambda))*(T_1(\lambda)/T_2(\lambda))*(K_L/K_E)$$

$$R_2(\lambda) = F_{L2}(\lambda)/F_{E1}(\lambda) = (L(\lambda)/E(\lambda))*(T_2(\lambda)/T_1(\lambda))*(K_L/K_E)$$

We compute: $(R_1(\lambda)*R_2(\lambda))^{1/2} = L(\lambda)/E(\lambda)*(K_L/K_E)$

We notice that the response ratio is independent of the mirrors reflectivity

$$E(\lambda) = L(\lambda)/(R_1*(\lambda)R_2(\lambda))*(K_L/K_E) \quad (3.1)$$

The ratio $\mathbf{(K_L/K_E)}$ cannot be evaluated with the required uncertainty then it is considered as unknown but it does not vary with wavelength. So we compute the relative irradiance value from equation (3.1) $E_{r\lambda 0}(\lambda)=E(\lambda)/E(\lambda_0)$

3.2.3 Assembly of absolute and relative values

As the spectral range of the relative and absolute measurements have a common part (310 nm to 350 nm), we can calculate the ratio between the two results. This ratio, so called 'spectral to Absolute coefficient', is not depending on wavelength according to its uncertainty over the 310 nm to 350 nm range.

Then, the relative spectral values in the range (200 nm-310 nm) are multiplied by the mean of this ratio in order to be presented in the unit of irradiance ($W.m^{-2}.nm^{-1}$). An uncertainty component corresponding to this operation is added in the 200 nm-310 nm spectral range.

3.3 Uncertainty

We show the uncertainty table split in two parts depending on the spectral range. All uncertainties are given as standard uncertainties.

3.3.1 Lower spectral range measurement uncertainty

The key comparison lamps are compared to radiance standards lamps in relative spectral values.

Table 3.1 Lower spectral range measurement uncertainty

Description of uncertainty parameter	type	uncertainty parameter		Irradiance uncertainty (%)			
Wavelength range (nm)			unit	200	210	220 to 290	300
Repeatability of reference	A			-	-	-	-
Repeatability of transfer	A			11.6%	3.6%	0.8%	0.5%
Scale (Radiance reference)	B			3.5%	3.5%	3.5%	3.5%
Radiance sources position(transversal)	B	0.05	mm	0.2%	0.2%	0.2%	0.2%
Irradiance sources position(longitudinal)	B	0.05	mm	0.0%	0.0%	0.0%	0.0%
Current source (reference)	B	0.4	mA	0.1%	0.1%	0.1%	0.1%
Current source (in test)	B	0.4	mA	0.1%	0.1%	0.1%	0.1%
Wavelength	B	0.05	nm	0.0%	0.0%	0.0%	0.0%
Cosine correction	B						
Optical dissymmetry	B			5.0%	2.0%	0.5%	0.3%
Detector linearity	B			0.1%	0.1%	0.1%	0.1%
Spectral width	B			0.0%	0.0%	0.0%	0.0%
Stray light	B			0.1%	0.1%	0.0%	0.0%
Spectral to Absolute coefficient	B			1.5%	1.5%	1.5%	1.5%
Combined standard uncertainty (k=1)				13.2%	5.6%	3.9%	3.9%

Repeatability of reference: This component is included in the repeatability of transfer

Scale (Radiance reference): traceability to PTB. Calibration certificate: PTB-7.11-129/99

Radiance source position: In spite of a strong dependence of radiance with position, the effect on the relative spectral values is low because of the correlation between radiance variation at different wavelength. The uncertainty of this parameter is the repeatability of positioning.

The orientation effect is very low, then it has been neglected.

The spectrum of both lamps (standard and measured) are almost the same., then the wavelength uncertainty as well as the stray light give rise to a low uncertainty in transfer.

Optical dissymmetry: Term due to our optical arrangement: difference between the reflectivity of mirrors in first and second configuration (cf 3.2.2)

Spectral to Absolute coefficient: This component is calculated as the standard deviation of the ratio between absolute and relative measurement (cf 3.2.3). Its value is significantly lower than the expected value computed from the combination of the standard uncertainties of each term of the ratio. We explain this effect by the correlation with wavelength.

3.3.2 Higher spectral range measurement uncertainty

Comparison of standard quartz halogen lamps and key comparison deuterium lamps.

Table 3.2 Higher spectral range measurement uncertainty

Description of uncertainty parameter	type	uncertainty parameter	Irradiance uncertainty (%)				
Wavelength range(nm)			310	320	330	340	350
Repeatability of reference	A		0.50%	0.50%	0.50%	0.50%	0.50%
Repeatability of transfer	A		0.50%	0.50%	0.50%	0.50%	0.50%
Scale (irradiance reference)	B		2.5%	2.0%	2.0%	2.0%	1.0%
Irradiance sources position(longitudinal)	B	0.5mm	0.3%	0.3%	0.3%	0.3%	0.3%
Current source (reference)	B	1mA	0.13%	0.13%	0.12%	0.12%	0.12%
Current source (in test)	B	0.4mA	0.1%	0.1%	0.1%	0.1%	0.1%
Wavelength	B	0.25nm	1.28%	1.15%	1.00%	0.88%	0.73%
Cosine correction	B		0.10%	0.10%	0.10%	0.10%	0.10%
Optical dissymmetry	B	-	-	-	-	-	-
Detector linearity	B		0.10%	0.10%	0.10%	0.10%	0.10%
Spectral width	B		0.10%	0.10%	0.10%	0.10%	0.10%
Stray light	B		0	0	0	0	0
Spectral to Absolute coefficient	B		-	-	-	-	-
Combined standard uncertainty (k=1)			2.9%	2.4%	2.4%	2.3%	1.5%

Repeatability of reference: estimated from the difference of results obtained with different reference sources

3.4 Results

3.4.1 Calculation

Our two measurements are assembled as explained in 3.2.3.

First, we compute the ratios of the absolute values over the relative values in the common range (310 to 350 nm).

Then, in the lower spectral range (200 nm to 300 nm), the provided values of lamps are the relative values multiplied by the mean of the ratios.

In the higher part of the spectrum (310 nm to 350 nm) the provided values are simply the so-called absolute values.

3.4.2 Deuterium Lamp systems used

The following components were used by BNM/INM during the intercomparison:

Power supply: DLS-INM-PS

Monitor detector: DLS-INM-MD

Lamps: DLS-INM-L#01, DLS-INM-L#02, DLS-INM-L#03

If necessary the power supply has been switched between the primary voltage settings that are common in the different countries.

3.4.3 Lamp system electrical stability

The Deuterium Lamp systems were operated at 0.2996 A, the average lamp voltages measured were:

Table 3.3 Average Lamp voltages for the different INM lamp systems

Lamp	PTB round 1	Participant round 1	PTB round 2	Participant round 2
DLS-INM-L#01	77,23 V	76,89 V	77,38 V	77,19 V
DLS-INM-L#02	75,82 V	75,75 V	75,94 V	75,84 V
DLS-INM-L#03	77,29 V	77,33 V	77,77 V	77,78 V

3.4.4 Numerical results

BNM/INM measured all three lamp systems for the intercomparison. The results for the mean of the spectral irradiance of each lamp in each measurement round are given in the following tables. λ represents the wavelength in nm, $E(\lambda)$ stands for the spectral irradiance in $W \cdot m^{-2} \cdot nm^{-1}$ and $u(E)$ is the combined relative standard uncertainty for the measurement as reported by the participant. In the case that the participant reported spectral irradiance values for each single measurement of one round, the average calculated by the pilot is shown in Table 3.4.

Table 3.4 Results for the Lamp systems calibrated by BNM-INM

	DLS-INM-L#01		DLS-INM-L#02		DLS-INM-L#03		
	Round 1	Round 2	Round 1	Round 2	Round 1	Round 2	Uncertainty
λ	$E(\lambda)$	$E(\lambda)$	$E(\lambda)$	$E(\lambda)$	$E(\lambda)$	$E(\lambda)$	$u(E)$
[nm]	[W m^{-2}nm^{-1}]	[W m^{-2}nm^{-1}]	[W m^{-2}nm^{-1}]	[W m^{-2}nm^{-1}]	[W m^{-2}nm^{-1}]	[W m^{-2}nm^{-1}]	[%]
200	0,001249	0,001009	0,00123	0,0009751	0,00102	0,001398	13,2
210	0,001107	0,001039	0,001155	0,001162	0,001097	0,0012	5,6
220	0,001023	0,0009782	0,001117	0,001091	0,001024	0,001009	3,9
230	0,000896	0,0008595	0,001001	0,0009844	0,0009313	0,0009109	3,9
240	0,0007786	0,0007364	0,000883	0,0008613	0,000818	0,0008025	3,9
250	0,0006611	0,0006352	0,000766	0,0007389	0,0007216	0,0007072	3,9
260	0,000559	0,0005314	0,0006492	0,00063	0,0006156	0,0005958	3,9
270	0,0004696	0,0004501	0,0005468	0,000532	0,0005209	0,0005086	3,9
280	0,0003969	0,0003796	0,0004608	0,0004481	0,0004439	0,0004288	3,9
290	0,0003393	0,0003243	0,000393	0,0003827	0,0003791	0,0003676	3,9
300	0,0002917	0,0002779	0,0003356	0,0003276	0,0003222	0,0003154	3,9
310	0,0002501	0,0002371	0,0002873	0,0002763	0,0002786	0,0002683	2,9
320	0,0002241	0,0002139	0,0002562	0,0002494	0,0002498	0,0002416	2,4
330	0,0001943	0,0001845	0,0002223	0,0002138	0,0002169	0,0002088	2,4
340	0,0001745	0,000168	0,0001989	0,000194	0,0001954	0,00019	2,3
350	0,0001509	0,0001457	0,0001706	0,0001689	0,0001678	0,0001656	1,5

3.4.5 Repeatability between measurement rounds

With the results reported in 3.4.4 the repeatability of the measurements of each lamp system between each round was calculated. The difference from round 2 to round 1 as shown in Figure 3.3 might indicate outliers or a high drift of a single lamp.

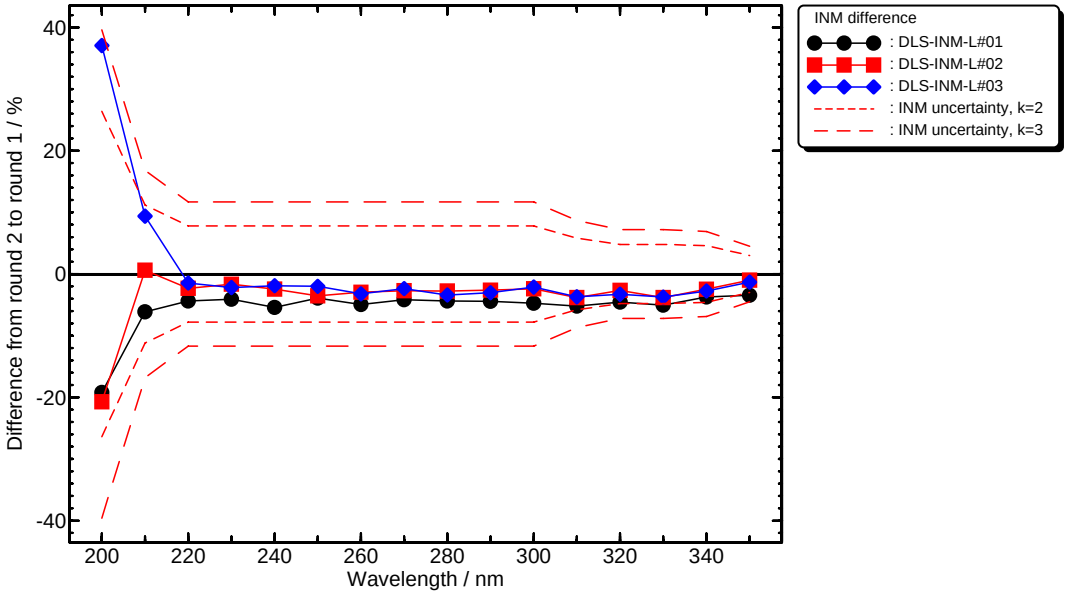

Figure 3.3 Repeatability between the measurement rounds calculated from the INM data.
The lines indicate the expanded measurement uncertainties for k = 2 and k = 3.

All participants' lamps were calibrated in one group during the two measurement campaigns at the PTB. Therefore the PTB could assign a spectral irradiance distribution for each participant's lamps. The repeatability of these measurements is shown in Figure 3.4. In combination with the participant's outcome these results can support the indication of an exceptional drift of a lamp system. Nevertheless, the PTB calibrations are only an additional indication for the participants' lamp stabilities (see also section 9.1.2)

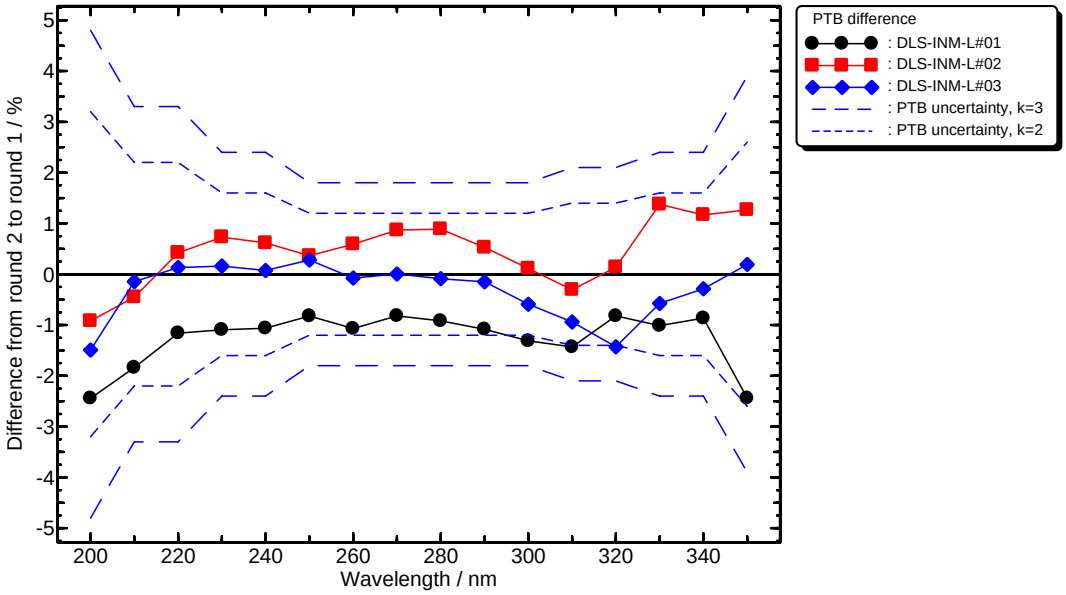

Figure 3.4 Repeatability between the measurement rounds calculated from PTB data.
The lines indicate the expanded measurement uncertainties for k = 2 and k = 3.

3.4.6 Normalized inner consistency of participants measurements

Additionally the inner consistency of the spectral irradiance calibrations of the lamps as described in section 9.1.2 was calculated (see equation (9.4)). It has to be pointed out, however, that the results presented here allow no conclusion of the absolute difference between participant and PTB.

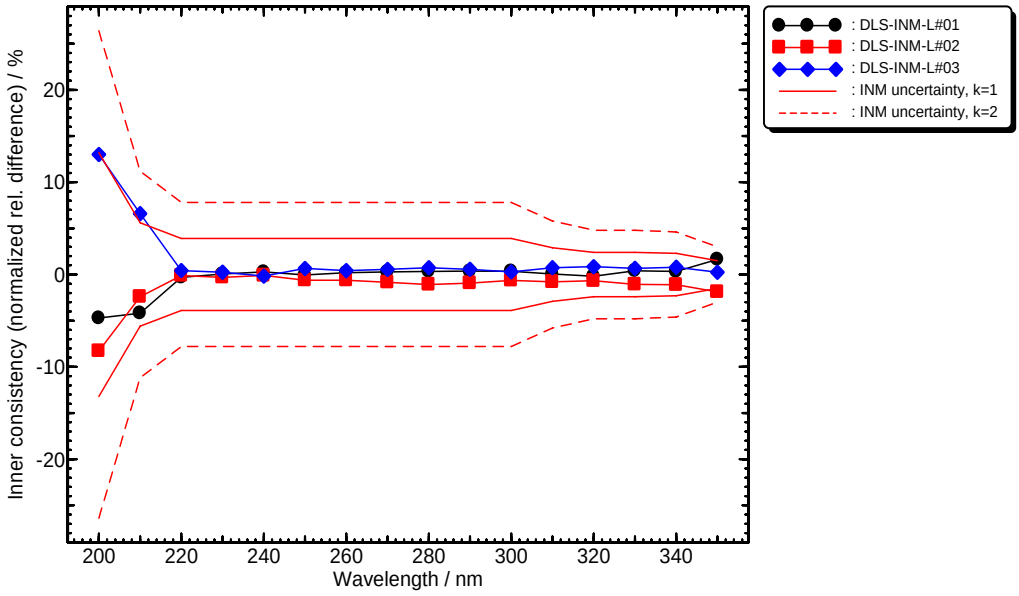

Figure 3.5 Normalized inner consistencies of the INM results compared to that of the PTB. The lines indicate the expanded measurement uncertainties for k = 1 and k = 2.

3.4.7 Acceptance of measurements

The results presented in the last sections indicate that all measurement results of all lamps during both measurement rounds at the participant can be used and that no data should be rejected.

4 NIST

This document describes the measurements and the NIST spectral irradiance scale realization of the deuterium (D2) lamps used for the Consultative Committee on Photometry and Radiometry (CCPR) Key Comparison, k1b. More detailed analysis and descriptions of the setup and the uncertainties can be found [1].

The CCPR k1b deuterium (D2) lamps were measured according to the following timetable. The lamps originated from PTB Braunschweig. The lamps were hand transported as carry-on luggage for all the transfers between the PTB and NIST.

Table 4.1 Dates and location of the measurements

Location	Measurement Date
1st PTB	July 2003
1st NIST	April 2004
2nd PTB	May 2004
2nd NIST	November 2004

4.1 Make and type of spectroradiometer (or equivalent)

For the measurements of spectral irradiance an Oriel# MS257 F/3.9 single Czerny-Turner monochromator with a bi-alkali side-on PMT (Hamamatsu R106) cooled to –15 °C was used. An integrating sphere receiver was directly attached to the entrance aperture of the monochromator. The 1st NIST measurements utilized a Spectralon-coated sphere which was changed to a NIST-fabricated packed PTFE sphere for the 2nd NIST measurements. The change of the integrating sphere was due to changes in the throughput and the fluorescence of the sphere resulting from the exposure to the synchrotron radiation [2]. The integrating sphere receiver is needed to remove the polarization sensitivity of the spectroradiometer when comparing the unpolarized D2 lamp with the polarized synchrotron radiation, especially since the throughput of spectrometers are sensitive to polarization. The opening of the spectroradiometer was set to 2.5 mm wide by 10 mm high to achieve a spectral bandwidth of < 5 nm from 200 nm to 350 nm.

4.2 Laboratory transfer standards used:

The NIST synchrotron, SURF III, was used as an absolute, calculable source from the use of the Schwinger equation and the parameters of the synchrotron. The synchrotron was compared against filter radiometers centered at 254 nm, 400 nm and at 800 nm which are calibrated for absolute, spectral irradiance responsivity. The filter radiometers are calibrated in the NIST SIRCUS facility and are traceable to the electrical standards from the cryogenic electrical substitution radiometer. The filter radiometer comparisons against the synchrotron were performed to validate the synchrotron scale.

Briefly, the NIST synchrotron, SURF III, consists of an electron beam accelerated about a 168 cm diameter, circular track [3]. The electron beam energy can be set and the beam current measured. The spectral irradiance calibrations of the D2 lamps were performed with the electron beam energy at 380 MeV with a beam current of 15 mA. The beam parameters were set to match the irradiances from the D2 lamp. The spectral irradiance from the synchrotron can be calculated from the physical parameters if the angular extent of the entrance to the spectroradiometer from the point of emission of the accelerated electrons is known. The angular extent is found using the distance from the

tangent point of the circular beam which was measured with a physical technique and optical triangulation for comparison.

Since the synchrotron requires ultra-high vacuum for operation, the comparisons of air-UV require windows which need to be measured for spectral transmittance. The window spectral transmittance was measured using the same spectroradiometer as used for the D2 lamp measurements. The window transmittance was determined by a dual-window technique alternately placing the windows into the synchrotron radiation to obtain the ratios of transmitted irradiances. The temporal stability of the window spectral transmittance was monitored, and the uncertainties of the spectral transmittance are included in the total uncertainties.

4.3 Description of measuring technique (please include a diagram):

The spectroradiometer with the integrating sphere receiver was placed on a motorized stage with both x- and y-axis controls with the z-axis being the direction along the radiation from the synchrotron. The D2 lamp was also placed directly to the side of the synchrotron window as shown in Fig. 1. The motorized stages were needed to both scan for the plane of the synchrotron and to switch between the lamp source and the synchrotron for the measurements. The D2 lamp or the device-under-test (DUT) was placed on a moveable stage for positioning to the specified 30 cm distance from the alignment plate.

The sequence of measurements starts with measurement of the synchrotron source to determine the spectral irradiance responsivity of the spectroradiometer with a known, calculable source. Each of the three CCPR k1a lamps is then measured. The synchrotron is measured again at the end of the lamp measurements to determine that the spectral irradiance responsivity of the spectroradiometer has not changed. Since the synchrotron beam current decays with time, measurement at each wavelength is scaled by the beam current.

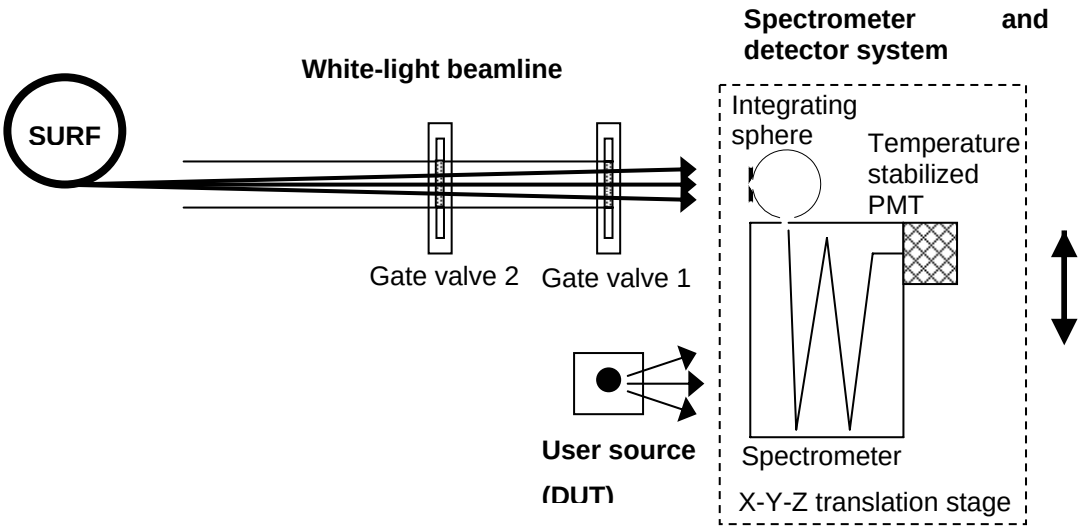

Figure 4.1 Schematic of the measurement setup showing the placement of the synchrotron with the deuterium lamp at the side of the beamline.
The spectroradiometer can alternatively measure the synchrotron and the deuterium lamp.

The spectral irradiances of the D2 lamps are obtained from the spectral irradiance of the synchrotron by using

$$E_{D2,S} = \frac{E_S}{i_S} \cdot i_{D2} \quad , \qquad (4.1)$$

where E_S is the spectral irradiance of the synchrotron, i_S is the photocurrent measured when the spectroradiometer is placed in front of the synchrotron, $E_{D2,S}$ is the spectral irradiance of the D2 lamp, and i_{D2} is the photocurrent when measuring the D2 lamp. The spectral irradiance of the synchrotron is modified from that as given by the Schwinger equation by the spectral transmittance of the window. The in-air transmittance only affects the 200 nm spectral irradiance and the change due to the small path length of ~ 15 cm is taken into account in the uncertainty budget.

Since a single grating monochromator was used for increased throughput, the spectroradiometer was measured for stray-light scattering in the NIST Spectral Irradiance and Radiance responsivity Calibrations using Uniform Sources (SIRCUS) [4]. The spectroradiometer with the integrating sphere input was taken to SIRCUS for determining the stray-light along with the fluorescence of the integrating sphere with tunable lasers from 220 nm to 400 nm. A total scattering matrix is developed and the spectral irradiances of the D2 lamps are corrected for the scattered radiation [5].

4.4 Establishment or traceability route of primary scale including date of last realisation and breakdown of uncertainty:

Since the synchrotron is directly used to calibrate the D2 lamps, the scale realization is performed every time the D2 lamps are measured. The uncertainties are stated in an Excel spreadsheet titled <CCPR-K1.b uncertainty sent to PTB>. The uncertainties of the synchrotron are listed in Table 4.2.

Table 4.2 Components of the relative uncertainties (k=2) of spectral irradiance of synchrotron radiation.

Source of uncertainty	Nominal value	Relative uncertainty	Sensitivity coefficient	Uncertainty in irradiance
Electron energy	380 MeV	0.02%	0.057	0.0011%
Beam current	~15 mA	0.4%	1	0.4%
Orbital radius	83.70773 cm	10^{-10}	0.66	10^{-10}
Window transmittance	~0.8	0.5%	1	0.5%
Distance	692.6 cm	0.086%	2.0	0.17%
Positioning		±0.6 mm*	0.0011	0.066%
Aperture size	0.95 cm	6.3%	0.015	0.096%
Air absorption**			1	0.24%
Combined				0.72%

* absolute uncertainty
** for wavelengths below 205 nm, <0.1% for wavelengths longer than 205 nm.

The uncertainties of the spectral irradiance calibration of the deuterium lamp are listed in Table 4.3.

Table 4.3 Components of the relative uncertainty (k=2) of spectral irradiance of deuterium lamp calibration.

Source of uncertainty	Nominal value	Relative uncertainty	Sensitivity coefficient	Uncertainty in irradiance
SURF radiation			1	0.72%
Wavelength		±0.1 nm*	0.013	0.27%
Stray light and fluorescence			1	0.5%
Lamp distance	30 cm	0.033%	2.0	0.13%
Lamp stability			1	0.5%
Random uncertainty			1	0.6%
Combined				1.2%

* absolute uncertainty

4.5 Description of calibration laboratory conditions: e.g. temperature, humidity etc.

The temperature of the laboratory was nominally maintained at 23.4 °C . The relative humidity was not controlled and could fluctuate with atmospheric conditions limited by the air conditioning of the room. During the measurements one recorded value of the relative humidity was 48.8 %.

#Certain commercial equipment, instruments, or materials are identified in this paper to foster understanding. Such identification does not imply recommendation or endorsement by the National Institute of Standards and Technology, nor does it imply that the material or equipment are necessarily the best available for the purpose.

4.6 References

[1] Shaw P-S, Arp U, Saunders R. D., Shin D. J., Yoon H. W., Gibson C. E., Li Z, Parr A. C., and Lykke K. R., "Synchrotron radiation based irradiance calibration from 200 nm to 400 nm at SURF III," submitted to Applied Optics.

[2] Zhigang Li, Ping-Shine Shaw, Uwe Arp, Howard W. Yoon, Robert D. Saunders, and Keith Lykke, "Characterization of Integrating Spheres for Ultraviolet Radiometry," presented at the 6th Workshop on Ultraviolet Radiation Measurements, Davos, Switzerland, October 2005.

[3] Shaw P-S., Arp U., Yoon H.W., Saunders R.D., Parr A.C., Lykke K.R., "A SURF beamline for synchrotron source-based absolute radiometry," Metrologia 40, 2003, S124-S127.

[4] Brown S. W., Eppeldauer G. P., Lykke K. R., "NIST Facility for Spectral Irradiance and Radiance Responsivity Calibrations with Uniform Sources," Metrologia 37, 2000, pp. 579-582.

[5] Shumaker J.B., Deconvolution, Chap. 8 in Self-Study Manual on Optical Radiation Measurements: Part I- Concepts, Chapters 7, 8, and 9, National Bureau of Standards, June 1979.

4.7 Results

4.7.1 Deuterium Lamp systems used

The following components were used by NIST during the intercomparison:

Power supply: DLS-NIST-PS

Monitor detector: DLS-NIST-MD (detector failed during first round)

Lamps: DLS-NIST-L#01, DLS-NIST-L#02, DLS-NIST-L#03

If necessary the power supply has been switched between the primary voltage settings that are common in the different countries.

4.7.2 Lamp system electrical stability

The Deuterium Lamp systems were operated at 0.2996 A, the average lamp voltages measured were:

Table 4.4 Average Lamp voltages for the different NIST lamp systems

Lamp	PTB round 1	Participant round 1	PTB round 2	Participant round 2
DLS-NIST-L#01	76,45 V	76,51 V	76.61 V	75,56 V
DLS-NIST-L#02	73,61 V	73,86 V	74,04 V	74,09 V
DLS-NIST-L#03	70,96	70,71	70,64	70,38

4.7.3 Numerical results

The participant measured all three lamp systems for the intercomparison. The results for the mean of the spectral irradiance of each lamp in each measurement round are given in the following tables. λ represents the wavelength in nm, $E(\lambda)$ stands for the spectral irradiance in $W \cdot m^{-2} \cdot nm^{-1}$ and $u(E)$ is the combined relative standard uncertainty for the measurement as reported by the participant. In the case that the participant reported spectral irradiance values for each single measurement of one round, the average calculated by the pilot is shown in Table 4.5.

Table 4.5 Results for the Lamp systems calibrated by NIST

	DLS-NIST-L#01		DLS-NIST-L#02		DLS-NIST-L#03		
	Round 1	Round 2	Round 1	Round 2	Round 1	Round 2	Uncertainty
λ	$E(\lambda)$	$E(\lambda)$	$E(\lambda)$	$E(\lambda)$	$E(\lambda)$	$E(\lambda)$	$u(E)$
[nm]	[W m^{-2}nm^{-1}]	[W m^{-2}nm^{-1}]	[W m^{-2}nm^{-1}]	[W m^{-2}nm^{-1}]	[W m^{-2}nm^{-1}]	[W m^{-2}nm^{-1}]	[%]
200	0,0009196	0,0009118	0,0009687	0,0009537	0,001006	0,001004	0.7
210	0,0009473	0,0009433	0,0009813	0,0009757	0,001012	0,001016	0.6
220	0,0009145	0,0009105	0,0009359	0,0009269	0,0009601	0,00096	0.6
230	0,0008531	0,0008498	0,0008641	0,0008563	0,0008794	0,0008799	0.6
240	0,0007702	0,0007662	0,0007735	0,0007676	0,0007821	0,0007824	0.5
250	0,0006778	0,0006764	0,0006777	0,0006726	0,0006806	0,0006809	0.5
260	0,0005843	0,0005842	0,0005823	0,0005793	0,0005815	0,0005823	0.5
270	0,0005007	0,0005004	0,0004981	0,0004945	0,000496	0,0004954	0.5
280	0,0004277	0,0004283	0,0004259	0,000424	0,0004207	0,0004228	0.6
290	0,0003664	0,0003665	0,0003651	0,0003636	0,0003586	0,000359	0.5
300	0,0003169	0,0003163	0,0003165	0,000314	0,0003086	0,0003094	0.5
310	0,0002742	0,0002743	0,0002742	0,0002732	0,0002661	0,0002673	0.6
320	0,0002398	0,0002408	0,0002402	0,0002397	0,0002315	0,000233	0.6
330	0,0002119	0,0002116	0,0002122	0,0002105	0,0002035	0,0002038	0.6
340	0,0001878	0,0001872	0,0001882	0,0001862	0,0001797	0,0001797	0.6
350	0,0001671	0,0001667	0,0001677	0,0001663	0,0001597	0,0001594	0.6

4.7.4 Repeatability between measurement rounds

With the results reported above the repeatability of the measurements of each lamp system between each round was calculated. The difference from round 2 to round 1 as shown in Figure 4.2 might indicate outliers or a high drift of a single lamp.

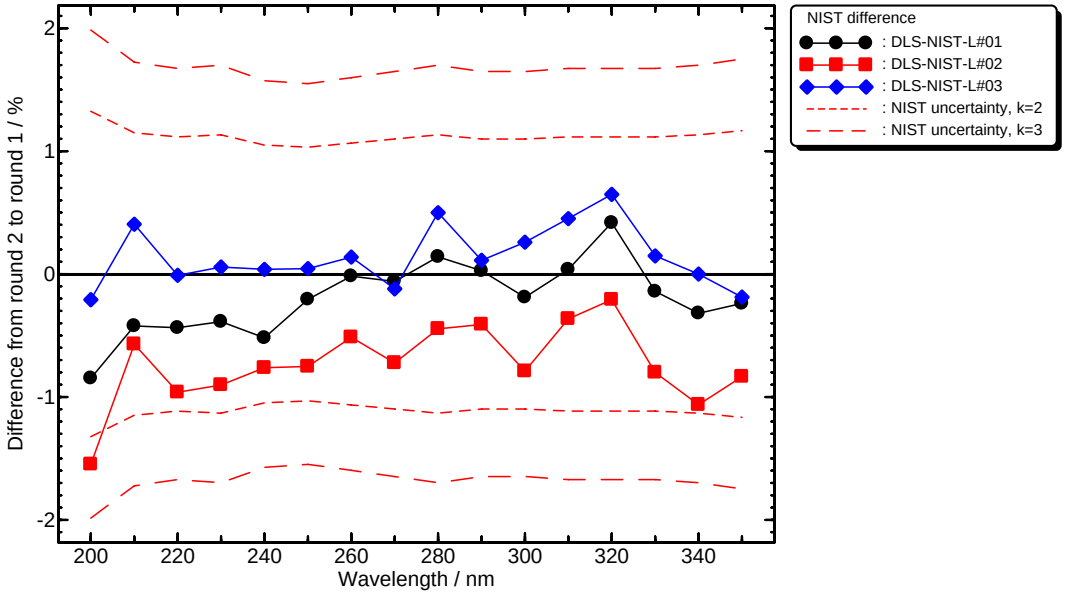

Figure 4.2 Repeatability between the measurement rounds calculated from the NIST data.
The lines indicate the expanded measurement uncertainties for k = 2 and k = 3.

All participants' lamps were calibrated in one group during the two measurement campaigns at the PTB. Therefore the PTB could assign a spectral irradiance distribution for each participant's lamps. The repeatability of these measurements are shown in Figure 4.3.

In combination with the participant's outcome these results can support the indication of an exceptional drift of a lamp system. Nevertheless, the PTB calibrations are only an additional indication for the participants' lamp stabilities (see also section 9.1.2)

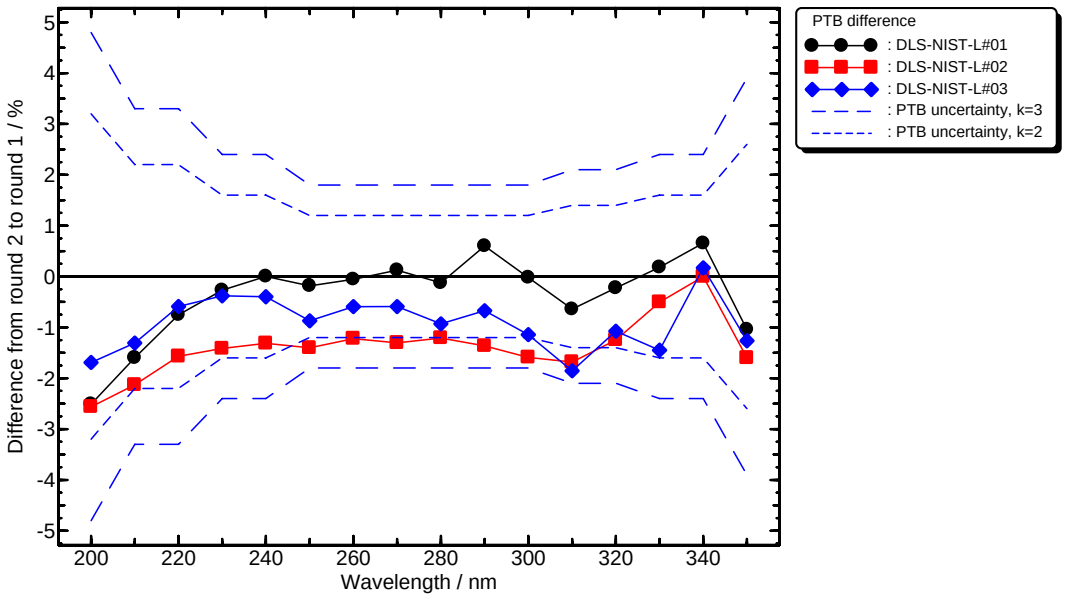

Figure 4.3 Repeatability between the measurement rounds calculated from PTB data.
The lines indicate the expanded measurement uncertainties for k = 2 and k = 3.

4.7.5 Normalized inner consistency of participants measurements

Additionally the inner consistency of the spectral irradiance calibrations of the lamps as described in section 9.1.2 was calculated (see equation (9.4)). It has to be pointed out, however, that the results presented here allow no conclusion of the absolute difference between participant and PTB.

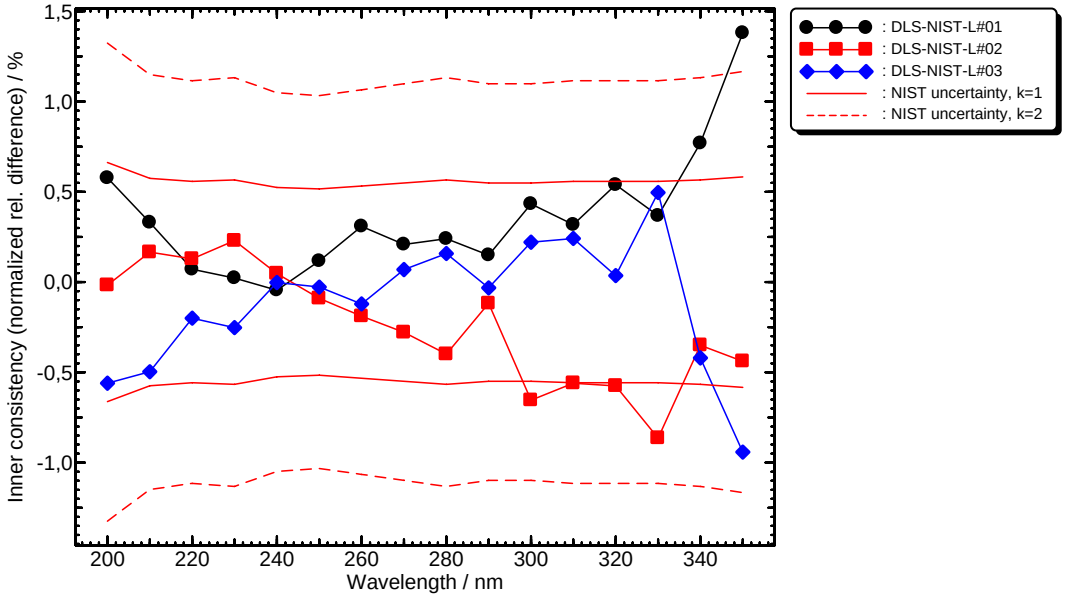

Figure 4.4 Normalized inner consistency of the NIST result compared to that of the PTB.
The lines indicate the expanded measurement uncertainties for k = 1 and k = 2.

4.7.6 Acceptance of measurements

The results presented in this section indicate that all measurement results of all lamps during both measurement rounds at the participant can be used and that no data should be rejected.

5 NPL

5.1 Introduction

The NPL spectral irradiance scale from 250 to 2500 nm was formerly integrated into our measurement services and consequently became our disseminated scale in May 2003, as reported at the last CCPR meeting. This scale was extended to cover the region of this comparison during the measurements for this comparison and is now disseminated to our customers down to 200 nm. The scale is based on the use of the absolute spectral radiance emitted from a high temperature blackbody through Planck's law. The critical input variable being thermodynamic temperature, which is determined by a filter radiometer whose spectral response has been calibrated against the NPL primary standard cryogenic radiometer. This traceability chain is shown schematically in Figure 5.1. A brief overview of the various components and stages involved in this process, together with their associated uncertainty follows below.

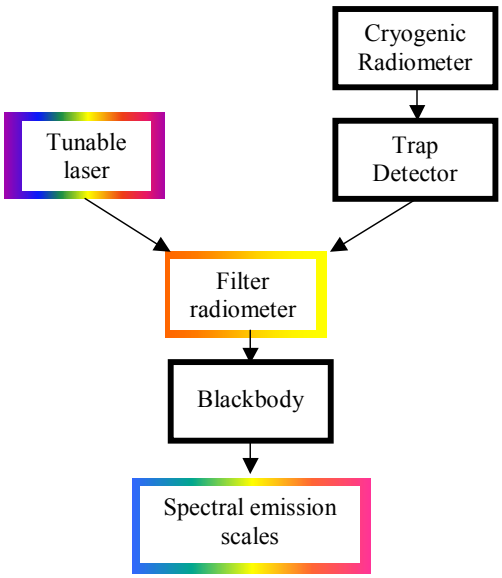

Figure 5.1 Traceability chain for the primary spectral irradiance scale at NPL

5.2 The Spectral Radiance and Irradiance Primary Scales (SRIPS) Facility

The Spectral Radiance and Irradiance Primary Scales (SRIPS) facility, shown schematically below in Figure 5.2, was used not only for establishing the NPL UV spectral irradiance scale, but also for all NPL's measurements of the deuterium lamps for this comparison. The primary source was a BB3500 blackbody source, operated at temperatures around 3060 K and 3160 K. The thermodynamic temperature of the blackbody was determined absolutely using a group of filter radiometers built at NPL and calibrated traceably to the primary cryogenic radiometer at NPL.

A Bentham DTM300 turret grating monochromator was used to select the wavelengths and measurements were made with a photo-multiplier tube. The monochromator and detector were mounted on a large translation stage that could be moved in front of each source in turn. The entire facility was computer controlled.

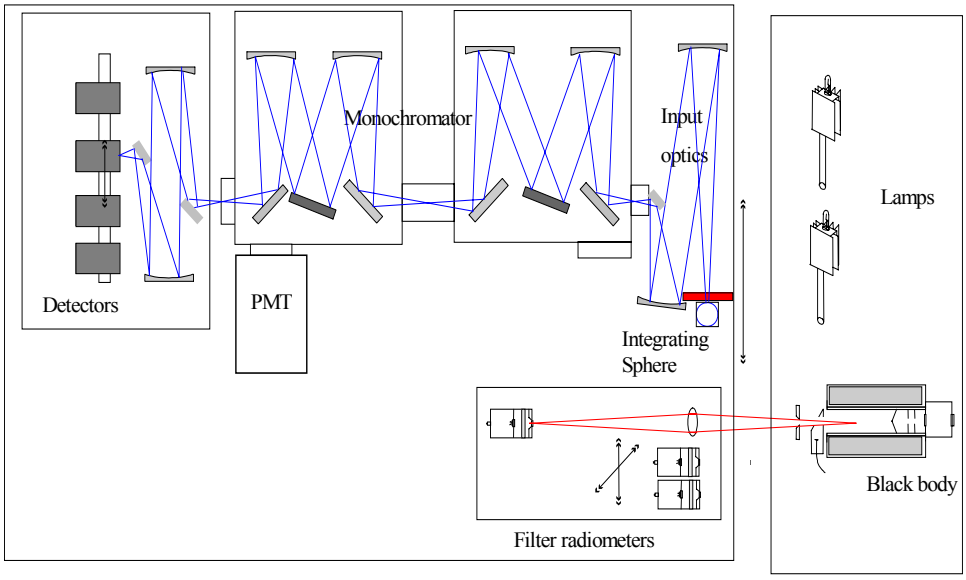

Figure 5.2 SRIPS Facility diagram

5.2.1 The Blackbody Source

The primary source was a BB3500 blackbody supplied to NPL by VNIIOFI in early 1999. The source has been extensively investigated and shown to be uniform and stable under active optical stabilisation from the front.

Investigations have shown [1] that this blackbody suffers from the same ultraviolet absorption around 380 nm as has been observed with the BB3200pg [2]. Further investigations in preparation for this comparison showed that there were further absorption features at shorter wavelengths. For this reason, the blackbody temperature was kept relatively low, around 3050 K for the longer wavelengths. However, for the shortest wavelengths, the need for a high blackbody temperature was unavoidable; here the absorption effect has been characterised and corrected.

The radiance of the blackbody was determined from Planck's law, based on a measure of its thermodynamic temperature via filter radiometers, and the geometry defined by a water-cooled, brass, diamond-turned, aperture in front of the blackbody and the aperture on the integrating sphere at the front of the monochromator.

5.2.2 The Monochromator

The monochromator used was a Bentham DTM300 monochromator, arranged in a subtractive mode configuration. The monochromator used a pair of UV optimised gratings. Details of the UV gratings are shown in Table 5.1.

Table 5.1 Description of the UV grating.

Grating	Grooves per mm	Blaze Wavelength	Recommended Wavelength Range
UV	2400	250 nm	200 nm – 675 nm

Light enters the monochromator via pair of off-axis parabolic mirrors which image the exit port of a 50 mm diameter Spectralon coated integrating sphere, onto the entrance slit of the monochromator. Both mirrors are UV enhanced, $MgFl_2$ protected and aluminium-coated. There is a 1.6 times demagnification between the integrating sphere and the entrance slit of the monochromator.

5.2.3 Detector

The Photomultiplier tube (PMT) is directly mounted on the exit port of the monochromator. The PMT has its own power supply and controller that stabilises it at 780V and –10 °C. For the wavelength range of this comparison, the PMT was the only detector used.

5.2.4 Filter Radiometers

The blackbody temperature was measured with an 800 nm filter radiometer used in conjunction with a geometric system to allow it to measure spectral radiance, in a similar manner to that described previously [3].

The filter radiometer comprised a diamond-turned brass aperture, a wedged 10 nm bandwidth interference filter and a silicon photodiode and was housed in a water-cooled jacket. A Vinculum transimpedance amplifier was connected to the silicon photodiode and held in the same water jacket.

A 300 mm focal length lens was used at a distance of 600 mm to image light from the blackbody aperture so as to overfill the filter radiometer aperture. This aperture and a thin-film aperture on the lens defined the geometry of the measurement. The filter radiometer was used in the same f /55 geometry in which it had been calibrated. The lens transmittance was calculated using the Fresnel equations, which had previously [9] been shown to agree within 0.05 % of the measured value at this wavelength. A correction was also applied for differences in "size-of-source" based on measurements using similar techniques to those described previously [3].

Additional filter radiometers operating in "irradiance mode" (without a lens) were used to monitor any drift in the primary filter radiometer.

5.2.5 Laboratory Conditions

Measurements were made in a laboratory maintained at 20 ± 3 ºC. The humidity of the laboratory was not controlled.

5.3 Scale realisation and traceability

5.3.1 Overview

The traceability to SI comes from the determination of the blackbody temperature through filter radiometry. Filter radiometers were calibrated by comparison with two trap detectors against a tuneable laser-illuminated integrating sphere source. Measurements were made in approximately 0.1 nm intervals across the full transmittance range of the filter radiometer. The trap detectors, in turn, were calibrated against the cryogenic radiometer. This was done with a direct laser beam as a source. The calibrated aperture on the trap detector was used to convert spectral responsivity to spectral irradiance responsivity. A more detailed description of this process can be found in the literature [4].

5.3.2 Measurement Sequence

All lamps were measured on at least three occasions. The lamps were realigned between these measurements. Each calibration was made in four spectral regions, which overlapped with the neighbouring region by at least 2 wavelengths, with one exception. Regions 3 and 4 can be considered one region – a break was made simply to measure the blackbody temperature – therefore there were no wavelength overlaps between these two regions. The different regions are listed in Table 5.2.

Table 5.2 Wavelengths measured at NPL for the CCPR-K1.b comparison

Name	Start wavelength	Stop wavelength	Step size and extra wavelengths	Input optics	Slit size (mm) [Entrance – Middle – Exit] *Bandwidth*	UHTBB Temp
Region 1	200 nm	230 nm	10 nm	Tile	[3-3-5] *4 nm*	3160 K
Region 2	220 nm	260 nm	5 nm	Tile	[1-1-2] *1.5 nm*	3160 K
Region 3	220 nm	280 nm	10 nm + 225 nm	Sphere	[1-1-2] *1.5 nm*	3050 K
Region 4	290 nm	350 nm	10 nm	Sphere	[1-1-2] *1.5 nm*	3050 K

Due to low signal levels between 200 and 260 nm, the integrating sphere on the SRIPS facility was replaced with a Spectralon tile diffuser. These measurements are considered only relative, as there was no defining aperture used. The results have been corrected and shifted to overlap the results from regions 3 and 4, which were made with the integrating sphere.

To further increase the signal level at the lowest wavelengths (200 – 230 nm), the entrance slits of the monochromator were widened. This introduces a further shift to the data in that region due to the bandwidth, which was corrected as described in section 5.4.2.1.

For region 1 and 2 the measurements were made in the following sequence:

1) Measurement of the temperature of the blackbody with a filter radiometer.
2) Measurement of the blackbody with the SRIPS monochromator over a particular wavelength range, e.g. 220 nm – 260 nm.
3) Measurement of the temperature of the blackbody with the filter radiometer. If it had changed more than 0.2%, steps 1-3 were repeated and the previous results discarded.
4) Measurement of the lamps with the SRIPS monochromator over the same wavelength range.
5) Measurement of the temperature of the blackbody with a filter radiometer
6) Measurement of the blackbody with the SRIPS monochromator over the same wavelength range
7) Measurement of the temperature of the blackbody with the filter radiometer.

In regions 3 and 4, the PMT detector suffered from short-term fatigue and long-term drift because of the higher signal levels. Therefore, the measurement sequence was altered:

1) Measurement of the temperature of the blackbody with a filter radiometer
2) Measurement of the blackbody with the SRIPS monochromator at one wavelength
3) Measurement of the lamp with the SRIPS monochromator at that wavelength
4) Measurement of the blackbody with the SRIPS monochromator at that wavelength
5) Repetition of steps 2 to 4 for all the other relevant wavelengths
6) Measurement of the temperature of the blackbody with the filter radiometer.

This process increased the time between measurements, and therefore allowed the PMT to recover between each light reading and also, by placing the blackbody and lamp measurements at one wavelength next to each other, reduced the effect of long-term drift.

5.4 Analysis of Measurement Results

5.4.1 Measurement Equation — Monochromator

At any wavelength, the SRIPS facility measures both the blackbody and the lamp. The signal when measuring the blackbody is:

$$V^{\mathrm{BB}}(\lambda) = \pi\, g \cdot \int R^{\mathrm{SRIPS,BB}}(l) \cdot L^{BB}(T,l) \cdot S(l,\lambda) \cdot dl + \text{stray light} + \text{electronic noise} \quad (5.1)$$

Here, g is the geometric factor, which is described below. V^{BB} is the signal measured by the SRIPS detector, $R^{\mathrm{SRIPS,BB}}$ is the responsivity of the SRIPS facility during the blackbody measurements, L^{BB} is the radiance of the blackbody as given by Planck's law. S is the slit function of the monochromator, normalised to have a unit area and l is an integration constant, equivalent to wavelength, but only over the slit width. The integral is over the extent of the slit function, usually 5–10 nm. Over this wavelength range there will be a small change in the blackbody radiance and also a (usually small) change in the SRIPS responsivity, therefore these functions lie inside the integral. Stray light and electrical noise are determined with a shutter.

The signal SRIPS measures when calibrating the lamp is given by a similar equation (A is the area of the integrating sphere aperture):

$$V^{\mathrm{lamp}}(\lambda) = A \cdot \int R^{\mathrm{SRIPS,lamp}}(l) \cdot E^{\mathrm{lamp}}(\lambda) \cdot S(l,\lambda) \cdot dl + \text{stray light} + \text{electronic noise} \quad (5.2)$$

When the second blackbody scan is made, the signal is given by Equation (5.1) again, although the stray-light and electrical noise may be different and the responsivity of SRIPS may have drifted a small amount. If the sources can be considered to be varying only slowly with wavelength over the slit function, then the integrals can be removed. This approximation is reasonable when the two sources are spectrally similar, as for a blackbody and lamp. However, for dissimilar sources, an error is introduced, as is discussed in section 5.4.2.1. Taking this approximation, the two equations can be combined to give:

$$E^{\mathrm{lamp}}(\lambda) = K\kappa(\lambda)\frac{\pi g}{A} L^{\mathrm{BB}}(\lambda;T)\frac{V^{\mathrm{lamp}}(\lambda)}{V^{\mathrm{BB}}(\lambda)}\frac{R^{\mathrm{SRIPS,BB}}(\lambda)}{R^{\mathrm{SRIPS,lamp}}(\lambda)} \quad (5.3)$$

where E^{lamp} is the desired lamp irradiance. The final term should be unity, if the SRIPS facility has not drifted. It is left in at this stage for the purposes of uncertainty calculations. Here K is an additional constant introduced to account for any difference between the measured lamp geometry (alignment distance, tilt etc) and the defined lamp geometry at which the lamp should be measured. K is unity, but has an associated uncertainty.

In practice two measurements of the blackbody have been made at potentially different temperatures. The average of the two ratios: $L^{\mathrm{BB}}/V^{\mathrm{BB}}$ is used, where L^{BB} is calculated for the average of the blackbody temperature measured before and after the relevant monochromator scan.

The geometric factor comes from the form factor for radiative transfer between two coaxial circular discs, but is multiplied by the area of the emitting aperture in order to make a version that is symmetrical from one disc to the other:

$$g = \frac{2\pi r_1^2 r_2^2}{(r_1^2 + r_2^2 + d^2) + \sqrt{(r_1^2 + r_2^2 + d^2)^2 - 4r_1^2 r_2^2}} \quad (5.4)$$

Here r_1 and r_2 are the radii of the two discs and d is the distance between them. For SRIPS measurements these are the radii of the blackbody and the integrating sphere aperture that is the entrance aperture to the monochromator system.

The radiance of a blackbody in air is calculated from Planck's law using air wavelengths and the refractive index of air, n.

$$L_{BB} = \frac{2h(c/n)^2}{\lambda^5(\exp[hc/n\lambda kT]-1)} \tag{5.5}$$

5.4.2 Measurement Analysis

Due to the complicated nature of the measurements taken of the deuterium lamps, the measurement analysis occurs in several parts. Weighted shifts need to be applied to the data taken with the Spectralon tile diffuser since these measurements are considered only relative. Before the data was shifted, errors due to the finite bandwidth of the monochromator and blackbody absorption were corrected for.

5.4.2.1 Bandwidth Correction

Equation (5.3) makes the assumption that when Equation (5.2) is divided by (5.1) after the dark signal is removed, the responsivity of SRIPS cancels out. This would only be true if the slit function were infinitely narrow.

How similar the measured ratio $\tilde{V}_{\text{lamp}}(\lambda)/\tilde{V}_{\text{BB}}(\lambda)$ is to the assumed ratio $V_{\text{lamp}}(\lambda)/V_{\text{BB}}(\lambda) = \dfrac{R(\lambda)E_{\text{lamp}}(\lambda)A}{R(\lambda)L_{\text{BB}}(\lambda)\pi g}$ needs to be determined. The full integral equation is generally unsolvable. However, under certain specific conditions a solution can be found.

This problem has been investigated as part of a project [5] on lamp spectral modelling, and for a triangular slit function an approximation can be made. For a triangular slit function, of full width $2\Delta\lambda$ and unit area, the following equation holds:

$$V(\lambda) = \tilde{V}(\lambda) - \tfrac{1}{12}(\Delta\lambda)^2\tilde{V}''(\lambda) + \tfrac{1}{240}(\Delta\lambda)^4\tilde{V}^{iv}(\lambda) + \ldots \tag{5.6}$$

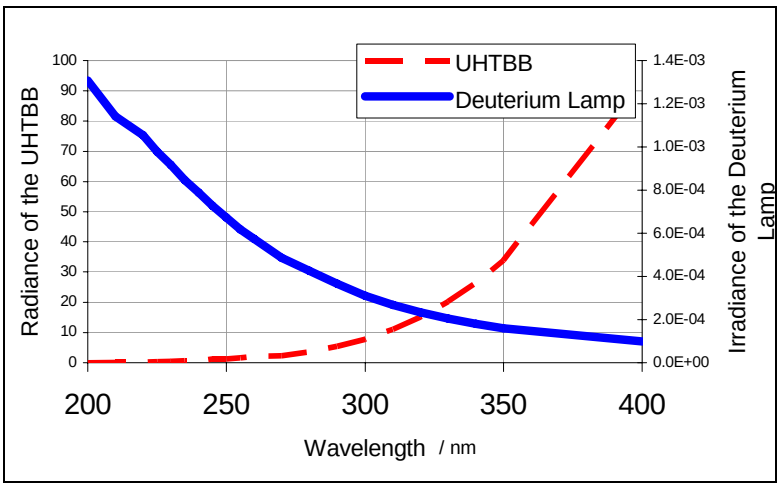

Figure 5.3 Irradiance of the UHTBB and deuterium lamps

Equation (5.6) can be applied to each source and then the ratio taken. If the two sources are very similar (as is the case for an FEL calibrated against a blackbody), the correction to the ratio is tiny,

even if the correction to each individual source is significant. This means that Equation (5.3) can be used without correction for FELs. However, Figure 5.3 shows how the blackbody and the deuterium lamps are very different sources and are changing rapidly and non-linearly in different directions. This means that Equation (5.3) can be used, but only after the raw signals (in V) are corrected for using Equation (5.6).

The correction that needs to be applied is the second term in Equation (5.6). The second derivative was calculated from the raw measurement data using the following equation:

$$\frac{d^2\tilde{V}_i}{d\lambda^2} = \frac{\tilde{V}_{i-1} - 2\tilde{V}_i + \tilde{V}_{i+1}}{d^2} \tag{5.7}$$

Where i represent the discrete ith measurement and d is the step size between measurements. Therefore the correction is:

$$\Delta V = -\frac{(\Delta\lambda)^2}{12}\left[\frac{\tilde{V}_{i-1} - 2\tilde{V}_i + \tilde{V}_{i+1}}{d^2}\right] \tag{5.8}$$

This correction was applied to all of the lamp data before the weighted shifts were applied. In order to have measurements at appropriately spaced wavelengths to determine an accurate second derivative, measurements were made additionally on one day in each round in 2.5 nm steps. The correction calculated on that day was applied at the comparison wavelengths for the comparison lamps on all days.

The bandwidth was determined by scanning a mercury line with the monochromator for the two slit widths used for the comparison measurements (slits of [3-3-5] corresponded to a bandwidth of 4.06 ± 0.05 nm, and slits [1-1-3] corresponded to a bandwidth of 1.46 ± 0.05 nm).

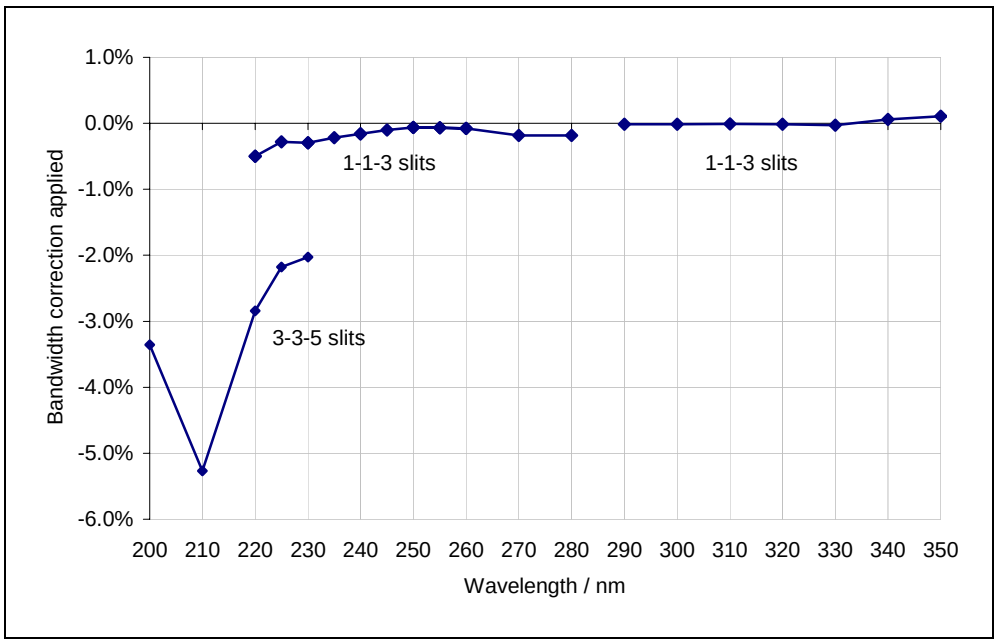

Figure 5.4 Bandwidth correction applied.
Where there are two values for one wavelength it is because the monochromator is operated with different sized slits at those wavelengths. The stronger effect corresponds to the wider slits

5.4.2.2 Absorption Correction

Investigations have shown [2] that the blackbody suffers from ultraviolet absorption around 380 nm. For this reason, the blackbody temperature was kept relatively low, around 3050 K for the longer wavelengths (regions 3 and 4).

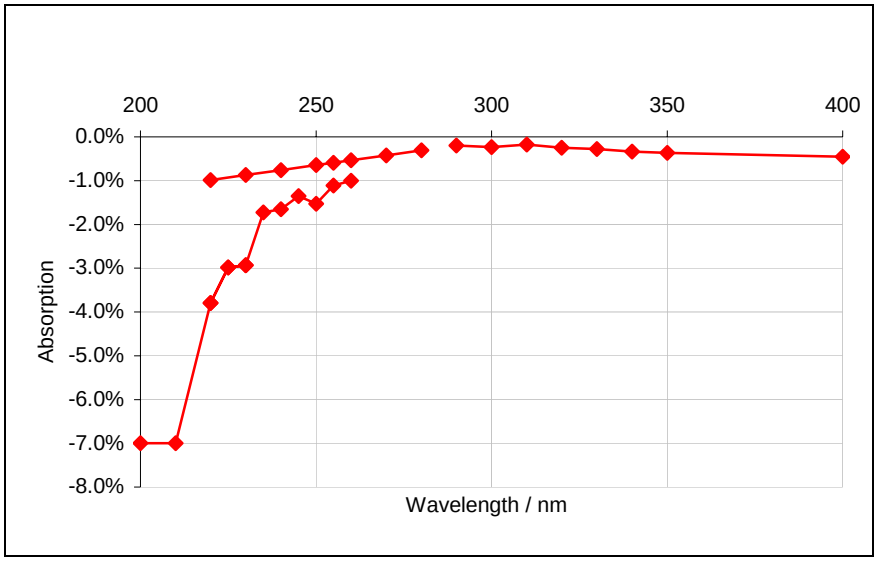

Figure 5.5 Absorption effect: Correction applied.
Where there are two values for one wavelength, this is because the blackbody is operated at two temperatures at that wavelength. The stronger effect is seen at the higher temperature

To understand, and correct for, this absorption effect, the blackbody was measured at different temperatures and the ratio of the measured signals between the hotter and cooler blackbodies was compared with the expected ratio from the Planck equation. A comparison of a blackbody at 3050 K with one at 2450 K, at which temperature there is no sublimed carbon, showed a broad absorption feature in the region from 300 to 450 nm. The difference between these measurements was used as a correction in region 4.

These tests were also made as part of this comparison at shorter wavelengths and for a hotter blackbody, since that was required for the shortest wavelengths to maximise signals there. It was not possible to make a comparison to a blackbody cool enough to show no absorption; instead blackbodies at 3170 K and 3050 K were compared to one at 3000 K. Some absorption around 210 nm was discovered. The absorption is probably due to C_2N_2, which has strong lines at 209.31 nm and 210.74 nm [6].

The absorption correction for region 3 was based on the 3050 K blackbody results and the absorption correction for regions 2 and 1 were based on the 3170 K blackbody results. The overall absorption correction is plotted in Figure 5.5. The uncertainty associated with this correction is discussed in section 5.5.2.5.

5.4.2.3 Weighted Shift

The measurements made with the Spectralon tile diffuser at the lowest wavelengths are considered to be relative as they were made with no defining aperture. These measurements need to be shifted to agree with the measurements made with the integrating sphere. This shift was applied to the data after the absorption and bandwidth corrections had been applied.

Because the measurement was slightly different for regions 1 and 2, because of the slit size differences, region 1 requires two shifts, and region 2 requires one shift to be performed. Figure 5.6

shows an example of the simple calculation based on Equation (5.3) made for the lamp calibration on one day.

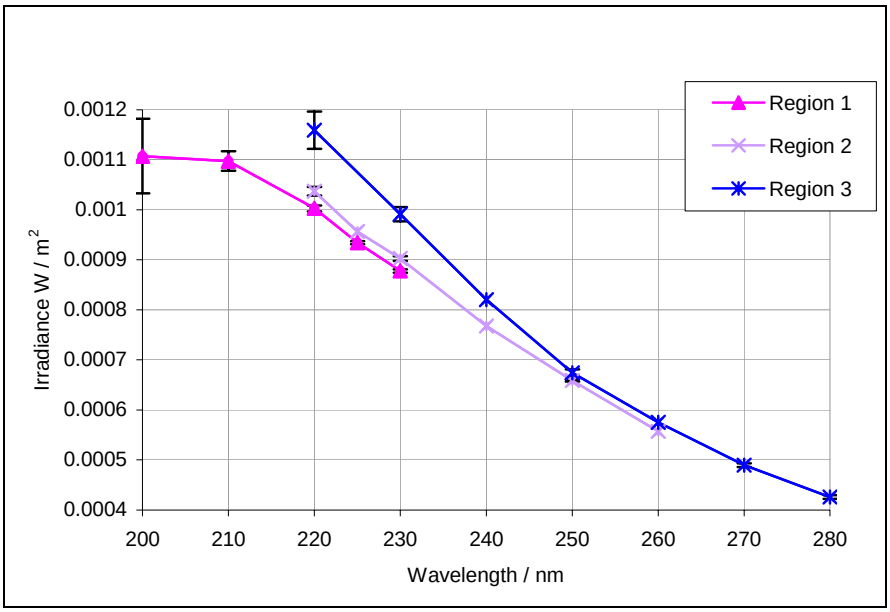

Figure 5.6 Raw calculation of deuterium irradiance, showing as "error bars" the blackbody repeatability during these measurements

In Figure 5.6 the "error bars" at each wavelength are different due to the repeatability of the blackbody. In region 3 the repeatability of the blackbody worsens at the lower wavelengths, and this also occurs with the lowest wavelengths in region 1. Since varying repeatability is highly wavelength dependent, the shifts that are applied are weighted according to their associated uncertainty. The uncertainty used for each wavelength was the standard deviation of the blackbody repeatability during each round of the comparison, or the repeatability of the blackbody on the day of the measurement, whichever was greater. This method was used to average out any coincidently 'good' repeatability for an individual wavelength, so that an unbiased shift could be applied to the data.

The measurement made in region 1 [$A(\lambda)$], needs to be shifted by [α] and [β], to agree with the measurements made in region 3, [$A'(\lambda)$], Equation (5.9). Similarly the measurements made in region 2, [$B(\lambda)$], need to be shifted by [β] to agree with region 3, [$B'(\lambda)$]. α and β are the shift factors required, which were calculated by taking the weighted average of the overlapping wavelengths, Equation (5.10). ω_i is calculated using the repeatability of the blackbody, Equation (5.11).

$$A'(\lambda) = \alpha\beta A(\lambda) \qquad B'(\lambda) = \beta B(\lambda) \quad (5.9)$$

$$\beta = \frac{\sum_{i=1}^{N} \omega_i \left(\frac{C_i}{B_i}\right)}{\sum_{i=1}^{N} \omega_i} \qquad (5.10)$$

$$\omega_i = \frac{1}{U\left(\frac{B_i}{C_i}\right)}, \text{ where } \quad U\left(\frac{B_i}{C_i}\right) = \sqrt{\left(\frac{U(B_i)}{B_i}\right)^2 + \left(\frac{U(C_i)}{C_i}\right)^2} \qquad (5.11)$$

5.5 Uncertainty Analysis

5.5.1 Uncertainty associated with Constants

This section discusses the uncertainty associated with the constants in Equation (5.3) in section 5.4.1, K, g and A. K is a measure of the quality of the alignment of the lamp on the day of measurement. The lamps were aligned at a distance of 300 mm, and the uncertainty of that distance is estimated to be 0.3 mm. The lamp alignment uncertainty also contains estimates for the effect of minor tilt and similar alignment errors and has been estimated at 0.19% for the comparison lamps. Therefore K has a value of 1 ± 0.0019 for the comparison lamps.

The lamp stability during the calibration was determined for the comparison lamps by comparing the photodiode reading at the beginning and end of each day. This showed a standard deviation of 0.04%. The stability from switch on to switch on was estimated by comparing the photodiode readings from one day to the next during one measurement round. This gave an uncertainty of 0.23%.

The uncertainty associated with an estimate of the value $\pi g / A$ is due to geometry. It is a constant at all wavelengths and for all separate lamp measurements. The effect is taken as a Type B uncertainty of 0.08%. The relevant apertures are r_1=4 mm ± 0.1 µm, r_2=8 mm ± 0.1 µm and the distance between them is 500 ± 0.2 mm.

5.5.2 Uncertainty associated with Blackbody Radiance

The blackbody temperature is given by the Planck equation.

$$L^{BB}(\lambda;T) = \alpha(\lambda)\varepsilon \frac{2h(c/n)^2}{\lambda^5(\exp[hc/n\lambda kT]-1)} \tag{5.12}$$

Here h is the Planck constant, 6.626 0693(11) × 10^{-34} J s, c is the speed of light, 299 792 458 m s^{-1} (exact), k is the Boltzmann constant, 1.380 6505(24) × 10^{-23} J K^{-1}, n is the air refractive index, 1.00029 ± 0.00005 and ε is the emissivity of the blackbody, which is 0.99988 ± 0.00010.

$\alpha(\lambda)$ is from the absorption of the blackbody. A correction for this effect has been applied as shown in section 5.4.2.2. The associated uncertainty associated with the correction is discussed later in this section.

5.5.2.1 Uncertainty associated with blackbody temperature

The temperature of the blackbody is measured using a filter radiometer whose spectral responsivity, $R(\lambda)$, has been calibrated. The filter radiometer is placed in front of the blackbody and light is focussed onto it using a lens. Four measurements are taken: a light reading, V^{light}, a dark reading, V^{dark}, an out-of-band reading V^{OOB} (with a long-pass filter in front of the filter radiometer — this accounts for any filter radiometer responsivity at wavelengths longer than the longest calibration wavelength) and a dark out-of-band reading $V^{\text{OOB, Dark}}$, with the long pass filter and the shutter.

The signal, V, can be compared with the expected signal in the following equation:

$$\begin{aligned} V &= V^{\text{light}} - V^{\text{dark}} - V^{\text{OOB}} + V^{\text{OOB,Dark}} \\ &= sGUS \cdot g\pi R \cdot \int_{\lambda_0}^{\lambda_1} r(\lambda)\,\tau(\lambda)\,L(\lambda;T)\,d\lambda \end{aligned} \tag{5.13}$$

Here L is the radiance of the blackbody given by Equation (5.5), $\tau(\lambda)$ is the wavelength-dependent lens transmittance, g is the geometric factor, given by Equation (5.4), but this time with the lens and filter radiometer apertures, G is the electronic gain of the amplifier and s is the size-of-source effect,

a measure of the amount of light scattered by imperfections in the lens. U is the uniformity of the blackbody—the difference between the signal measured and the signal that would be measured if a larger area of the blackbody were observed (because the spectral irradiance calibration facility sees a larger area of blackbody). S is a measure of the blackbody stability between the time when the temperature is measured and the time when the spectral irradiance is measured. S has a value of unity, but an associated uncertainty.

The responsivity of the filter radiometer has been split into two components. The absolute responsivity, R, (in A W^{-1}) has been separated from the relative spectral responsivity $r(\lambda)$ to simplify the error analysis (R is the component correlated at all wavelengths; r is entirely uncorrelated from one wavelength to the next).

The filter radiometer responsivity has been calibrated at discrete wavelengths; therefore, Equation (5.13) is replaced by a discrete version, using the trapezium rule:

$$V(T) = C\sum_{j=1}^{N} r_j L(\lambda_j, T)\cdot \delta\lambda_j \tag{5.14}$$

Here C combines all the uncertainties on the outside of the integral in Equation (5.13). $\delta\lambda_j$ is $\left(\lambda_{j+1} - \lambda_{j-1}\right)/2$ for all but the first $\left(\left(\lambda_2 - \lambda_1\right)/2\right)$ and last $\left(\left(\lambda_N - \lambda_{N-1}\right)/2\right)$ values.

The Newton-Raphson technique is used to determine the temperature of the blackbody given the signal. This is robust for this calculation because only one value of temperature can be associated with each signal.

According to normal uncertainty analysis, as described in the Guide to the Uncertainty of Measurement (GUM) [7], given a function $f(x_1,x_2,x_3...)$, the uncertainty associated with the function, u_f should be derived from the uncertainties calculated from the individual parts. However, here the temperature cannot be described as a function of the other variables. Instead we must use the techniques for a "multivariate, implicit, real valued model" as described in section 6.3.4 of the 6th best practice guide from the Software Support for Metrology programme at NPL [8]. This requires Equation (5.14) to be written in the form $h(Y, X) = 0$:

$$h(T, C, V, r_1...r_N, \tau_1...\tau_N) = \left[C\sum_{j=1}^{N} r_j L(\lambda_j, T)\cdot \delta\lambda_j\right] - V = 0 \tag{5.15}$$

The best practice guide supplies methods for determining the uncertainty associated with T due to the uncertainties in all the other components. The following equations are therefore needed to determine the uncertainty associated with temperature due to uncertainties in each of the components:

$$\left(\frac{\partial h}{\partial T}\right)^2 u^2(T) = u^2(V)\left(\frac{\partial h}{\partial V}\right)^2 + u^2(C)\left(\frac{\partial h}{\partial C}\right)^2 + \sum_{i=1}^{N} u^2(r_i)\left(\frac{\partial h}{\partial r_i}\right)^2 \tag{5.16}$$

$$\left(\frac{\partial h}{\partial T}\right)^2 = \left[C\sum_{j=1}^{N}\left(r_j\,\tau_j\,\delta\lambda_j\,\frac{\partial L(\lambda_j;T)}{\partial T}\right)\right]^2 \tag{5.17}$$

$$\left(\frac{\partial h}{\partial V}\right)^2 = 1 \tag{5.18}$$

$$\left(\frac{\partial h}{\partial C}\right)^2 = \left(\frac{V}{C}\right)^2 \tag{5.19}$$

$$\sum_{j=1}^{N}\left(\frac{\partial h}{\partial r_j}\right)^2 u^2(r_j) = \sum_{j=1}^{N}\left[C\,\tau_j\,L(\lambda_j;T)\delta\lambda_j\right]^2 u^2(r_j) \tag{5.20}$$

$$\frac{\partial L(\lambda_j;T)}{\partial T} = \frac{2h^2c^3\exp[hc/n\lambda kT]}{n^3\lambda^6kT^2\left(\exp[hc/n\lambda kT]-1\right)^2} \tag{5.21}$$

These equations assume no correlation and there are no correlations between V and C (although there may be some correlations within C), nor between either of these and the r_j s. Since the blackbody was used at two different temperatures for the different regions for the comparison, there are slightly different uncertainties that arise from the higher temperature and higher signal levels.

Uncertainty associated with signal levels

The signal level used in Equation (5.14) is the light signal level minus the dark signal and minus the out-of-band. This is treated as a type B uncertainty and comes dominantly from the uncertainty associated with the calibration of the voltmeter and the electrical noise in the dark reading. The uncertainty associated with the out-of-band comes from the quality of the filter used for the out-of-band measurements along with any differences between the temperature of the blackbody during out-of-band measurements and during blackbody temperature measurements.

The uncertainty associated with the measured signal is:

$$u_V^2 = u_{V\,\mathrm{light}}^2 + u_{V\,\mathrm{dark}}^2 + u_{V\,\mathrm{OOB}}^2 + u_{V\,\mathrm{OOB,\,dark}}^2 + \left(\frac{V}{K}\right)^2 u_K^2 \tag{5.22}$$

The final term represents the calibration uncertainty of the voltmeter. It assumes that it is the same for all four measurements and that they should all be multiplied by a, nominally unity, correction factor K. Therefore voltmeter non-linearities are assumed to be negligible. K is 1 with an uncertainty of 0.005%.

Typically, V is 1.8 V and u_V is 0.09 mV. From Equations (5.18) and (5.16), this corresponds to a temperature uncertainty of 0.027 K.

Size-of-source

The size-of-source effect is 0.22 ± 0.02%. From Equations (5.19) and (5.16), this corresponds to a temperature uncertainty of 0.10 K.

Amplifier gain

The amplifier was calibrated at an accredited laboratory. The quoted uncertainty on the amplifier measurements is 0.01% at 95% confidence, or a standard uncertainty of 0.005%. From Equations (5.19) and (5.16), this corresponds to a temperature uncertainty of 0.03 K.

Lens transmittance

The lens transmittance was calculated using the Fresnel equations, which had previously [9] been shown to agree within 0.05% of the measured value at this wavelength. From Equations (5.19) and (5.16), this corresponds to a temperature uncertainty of 0.15 K. Although the lens transmittance is a wavelength dependent quantity and therefore inside the integral, the values are entirely correlated and therefore the uncertainty is considered in C.

Geometric factor

The geometric factor is derived from the size of the apertures on the filter radiometer and lens and the distance between them. However, the full expression for *g* is not required to work out the effect of these uncertainties. This is because the area of the filter radiometer aperture is used in calculating the spectral responsivity during its calibration, and this area is calculated from the same aperture calibration. This calculation is therefore exactly the same as that for the geometric factor in the spectral irradiance measurement. For a 0.1 μm uncertainty in the filter radiometer and lens aperture diameters and a 0.2 mm uncertainty in the distance, and for the normal set-up, *g/A* has a standard uncertainty of 0.07%, which corresponds to a temperature uncertainty of 0.34 K.

FR absolute responsivity

The absolute responsivity of the filter radiometer after a fresh calibration has a standard uncertainty of 0.02%. There is also an uncertainty due to any difference between the calibration set up of the filter radiometer and its use. The most significant problem with that is the size-of-source effect, which is large enough to be considered elsewhere, but the temperature of the filter radiometer and the f-number of the optical set-up are also important. Care is taken to make sure these conditions are matched as closely as possible. Therefore there is only a small additional uncertainty, of 0.01% from this. An additional uncertainty of 0.04% has been added to account for any filter radiometer drift. The overall uncertainty is 0.046%, corresponding to a temperature uncertainty of 0.24 K.

Blackbody stability

When the blackbody is used as a reference source on the SRIPS facility, its temperature is measured twice before the monochromator scan and twice afterwards. If the difference between the maximum and minimum filter radiometer readings with an 800 nm filter radiometer is greater than 0.2%, then the results are ignored and the scan repeated. The uncertainty associated with the averaged temperature is typically 0.05%, corresponding to a temperature uncertainty of 0.26 K.

Blackbody uniformity

The uniformity of the blackbody is measured by scanning a filter radiometer with a 5 mm aperture in front of the blackbody at the distance of the integrating sphere. The central reading is similar to the temperature measurement and the overall scan is similar to the area of the integrating sphere aperture. The average of all the measurements is compared with the central reading. Of course a uniformity scan takes time and therefore the stability of the blackbody will also affect the measurement. However the stability is noisy at the 0.1-0.2% level on a very short timescale. This means that there is no steady drift across the uniformity scan; instead, each individual point will have its own stability component completely uncorrelated with the points either side of it. This means that the averaging technique will also remove some of the stability uncertainty. The uncertainty associated with the uniformity correction is 0.11%, corresponding to a temperature uncertainty of 0.33 K.

Emissivity

In addition to its effect in calculating the irradiance of the blackbody, the emissivity will also play a part in calculating its temperature. At the filter radiometer wavelength the uncertainty associated with blackbody emissivity is 0.02%, corresponding to a temperature uncertainty of 0.06 K. This does give a mathematical correlation between the blackbody irradiance calculation and temperature measurement but it is far too small to be significant.

5.5.2.2 Filter radiometer relative responsivity

The calibration of the filter radiometer has three distinct regions. In the wings, where the responsivity of the filter radiometer is low, the predominant uncertainty is signal to noise at around 0.5% of the signal. On the steep slopes of the profile, the predominant uncertainty is due to

wavelength fluctuations, this is expressed as a responsivity uncertainty of around 0.14%. In the central, flatter region the signal to noise is good and any wavelength fluctuations are less significant. Here the uncertainty drops to 0.02%. These uncertainties are entirely random and therefore the integration will "average out" their effect. The overall effect on temperature, calculated from Equations (22) and (25), is 0.005 K.

5.5.2.3 Uncertainty associated with trapezium rule

The numerical integration is carried out using the trapezium rule, because the filter radiometers have been calibrated at discrete wavelengths. An estimate of the uncertainty introduced by this can be obtained by calculating the temperature using all the points and then by using only half the points. The difference gives an uncertainty of 0.003 K at this temperature. Because of the large number of points (1150), this difference is small enough that more involved methods for determining the integral, and its uncertainty, are not required.

5.5.2.4 Overall uncertainty associated with temperature

Combining these equations and these uncertainty sources for a blackbody at 3050 K measured with filter radiometer 800W50S1337A, the overall standard (66% confidence) uncertainty associated with temperature is 0.62 K. This value should be combined with the uncertainties of all the other components in Equation (5.12) to give the overall uncertainty associated with blackbody radiance. The effect of the temperature uncertainty on wavelength can be seen from that equation. The overall uncertainty associated with temperature is given in Table 5.3.

Table 5.3 Uncertainty components and overall uncertainty associated with the blackbody temperature measurement. All are standard uncertainties (k = 1)

Uncertainty component	Uncertainty as a percentage of value, where appropriate		Temperature uncertainty/ K	
	3050 K	3160 K	3050 K	3160 K
Geometric factor	0.067%	0.067%	0.344	0.369
Blackbody Uniformity	0.064%	0.064%	0.328	0.351
Blackbody Stability	0.050%	0.050%	0.258	0.277
FR absolute responsivity	0.046%	0.046%	0.236	0.254
Lens Transmission	0.029%	0.029%	0.149	0.160
Size of source	0.020%	0.020%	0.103	0.110
Emissivity	0.012%	0.012%	0.060	0.064
Voltage measurement			0.027	0.031
Amplifier gain	0.005%	0.005%	0.026	0.028
FR relative responsivity			0.005	0.006
Mathematical Approximations			0.003	0.003
Overall Temperature Uncertainty			0.621 K	0.666 K

5.5.2.5 Uncertainty associated with the absorption correction

Section 5.4.2.2, discusses the effect of absorption and the correction that has been applied to the data, since the absorption effect was significant. The ratios of the measurements at two different temperatures were compared to determine the absorption correction between 200 nm and 350 nm. The associated uncertainty associated with the correction is due to the uncertainty of the measurements made to determine the absorption effect, which is due to repeatability of those measurements. An approximation was also made to account for the daily changes in the absorption. This daily effect was determined using some results from measurements made of the absorption on three separate dates. This variability was of the order of half to a third the correction factor; therefore the correction was divided by 2.5. These two uncertainties were added in quadrature.

The measurements in region 3 and 4 were performed at 3050 K and therefore the absorption correction between 220 nm and 400 nm that was applied was from the measurements made at 3060 K. The uncertainties were determined in the same way, however the repeatability of these measurements and the correction applied was lower than for the shortest wavelengths, and therefore the uncertainties are lower.

5.5.2.6 Overall Uncertainty associated with blackbody radiance

The blackbody radiance is calculated from Equation (5.12). The uncertainty components to consider come from the temperature, as described in the previous section, the uncertainty associated with the correction of absorption due to carbon and, to a much smaller degree, to the uncertainty associated with the emissivity correction.

The overall standard uncertainty due to these factors is shown in Figure 5.7.

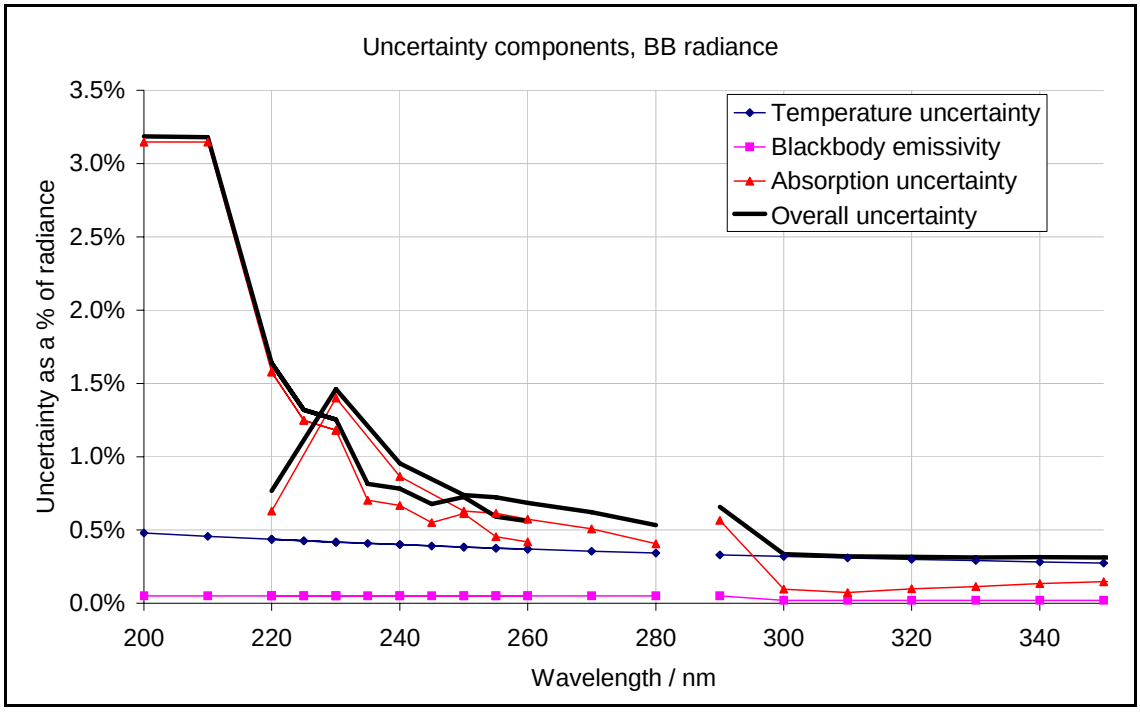

Figure 5.7 Standard uncertainty associated with blackbody radiance and a percentage of spectral radiance and as a function of wavelength

5.5.3 Uncertainty associated with Lamp-Blackbody Signal Ratios

The final uncertainty that needs to be considered is the uncertainty associated with the final two terms of Equation (5.3). That is the uncertainty associated with:

$$\frac{V^{\text{lamp}}(\lambda)}{V^{\text{BB}}(\lambda)}\frac{R^{\text{SRIPS,BB}}(\lambda)}{R^{\text{SRIPS,lamp}}(\lambda)} \tag{5.23}$$

The uncertainty associated with the ratios comes from any non-linearity in the response of the system or the measurement of the signals and in any drift in the facility between the measurement of the blackbody and the measurement of the lamp, along with the noise on the signals. However there is an additional uncertainty due to whether this ratio is really the desired ratio, this uncertainty comes from the wavelength accuracy and the effect of the monochromator bandwidth.

5.5.3.1 Linearity

The uncertainty associated with $V_{\text{lamp}} / V_{\text{BB}}$ is the uncertainty associated with the linearity and repeatability of the voltage measurements with the voltmeter. Because of the ratio, the absolute calibration of the voltmeter is irrelevant. The linearity of the PMT is better than 0.1% when the signal below 1 μA.

5.5.3.2 Geometry Match

When sources are compared to the blackbody they can illuminate the defining aperture of the SRIPS facility (the integrating sphere aperture) slightly differently. To test the uncertainty associated with these differences, an FEL lamp was measured in a variety of different geometries. The standard deviation of those measurements was 0.4%. However that included lamp realignment. For the comparison the blackbody and deuterium lamp illuminate the sphere in a reasonably similar way, so 0.2% is a reasonable estimate for the residual effect.

5.5.3.3 Noise

The predominant uncertainty at most wavelengths is the uncertainty associated with the ratio $R^{\text{BB}}_{\text{SRIPS}} / R^{\text{lamp}}_{\text{SRIPS}}$.

The blackbody is measured before and after the lamp. The difference between these two measurements (when any change in temperature is accounted for) is due to the stability of the source and the stability of SRIPS. The source stability is insignificant because the source is highly stable, as measured by the filter radiometer; its insignificance is confirmed by the fact that the blackbody differences show no spectral component. Therefore it can be assumed that these differences give the repeatability of SRIPS. There is typically no drift from the first to the second blackbody scan. This means that the repeatability calculated between blackbody measurements is equivalent to the SRIPS repeatability between the blackbody and lamp measurements.

The differences have been measured on many occasions and variations from day to day are or statistical rather than of experimental significance. This uncertainty has been determined from a standard deviation of the differences between the blackbody measurements on measurements made during round one of the comparison. The results are shown in Figure 5.8.

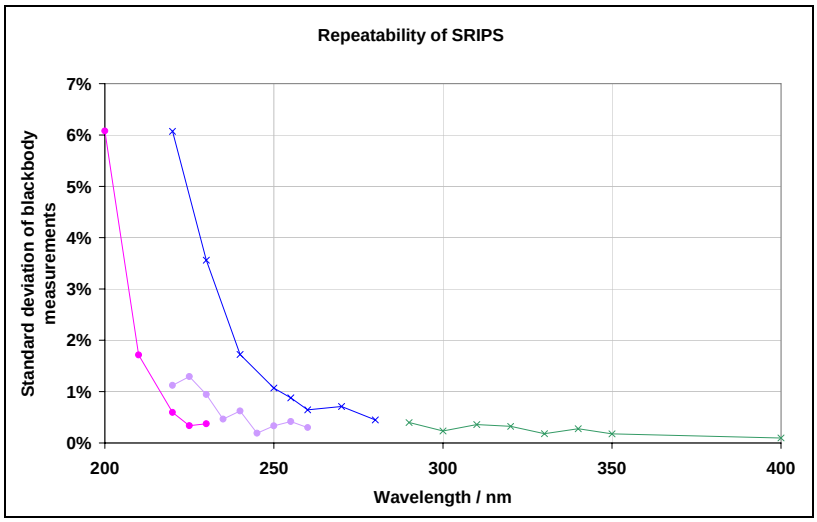

Figure 5.8 Repeatability of SRIPS.

The increases at the end of different spectral regions are due to the decrease in detector responsivity or grating throughput and therefore a lower signal and higher noise. For FEL calibrations, the standard deviation of the two blackbody measurements has been considered as the uncertainty associated with the stability of the SRIPS facility. Here the noise is actually worse than this because the lamp and blackbody are very different and so noise will affect one more than the other. This is particularly true in the longest wavelength regions, where the blackbody signal is very high, but the lamp signal is very low. Therefore, for region 4, only, this repeatability has been multiplied by 2.

In practice when calculating the uncertainty on a particular day, the uncertainty is calculated either from this standard deviation of all days, or from the specific uncertainty on the day in question, whichever is the greater. This means that statistically good days are not advantaged, but that statistically poor days are disadvantaged.

5.5.4 Wavelength accuracy

The ratios were carried out at the measured wavelengths, which may be slightly different to the calculated wavelengths because of uncertainty associated with the monochromator's wavelength accuracy. Strictly this should be treated as a wavelength uncertainty, however it can more easily be converted to an uncertainty associated with the ratio of irradiance levels of sources being compared.

There is an uncertainty associated with the wavelength of around 0.05 nm. The effect of this depends on how smoothly varying both sources are, as well as how smooth the responsivity of SRIPS is. If the ratio of the signals of the two sources varies strongly with wavelength, the wavelength uncertainty will become more important. The Taylor expansion of $V_{\mathrm{lamp}} / V_{\mathrm{BB}}$ is:

$$\tilde{V}(\lambda+\delta\lambda)=\frac{V^{\mathrm{lamp}}(\lambda+\delta\lambda)}{V^{\mathrm{BB}}(\lambda+\delta\lambda)}\approx\tilde{V}(\lambda)+\delta\lambda\cdot\frac{d\tilde{V}}{d\lambda} \tag{5.24}$$

Therefore the uncertainties are calculated from the ratio of the second to the first term in Equation (5.24).

5.5.5 Uncertainty associated with the bandwidth correction

The bandwidth correction applied is that given in Section 5.4.2.1 and Equation (5.6). This discusses the uncertainty associated with that correction.

5.5.5.1 Uncertainty from the measurement

This is the uncertainty due to the noise in the measurements on the day used to calculate the bandwidth correction. This noise is uncorrelated between the three points used to calculate the correction. Therefore the uncertainty due to the measurements can be obtained from:

$$\begin{aligned} u^2(\Delta V)=&\left[\frac{\Delta\lambda^2}{12d^2}\right]^2\left(u^2(V_{i-1})+4u^2(V_i)+u^2(V_{i+1})\right)\\ &+\left[\frac{2\Delta\lambda\cdot\left(V_{i-1}-2V_i+V_{i+1}\right)}{12d^2}\right]^2u^2(\Delta\lambda)\end{aligned} \tag{5.25}$$

The uncertainty associated with the bandwidth, required for the second term in Equation (5.25), has been estimated as 0.05 nm. The uncertainty associated with each of the measurements is given by the standard deviation of the two measurements. Note that this is an *absolute* uncertainty, with units of V.

This has been used to calculate the uncertainty associated with the correction for both the blackbody measurement and for the lamp measurement. These are uncorrelated, so the uncertainty associated

with the correction to the ratio of these can be obtained in the normal way by adding the two *relative* uncertainties in quadrature. The uncertainty calculated ranges from 1% at 200 nm to 0.2% for wavelengths above 220 nm.

5.5.5.2 Applicability to other days

To determine the bandwidth correction, measurements were required in very finely spaced intervals. This was only done on one day, so it is necessary to understand whether this correction can be applied to measurements of the other comparison lamps on other days.

The effect due to the bandwidth being slightly different on another day is likely to be smaller than the 0.05 nm bandwidth uncertainty already considered in Equation (5.25).

Effects due to minor variations in the spectral irradiance of the comparison lamps are considered negligible. This was tested by comparing this correction with that calculated for a different type of deuterium lamp calibrated at the same time.

The bandwidth correction was also calculated for measurements made on a day when the blackbody was 100 K hotter. The difference was trivial compared to the uncertainties and can be neglected entirely for the 20 K variation from day-to-day during the comparison measurements.

5.5.5.3 Mathematical uncertainties

The mathematical uncertainty because of the approximation to a triangular slit function is not known, but these slit functions appear "very triangular" and we have already considered the uncertainty due to bandwidth errors. Therefore this uncertainty can be considered negligible.

The uncertainty due to stopping at the second derivative term can be found by calculating the fourth derivative term. The effect is completely negligible above 207.5 nm, but is of the order of 1.5% for shorter wavelengths.

5.5.5.4 Overall uncertainty due to bandwidth correction

The overall uncertainty due to the bandwidth correction is given in Figure 5.9. The uncertainty associated with the correction is only significant at the shortest wavelengths where the monochromator is operated with wide slits and the original measurements were particularly noisy.

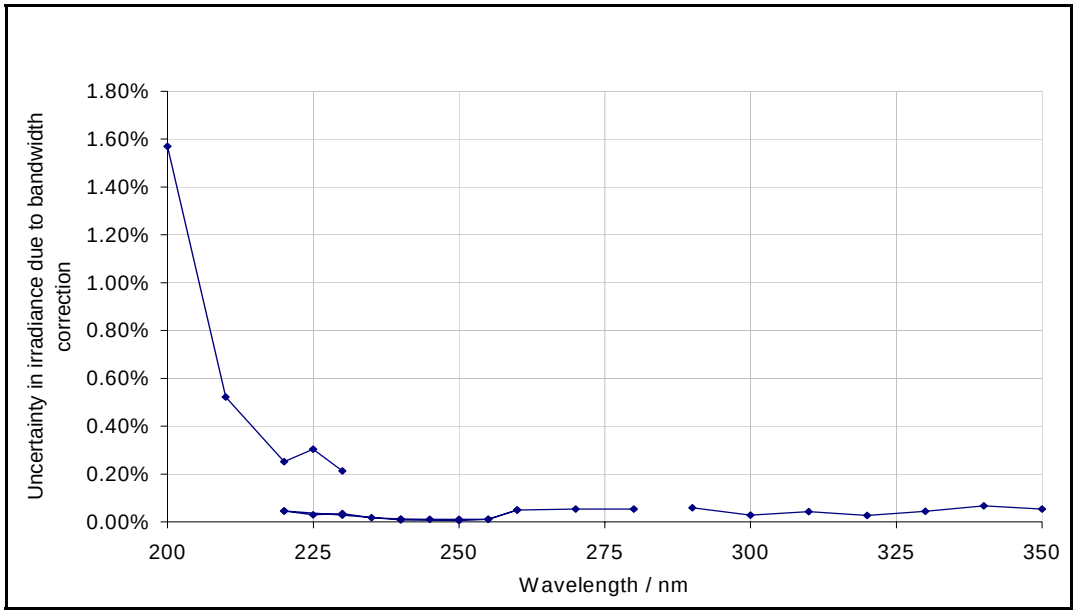

Figure 5.9 Uncertainty due to bandwidth correction (the correction itself is Figure 5.4)

This uncertainty has been tested by comparing measurements made with the monochromator using different slit widths. The measurements disagreed before the bandwidth correction was applied, but after correction agreed within the appropriate uncertainties.

5.5.6 Uncertainty associated with the overlap correction

The tile measurements in regions 1 and 2 must be corrected to overlap with the sphere measurements in regions 3 and 4. This is performed using the equations in section 5.4.2.1. Because this overlap is made, the systematic uncertainty associated with regions 1 and 2, due, for example to detector linearity, will not matter, except that because it is the same uncertainty associated with region 3 it will be reintroduced as the systematic component of the correction uncertainty[1].

In addition to this systematic uncertainty, there is a random component to the uncertainty. If the raw measurements are very noisy, then the correction will be less accurate. However, if some points are noisier than others, then the weight will have reduced their effect anyway. So, this has to be calculated to account for both these effects.

The uncertainty used was based on the comparison lamp DLS-NPL-L#01 and the measurements of it during the first round. Using the same notation as in section 5.4.2.1, the uncertainty due to noise in β can be calculated from:

$$u^2(\beta) = \sum \left[\left(\frac{C_i}{B_i} - \beta \right) \omega_i \right]^2 \qquad (5.26)$$

The uncertainty associated with α is similar, but the uncertainty associated with the A to C correction must add the β and α uncertainties in quadrature. This was done for the three calibrations of the comparison lamp DLS-NPL-L#01 in the first round and from these an overall uncertainty of 2.01% for the region 1 to region 3 correction and 1.94% for the region 2 to region 3 correction was deduced and applied to all calibrations of all lamps.

5.6 Overall Uncertainty associated with Lamp Irradiance

5.6.1 Single lamp calibration

The standard uncertainty (66% confidence) for a single calibration of a lamp can be obtained by combining in quadrature the uncertainties discussed in section 5.5. This is shown in Figure 5.10. This figure includes lines for each region, as listed in Table 5.2, which is why there is more than one value for some wavelengths. The final lamp results were calculated by combining the measurements from different regions using a weighted average. Because the average is weighted, the uncertainty will approach that of the lower uncertainty measurement at each wavelength.

[1] Of course if the systematic component was different in region 3 from region 2 it would be the region 3 uncertainty that would matter here.

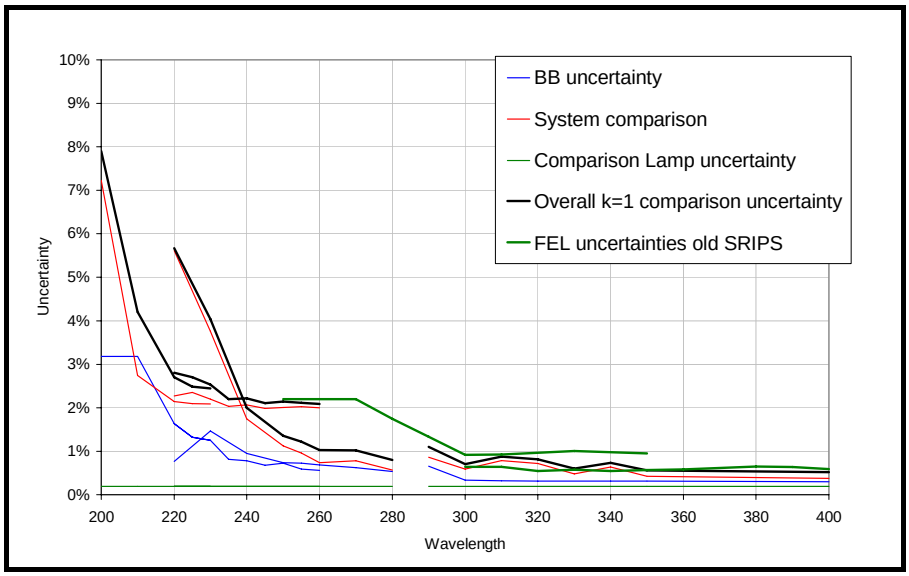

Figure 5.10 Overall k=1 uncertainty for a single measurement of a comparison lamp

5.6.2 Increased uncertainty in 270 nm to 310 nm region

As part of this comparison, the lamps were measured by NPL on two occasions. In most regions the repeatability of the lamps was exactly as statistically expected due to the calibration uncertainties. However, in the 270 nm to 310 nm region, the repeatability was noticeably larger than the uncertainty. A series of investigations were carried out but failed to identify a clear cause of this change.

NPL made the measurements to transfer the 2003 scale[2] down to 200 nm and to realise this scale on primary standard deuterium lamps at the same time as the lamps for this comparison were measured. With these 'scale' lamps, it was possible to compare the 2003 (blackbody based) scale with the scale that had previously been disseminated to customers, which was based relatively on synchrotron radiation (in the region 200 nm to 350 nm). The difference between the 'old' and 'new' scales was spectrally flat at approximately 4 % over the range from 200 nm to 350 nm, apart from in the region from 270 nm to 310 nm, where there was a distinct spectral feature.

This problem was only fully appreciated after the SRIPS facility was temporarily decommissioned to allow the software and hardware, such as the stage controllers, to be upgraded. Because the SRIPS facility has not been in operation since then, it has not been possible to investigate this error experimentally.

However, measurements on the dissemination facility to compare the deuterium lamps against FEL lamps, which hold the 2003 scale down to 250 nm, show the same feature. In addition, this is the spectral region in which a change was observed between the round 1 and round 2 values on SRIPS for this comparison. Therefore an assumption has been made that there was an error on the SRIPS facility that affected the calibration of a deuterium lamp against the spectrally very different blackbody.

NPL therefore took the decision to change the values of the 'scale' lamps for the dissemination of our scale to our customers. The 'scale' lamp values were adjusted, in the region from 270 nm to 310 nm, to ensure that the 4 % spectrally flat variation seen across most of the UV when comparing the 'new' (2003) scale with the 'old' scale applied to this central region as well. In other words, the

[2] NPL's primary spectral irradiance scale as realised on FEL lamps in the region from 250 nm to 2500 nm became our disseminated scale in May 2003, and is thus known as the 2003 scale.

'old' scale values, normalised to the 2003 scale at shorter and longer wavelengths, were used in the region from 270 nm to 310 nm. The uncertainty of this process was estimated pessimistically. The adjusted scale in this region is hereafter referred to as the 2003 scale and is the scale disseminated to customers.

Because during the first round of the comparison the 'scale' lamps were measured simultaneously with the comparison lamps, it was possible to treat the first round measurements, in the region 270 nm to 310 nm, as a calibration of the comparison lamps against the adjusted 'scale' lamp values i.e. the 2003 scale values.

This procedure was also used in the second round, although here the 'scale' lamps were measured immediately following the comparison lamps, rather than at the same time. Thus the average difference between the values measured on SRIPS against the blackbody in the second round for the scale lamps and the 2003 scale values for these lamps was applied to all the second round comparison lamp measurements.

These corrected values have been given in this report, and it should be re-emphasised that these corrected values are based on the scale NPL is currently disseminating to its customers. The uncertainties associated with first round spectral irradiance measurements in the 270 nm to 310 nm region are based on the uncertainty associated with the scale lamps and the uncertainty associated with the transfer from the scale lamps to the comparison lamps. The uncertainties associated with the second round have been estimated pessimistically, taking account of the adjustment made to the measured values.

5.6.3 Multiple calibrations of a lamp

Table 5.4 Uncertainty components split between correlated and uncorrelated

Correlated Effects	Uncorrelated Effects
Blackbody temperature	Measurement noise/repeatability
Blackbody emissivity	Overlap random effects
Original measurement of blackbody absorption	Day-to-day variability of blackbody absorption
Linearity	Lamp alignment
Geometry mismatch	Lamp daily stability
Bandwidth	Lamp stability between switch-ons
Wavelength error	
Systematic overlap correction	

The three calibrations of the lamp were combined using a simple average. The uncertainty on this average will be better than the uncertainty of the individual calibration because of the process of averaging. However this improvement will only affect the uncertainties associated with effects that are uncorrelated from one measurement to the next. These uncertainties can be reduced by $\sqrt{3}$, but the correlated uncertainties will remain unchanged. The correlated and uncorrelated effects are shown in Table 5.4.

5.6.4 Overall uncertainties submitted

The uncertainties have originally been calculated for one measurement of the lamp in each region independently. These uncertainties are shown in Table 5.5. Those uncertainties highlighted are reduced by $\sqrt{3}$ when combining three measurements of the lamp. Certain components within the blackbody radiance can also be reduced.

Table 5.5 Overall uncertainty components that make up the submitted uncertainties.
"Blackbody radiance" includes blackbody temperature (see Table 5.3), blackbody absorption, blackbody emissivity and blackbody–integrating sphere geometry. All uncertainties are standard uncertainties,

Wavelength, /nm	Blackbody radiance	Linearity of system	Geometry match	Bandwidth	Wavelength accuracy	Noise	Overlap systematic	Overlap random	Lamp alignment	Lamp stability during day	Lamp stability from on to on	270 - 310 nm extra round 1
200	3.19%			1.57%	0.62%	6.08%	0.22%	2.01%	0.19%	0.04%	0.23%	
210	3.18%			0.52%	0.21%	1.71%	0.22%	2.01%	0.19%	0.04%	0.23%	
220	1.64%			0.25%	0.29%	0.60%	0.22%	2.01%	0.19%	0.04%	0.23%	
225	1.32%			0.30%	0.30%	0.34%	0.22%	2.01%	0.19%	0.04%	0.23%	
230	1.26%			0.03%	0.33%	0.94%	0.22%	1.94%	0.19%	0.04%	0.23%	
235	0.82%			0.02%	0.30%	0.46%	0.22%	1.94%	0.19%	0.04%	0.23%	
240	0.78%			0.01%	0.30%	0.62%	0.22%	1.94%	0.19%	0.04%	0.23%	
245	0.68%			0.01%	0.31%	0.19%	0.22%	1.94%	0.19%	0.04%	0.23%	
250	0.74%	0.10%	0.20%	0.00%	0.23%	1.07%			0.19%	0.04%	0.23%	
255	0.73%	0.10%	0.20%	0.01%	0.31%	0.88%			0.19%	0.04%	0.23%	
260	0.69%	0.10%	0.20%	0.05%	0.28%	0.64%			0.19%	0.04%	0.23%	
270	See Table 5.6 and Table 5.7											
280												
290												
300												
310												
320	0.33%	0.10%	0.20%	0.03%	0.24%	0.64%			0.19%	0.04%	0.23%	
330	0.32%	0.10%	0.20%	0.04%	0.21%	0.36%			0.19%	0.04%	0.23%	
340	0.32%	0.10%	0.20%	0.07%	0.21%	0.55%			0.19%	0.04%	0.23%	
350	0.32%	0.10%	0.20%	0.05%	0.08%	0.35%			0.19%	0.04%	0.23%	
400	0.31%	0.10%	0.20%	0.10%	0.20%	0.20%			0.19%	0.04%	0.23%	

Those uncertainties highlighted are reduced by $\sqrt{3}$ when combining three measurements of the lamp.

In the corrected region (270-310 nm) the uncertainties in Round 1 are dominated by the scale lamp uncertainties, Round 1 uncertainties are given in Table 5.6.

Table 5.6 Overall uncertainty components that make up the submitted uncertainties, round 1.
All uncertainties are standard uncertainties, k=1.

Wavelength, /nm	Irradiance scale correlated	Irradiance scale uncorrelated	Wavelength accuracy	Noise	Alignment scale	Electrical scale	Alignment comp	Electrical comp
270	0.86%	1.75%	0.10%	0.71%	0.21%	1.60%	0.19%	0.23%
280	0.98%	1.66%	0.10%	0.45%	0.21%	1.60%	0.19%	0.23%
290	1.45%	1.78%	0.10%	0.79%	0.21%	1.60%	0.19%	0.23%
300	0.89%	1.66%	0.10%	0.47%	0.21%	1.60%	0.19%	0.23%
310	0.68%	1.75%	0.10%	0.72%	0.21%	1.60%	0.19%	0.23%

Those uncertainties highlighted are reduced by $\sqrt{3}$ when combining three measurements of the lamp.

In Round 2, the uncertainties are based on the blackbody measurements, with an additional uncertainty introduced for the correction; these uncertainties are given in Table 5.7.

Table 5.7 Overall uncertainty components that make up the submitted uncertainties, round 2.
"Blackbody radiance" includes blackbody temperature (see Table 5.3), blackbody absorption, blackbody emissivity and blackbody–integrating sphere geometry. All uncertainties are standard uncertainties, k=1.

Wavelength, /nm	Blackbody radiance	Linearity of system	Geometry match	Bandwidth	Wavelength accuracy	Noise	Lamp alignment	Lamp stability during day	Lamp stability from on to on	Additional correction uncertainty
270	0.62%	0.10%	0.20%	0.05%	0.24%	0.71%	0.19%	0.04%	0.23%	0.23%
280	0.53%	0.10%	0.20%	0.05%	0.27%	0.45%	0.19%	0.04%	0.23%	1.50%
290	0.66%	0.10%	0.20%	0.06%	0.25%	0.79%	0.19%	0.04%	0.23%	1.80%
300	0.34%	0.10%	0.20%	0.03%	0.27%	0.47%	0.19%	0.04%	0.23%	0.90%
310	0.32%	0.10%	0.20%	0.04%	0.25%	0.72%	0.19%	0.04%	0.23%	0.18%

Those uncertainties highlighted are reduced by $\sqrt{3}$ when combining three measurements of the lamp.

The results submitted for this comparison combine measurements made in different spectral regions, and combine three measurements of each lamp, thus reducing the uncertainties highlighted in Table 5.5, Table 5.6 and Table 5.7. The overall standard uncertainties have been split into those fully correlated between measurements of different lamps in both rounds, those correlated within the round, but not between rounds, and those fully uncorrelated between lamps. This combination is shown in Table 5.8.

Table 5.8 Uncertainties combined for three measurements of the lamp

Wavelength, /nm	Fully correlated	Correlated round 1	Correlated round 2	Fully uncorrelated round 1	Fully uncorrelated round 2
200	2.28%			4.04%	4.04%
210	1.63%			2.23%	2.23%
220	0.76%			1.50%	1.50%
225	0.74%			1.37%	1.37%
230	0.60%			1.43%	1.43%
235	0.57%			1.23%	1.23%
240	0.56%			1.25%	1.25%
245	0.56%			1.18%	1.18%
250	0.76%			0.66%	0.66%
255	0.78%			0.55%	0.55%
260	0.74%			0.43%	0.43%
270	0.00%	0.87%	0.72%	1.45%	0.46%
280	0.00%	0.98%	1.63%	1.37%	0.32%
290	0.00%	1.45%	1.94%	1.47%	0.49%
300	0.00%	0.89%	1.02%	1.38%	0.33%
310	0.00%	0.69%	0.49%	1.45%	0.45%
320	0.45%			0.41%	0.41%
330	0.43%			0.28%	0.28%
340	0.42%			0.37%	0.37%
350	0.37%			0.28%	0.28%
400	0.40%			0.23%	0.23%

5.7 References

[1] E. R. Woolliams, N. J. Harrison, B.B. Khlevnoy, L.J. Rogers, N.P. Fox, *Realisation and dissemination of spectral irradiance at NPL*. UV News, 7, 2002, pp 39-42

[2] P. Sperfeld, S. Galal Yousef, J. Metzdorf, B. Nawo, W. Möller, *The use of self-consistent calibrations to recover absorption bands in the black-body spectrum*. Metrologia, 37(5), 2000, pp. 373-376

[3] N.P. Fox, J. E. Martin, D. H. Nettleton, *Absolute spectral radiometric determination of the thermodynamic temperatures of the melting/freezing points of gold, silver and aluminium*, Metrologia, 28, 1991, pp 357-374

[4] V. E. Anderson, N. P. Fox, D. H. Nettleton, *Highly stable, monochromatic and tunable optical radiation source and its application to high accuracy spectrophotometry*, Applied Optics, 31(4), 1992, pp 536-545

[5] M. G. Cox,P. M. Harris,P. D. Kenward, E. R. Woolliams, *Spectral characteristic modelling*, NPL Report CMSC 27/03. Available at:www.npl.co.uk/ssfm/download/

[6] *The identification of molecular Spectra*. Third Edition, R.W.B Pearse and A.G.Gaydon. Chapman and Hall Ltd. 1965

[7] Guide to the Expression of Uncertainty in Measurement, Geneva, International Organization for Standardization, 1993

[8] M. G Cox, PM Dainton, PM Harris, Software Support for Metrology, Best Practice Guide No. 6: Uncertainty and statistical modelling", March 2001, available at: www.npl.co.uk/ssfm/download/

[9] E.R. Woolliams, D.F. Pollard, N.J. Harrison, E. Theocharous and N.P. Fox, New facility for the high-accuracy measurement of lens transmission. Metrologia, 37(5), 2000, pp 603-605

5.8 Results

5.8.1 Deuterium Lamp systems used

The following components were used by NPL during the intercomparison:

Power supply: DLS-NPL-PS

Monitor detector: DLS-NPL-MD

Lamps: DLS-NPL-L#01, DLS-NPL-L#02, DLS-NPL-L#03, DLS-NPL-L#04

If necessary the power supply has been switched between the primary voltage settings that are common in the different countries.

5.8.2 Lamp system electrical stability

The Deuterium Lamp systems were operated at 0.2997A, the average lamp voltages measured were:

Table 5.9 Average Lamp voltages for the different NPL lamp systems

Lamp	PTB round 1	Participant round 1	PTB round 2	Participant round 2
DLS-NPL-L#01	77,55 V	77,59 V	77,64 V	77,61 V
DLS-NPL-L#02	75,55 V	75,48 V	75,63 V	75,63 V
DLS-NPL-L#03	76,45 V	76,68 V	76,71 V	76,75 V
DLS-NPL-L#03	71,71 V	71,77 V	71,85 V	72,03 V

5.8.3 Numerical results

NPL measured all four lamp systems for the intercomparison. The results for the mean of the spectral irradiance of each lamp in each measurement round are given in the following tables. λ represents the wavelength in nm, $E(\lambda)$ stands for the spectral irradiance in $W \cdot m^{-2} \cdot nm^{-1}$ and $u(E)$ is the combined relative standard uncertainty for the measurement as reported by the participant. In the case that the participant reported spectral irradiance values for each single measurement of one round, the average calculated by the pilot is shown in Table 5.10.

5.8.4 Repeatability between measurement rounds

With the results reported in 5.8.3 the repeatability of the measurements of each lamp system between each round was calculated. The difference from round 2 to round 1 as shown in Figure 5.11 might indicate outliers or a high drift of a single lamp.

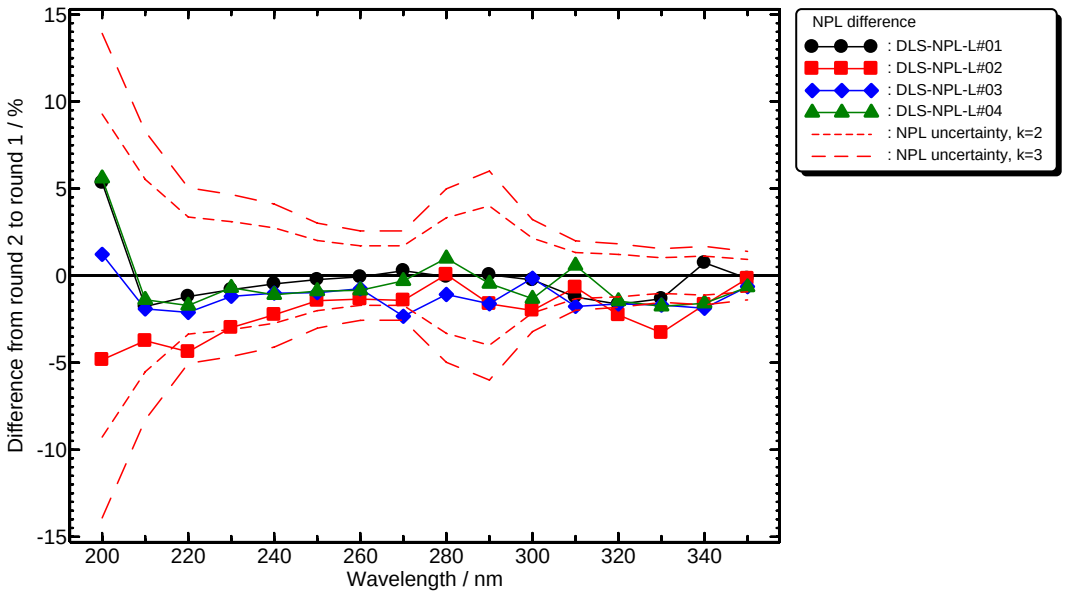

Figure 5.11 Repeatability between the measurement rounds calculated from the NPL data. The lines indicate the expanded measurement uncertainties for k = 2 and k = 3.

All participants' lamps were calibrated in one group during the two measurement campaigns at the PTB. Therefore the PTB could assign a spectral irradiance distribution for each participant's lamps. The repeatability of these measurements is shown in Figure 5.12. In combination with the participant's outcome these results can support the indication of an exceptional drift of a lamp

system. Nevertheless, the PTB calibrations are only an additional indication for the participant's lamp stabilities (see also section 9.1.2)

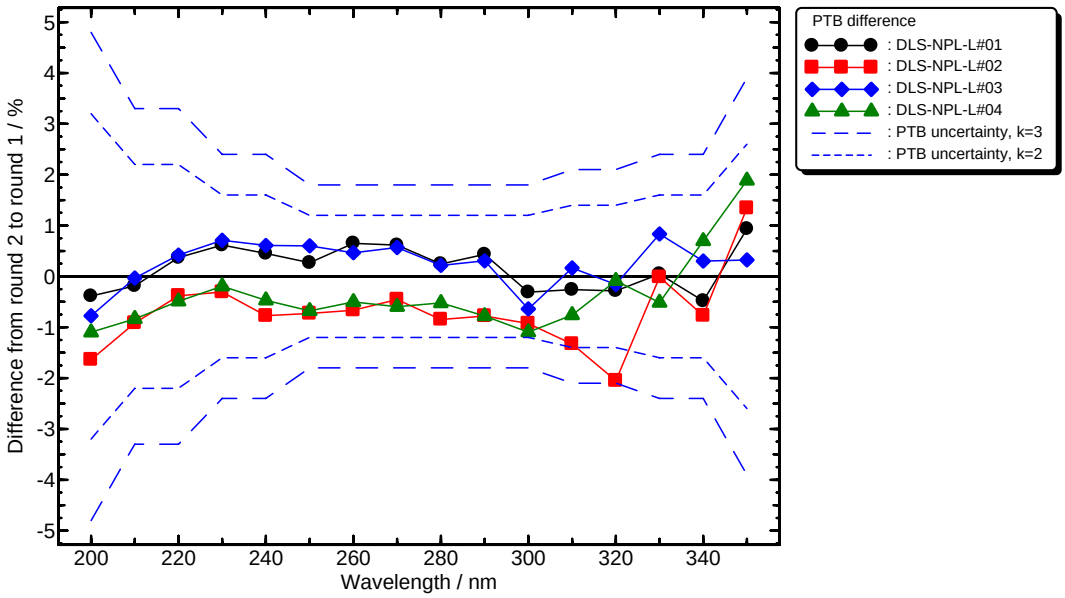

Figure 5.12 Repeatability between the measurement rounds calculated from PTB data.
The lines indicate the expanded measurement uncertainties for k = 2 and k = 3.

5.8.5 Normalized inner consistency of participants measurements

Additionally the inner consistency of the spectral irradiance calibrations of the lamps as described in section 9.1.2 was calculated (see equation (9.4)). It has to be pointed out, however, that the results presented here allow no conclusion of the absolute difference between participant and PTB.

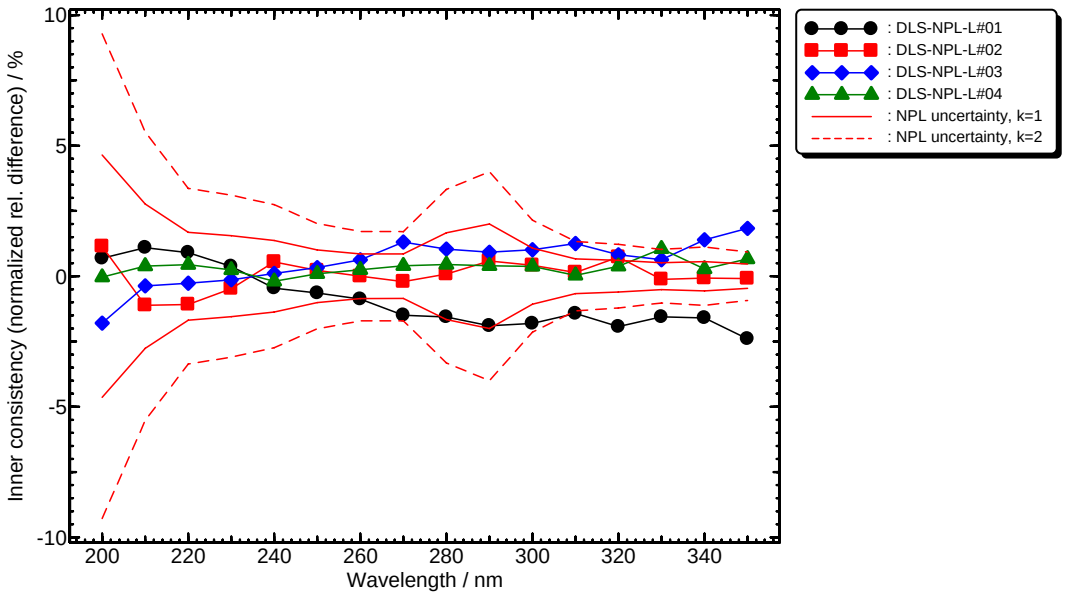

Figure 5.13 Normalized inner consistency of the NPL result compared to that of the PTB.
The lines indicate the expanded measurement uncertainties for k = 1 and k = 2.

5.8.6 Acceptance of measurements

The results presented in this section indicate that all measurement results of all lamps during both measurement rounds at NPL can be used and that no data should be rejected.

Table 5.10 Results for the lamp systems calibrated by NPL

	DLS-NPL-L#01		DLS-NPL-L#02		DLS-NPL-L#03		DLS-NPL-L#04		
	Round 1	Round 2	Round 1	Round 2	Round 1	Round 2	Round 1	Round 2	Uncertainty
λ	$E(\lambda)$	$E(\lambda)$	$E(\lambda)$	$E(\lambda)$	$E(\lambda)$	$E(\lambda)$	$E(\lambda)$	$E(\lambda)$	$u(E)$
[nm]	[W m^{-2}nm^{-1}]	[W m^{-2}nm^{-1}]	[W m^{-2}nm^{-1}]	[W m^{-2}nm^{-1}]	[W m^{-2}nm^{-1}]	[W m^{-2}nm^{-1}]	[W m^{-2}nm^{-1}]	[W m^{-2}nm^{-1}]	[%]
200	0,001178	0,001241	0,001387	0,00132	0,000886	0,0008968	0,001185	0,001252	4,6
210	0,001125	0,001105	0,001284	0,001236	0,000911	0,0008936	0,001174	0,001158	2,8
220	0,001035	0,001023	0,001214	0,001161	0,0009008	0,0008817	0,001113	0,001094	1,7
230	0,0009077	0,0009004	0,001085	0,001052	0,0008386	0,0008286	0,0009913	0,0009844	1,6
240	0,0007839	0,0007802	0,0009524	0,000931	0,0007595	0,0007519	0,0008656	0,0008561	1,4
250	0,0006693	0,0006678	0,00081	0,0007984	0,0006705	0,000664	0,0007433	0,0007368	1,0
260	0,0005702	0,0005698	0,000684	0,0006747	0,000584	0,0005796	0,0006325	0,0006272	0,9
270	0,0004813	0,0004826	0,0005738	0,0005657	0,0005091	0,0004972	0,0005322	0,0005306	1,3
280	0,0004071	0,0004069	0,0004738	0,000474	0,0004283	0,0004237	0,0004421	0,0004465	1,7
290	0,0003469	0,000347	0,0004035	0,0003969	0,0003694	0,0003634	0,0003748	0,0003731	2,1
300	0,0003017	0,000301	0,0003469	0,0003399	0,0003194	0,0003189	0,0003241	0,0003198	1,4
310	0,0002685	0,0002651	0,0002966	0,0002946	0,0002847	0,0002797	0,0002786	0,0002802	1,2
320	0,0002343	0,0002304	0,0002589	0,000253	0,0002489	0,0002449	0,0002456	0,0002421	0,6
330	0,0002056	0,0002029	0,000228	0,0002205	0,0002207	0,000217	0,0002162	0,0002124	0,5
340	0,00018	0,0001813	0,0001973	0,000194	0,0001951	0,0001915	0,0001896	0,0001865	0,6
350	0,0001586	0,0001583	0,000174	0,0001737	0,000171	0,0001699	0,0001659	0,0001649	0,5

6 NRC

NRC report to CCPR Key Comparison K1.b
Spectral Irradiance 200 nm to 350 nm

2005-February-28

A.A. Gaertner

Institute for National Measurement Standards

National Research Council of Canada

Ottawa, Ontario, Canada K1A 0R6

6.1 Introduction:

This report describes the NRC measurements of spectral irradiance for the four CCPR transfer lamps used for the NRC-INMS participation in the CCPR Key Comparison K1b of spectral irradiance in the wavelength range from 200 nm to 350 nm. The four lamps were deuterium lamps, selected, characterized, and mounted in a special lamp housing by the PTB, as described in the protocol for the intercomparison [1] and in Appendix A. The lamps were identified as:

DLS-NRC-L#01

DLS-NRC-L#02

DLS-NRC-L#03

DLS-NRC-L#04.

The lamp power supply was identified as DLS-NRC-PS.

The lamp monitor detector was identified as DLS-NRC-MD, with power supply DLS-NRC-PM.

6.2 Logistics

Phase 1:

The four lamp assemblies together with power supply and monitor detector were received 2003-October-07 from PTB by airfreight in two cartons.

The lamps were each measured on four different occasions on 2003-December-23 and 2004-January-06 to 08.

Phase 2:

The four lamp assemblies together with power supply and monitor detector were returned on 2004-January-13 by airfreight to PTB for the second phase of the CCPR comparison.

The four lamp assemblies together with power supply and monitor detector were received 2004-June-16 from PTB by airfreight in two cartons.

The four lamps were each measured on three different occasions on 2004-September-08 to 10.

6.3 NRC Lamp Standards

Two deuterium lamps, with the NIST type of bi-pin mounting socket, were used for calibrating the NRC spectroradiometer. The alignment of these lamps was done using the NIST type of alignment jig. The lamps are identified as NBS YE987 and NIST RC0864.

NBS YE987 is a Hamamatsu type L1128, operating at 300 ma, with the heater ON at 10V during warm-up (approximately 1 minute) and turned OFF during subsequent operation. It was allowed approximately 20 minutes to stabilise before measurements were taken. This lamp standard was purchased from NBS (now NIST) and received in 1982 with an NBS calibration from 200 nm to 350 nm at 10 nm intervals [2]]. The lamp had not been used since receipt until the measurements for this CCPR comparison.

NIST RC0864 is a Hamamatsu type L1627 (Super-Quiet Deuterium Lamp), operating at 300 ma, with the heater ON at 10V during warm-up (approximately 1 minute) and set to 7V during subsequent operation. It was allowed approximately 20 minutes to stabilise before measurements were taken. This lamp standard was purchased from NIST and received in 1994 with an NIST calibration from 200 nm to 400 nm at 10 nm intervals [3]. The lamp had not been used since receipt until the measurements for this CCPR comparison.

One FEL lamp, with the NIST type of bi-pin mounting socket, was used to check the operation of the above two deuterium lamps. The alignment of this lamp was done using the same NIST type of alignment jig as for the deuterium lamps. The lamp is identified as NBS F-176 and has an NBS calibration [4] for the wavelength region (250 nm $\leq \lambda \leq$ 1600 nm).

6.4 Measurement Facility

The input optical configuration to the monochromator used for the spectroradiometric measurements was different for each phase of the measurements. This difference was primarily used to determine any effects of stray light upon the measurements. A schematic of the measurement facility used for Phase 1 is given in Figure One, and in Figure Two for the measurements of Phase 2. The predominant difference between the two measurement configurations is the use of a flat diffuser and no prism predisperser on the input to the monochromator in Phase 1, and the use of a spherical diffuser and a prism predisperser in Phase 2.

6.4.1 Spectroradiometer:

The spectroradiometer is composed of the monochromator, the input optics, and the detectors.

6.4.1.1 Monochromator:

The monochromator was a GCA McPherson Model 2051, which is a 1-metre focal length grating instrument with a Czerny-Turner optical design. The grating used for these measurements was a 600 grooves*mm^{-1} ruled grating with a blaze at 200 nm and a coating of Al plus MgF_2.

Phase 1: The Prism Predisperser was not used for these measurements. It was considered that order sorting was not necessary for the wavelength region covered by this comparison, and we wished to obtain the largest signal size possible. The slit widths were adjusted to produce an optimum signal for the three types of spectral irradiance lamps to be used: the DLS lamps, the NRC deuterium lamp standards, and the NRC FEL lamp standards. The bandwidths used were triangular in shape (the input and output slits were set to be equal), with the Full Width at Half Maximum (FWHM) approximately 1.75 nm. The interior of the GCA-2051 was purged during all the measurements with a slight overpressure of air which had been cleaned of all water vapour and CO_2 using a Balston FT-IR Purge Gas Generator Model 75-62.

Phase 2: The GCA McPherson Model 608M1 (Suprasil) Prism Predisperser was used for these measurements. It was added for this phase of the measurements to determine the possible effects of stray light within the monochromator. The slit widths were adjusted to produce an optimum signal for the three types of spectral irradiance lamps to be used: the DLS lamps, the NRC deuterium lamp standards, and the NRC FEL lamp standards. The bandwidths used were triangular in shape (the input and output slits were set to be equal), with the Full Width at Half Maximum (FWHM) approximately 3.0 nm. The interior of the GCA-2051 was not purged for these measurements.

6.4.1.2 Monochromator Input Optics:

Phase 1: The input optics used to define the irradiance area measured, and couple this radiation to the monochromator, was a flat diffuser as shown in Figure One. The diffuser was formed of pressed polytetrafluorethylene (PTFE) with a final outside diameter of approximately 44 mm. The angle between the normal to the diffuser (set along the optical axis of the input lamp system) and the optical axis of the monochromator was 45 degrees as indicated in Figure One. The distance between the monochromator and the diffuser was set such that the input to the monochromator received light from an approximately square area, with sides of approximately 27 mm, centered on this diffuser.

Phase 2: The input optics used to define the irradiance area measured, and couple this radiation to the monochromator, was an integrating sphere as shown in Figure Two. The interior of the sphere was formed of pressed Halon (PTFE) with a final inside diameter of approximately 32 mm. The input port to the sphere was circular, 12 mm in diameter. This input port thus defines the region of the irradiance produced by the lamps which was measured. The output port of the sphere was rectangular in shape, design to provide optimum coupling to the input slits of the Predisperser unit. These two ports on the sphere are at 90 degrees to each other, so that region of the sphere wall seen by the monochromator does not overlap the region of the sphere wall irradiated by the input to the sphere. Note that the input port to this sphere defines the point from which the distance to the lamp filament must be measured.

There is also a small baffling unit attached to the input to this integrating sphere. The interior of this baffle unit is coated with black paint to reduce scattered light and the internal baffles are designed to reduce off-axis light which could enter the sphere. The smallest aperture in this baffle unit is an aperture of 26 mm diameter at approximately 60 mm from the input port. However, this aperture was not a limiting aperture of the input optics, as will be discussed in Section 5.1 describing the measurement configuration.

6.4.1.3 Detectors:

Two different detectors, both photomultipliers (PMTs), were used for these measurements. The two PMTs have a dissimilar spectral response that was useful in determining possible effects of stray light. As indicated in Figures One and Two, only the UV-PMT was used for the measurements of Phase 1, whereas both the VIS-PMT and the UV-PMT were used for the measurements of Phase 2.

UV-PMT: The photomultiplier used was an EMR Model 541F-09-17 operating at room temperature. This is an end-on solar-blind PMT with a MgF_2 window and a photocathode constructed from Cs_2Te which give a spectral response over a narrow UV wavelength range from 115 nm to 365 nm.

VIS-PMT: The photomultiplier used was a Hamamatsu Model R6872, cooled to approximately –12°C with a thermo-electric cooling unit. This is a side-on PMT with a quartz window and a multialkali photocathode which give a spectral response over a broad wavelength range from 185 nm to 900 nm.

6.4.2 Environmental Conditions:

The ambient temperature in the measurement laboratory was 23°C ± 1°C.

The relative humidity in the measurement laboratory was between approximately 5% and 10% for the Phase 1 measurements, and between approximately 35% and 40% for the Phase 2 measurements.

As indicated in Section 4.1.1, the monochromator, which is the greatest part of the optical path, was purged during the Phase 1 measurements.

6.5 Measurement Configuration:

6.5.1 Optical Configuration:

The basic optical configurations for the measurements are shown in Figures One and Two, which are approximately to scale.

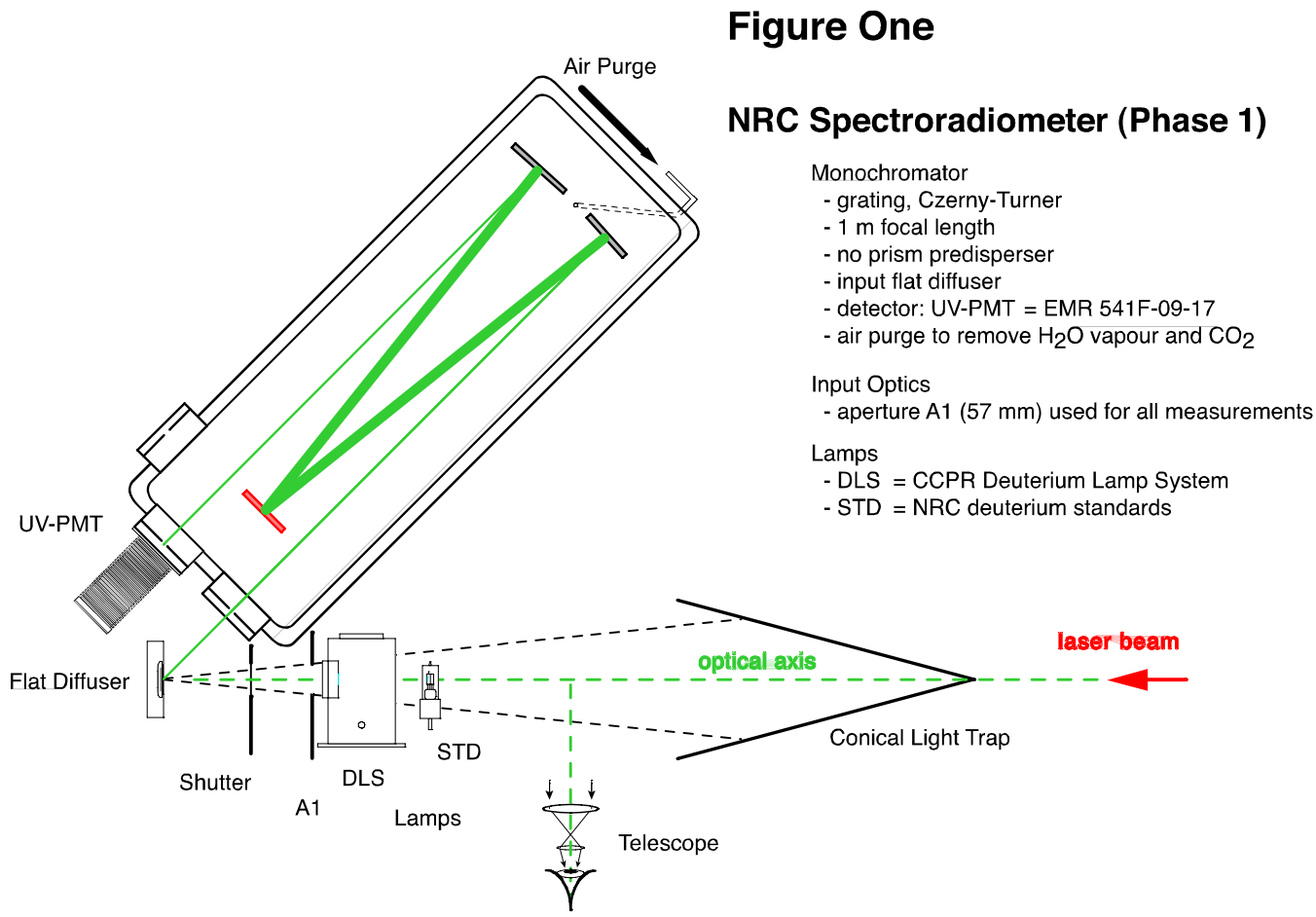

Figure 6.1 Schematic of the NRC Spectroradiometer (Phase 1)

The apertures A1 are sized and placed to limit the field-of-view (FOV) of the input diffuser (flat diffuser for Phase 1, sphere for Phase 2) to the desired portion of the NRC deuterium standard or NRC FEL standard lamp being measured. The aperture was left in place also during the measurements of the DLS lamps. It has no effect upon the measurements of the DLS lamps since it was very close to the DLS lamps and the aperture was larger than the output aperture of the DLS lamps.

The shutter was basically a moveable blade inside an aperture of diameter approximately 63 mm. It was placed close enough to the input diffuser (Phase 1) or the baffle system of the input sphere (Phase2) that it did not impinge on the FOV of any of the other apertures.

The conical light trap was placed 'behind' the lamps, as indicated in Figures One and Two, to enclose the entire FOV of the input diffuser as defined by the apertures A1. This was at approximately 1m from the diffuser for the NRC lamps (50 cm 'behind' the NRC lamps).

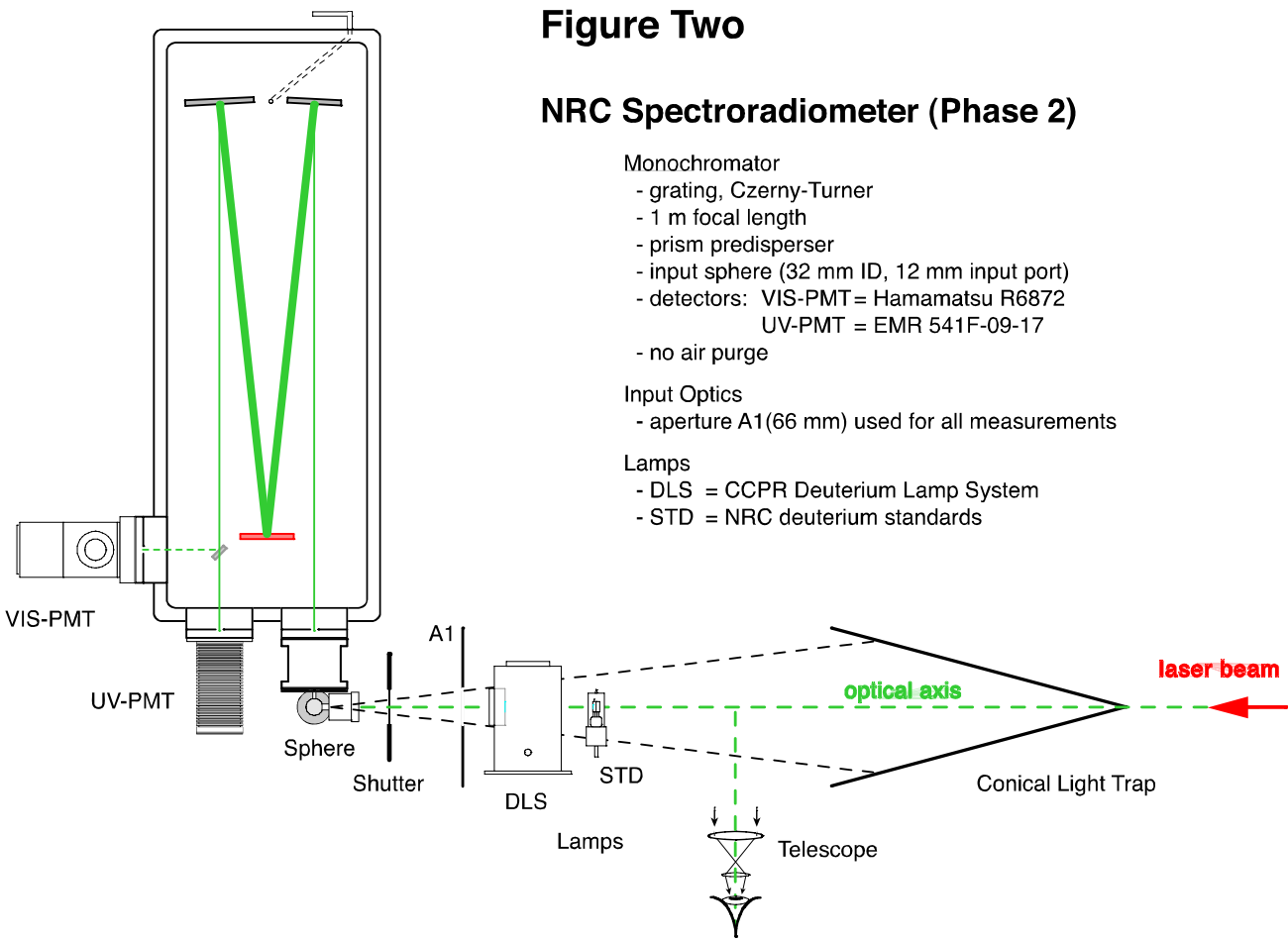

Figure 6.2 Schematic of the NRC Spectroradiometer (Phase 2)

The optical axis was set up using a laser beam placed 'behind' the light sources as indicated, and incident upon the input diffuser (flat diffuser for Phase 1, sphere for Phase 2). This beam was placed co-linear with the photometric bench upon which the shutter, apertures, lamps, and conical light trap were placed. The alignment of the monochromator and input diffuser was different for the two phases of measurement:

Phase 1: The flat diffuser could be replaced in its mount with a flat mirror. This allowed for standard procedures to be used to align the diffuser mount perpendicular to, and centered on, the optical axis, and to enable the monochromator to be aligned to this

axis at 45 degrees. The FOV of the monochromator at the flat diffuser could be checked using a white light shone into the output port of the monochromator and observing the region of the flat diffuser that was illuminated.

Phase 2: The input aperture plane of the monochromator input sphere was adjusted (by adjusting the position of the complete monochromator since the input sphere is firmly attached to the monochromator) such that the input aperture was centered on the optical axis and perpendicular to the optical axis.

A reference point for distance measurement along the optical axis was set using a telescope positioned as indicated. The axis of the telescope was set perpendicular to the optical axis and in a horizontal plane. The focal point of the telescope was set at the intersection of the telescope axis with the optical axis. The distance of this intersection from the input diffuser was set using calibrated length rods. This distance was approximately 70 cm between the surface of the flat diffuser and the telescope axis in Phase 1, and approximately 1.3 m between the input aperture (port) of the input sphere and the telescope axis in Phase 2. The distance of a lamp from the input diffuser could now be set by positioning the required point on the lamp at the telescope crosshair, and then moving the lamp mount assembly the required distance interval toward the input diffuser using the distance scale on the photometric bench. (The lamp mount assembly contains a crosshair indexed to the scale on the photometric bench.)

6.5.2 Lamp Configuration:

The NRC standard deuterium and FEL lamps were aligned to the optical axis using the NIST-style alignment jig to position the lamp socket at the correct angles and positions for measurement.

The necessity of aligning the DLS from the front required the use of a second laser beam. The position of the monochromator and detectors in the two Phases of measurements required a slightly different configuration for this second laser:

Phase 1: The flat diffuser and shutter were mounted such that they could be lowered out of the path of the two laser beams during the DLS alignment procedure. Therefore the second laser beam could be mounted exactly collinear with the original laser beam. This position is to the left side of Figure One. With each laser beam incident at the center of the output of the other laser, the two beams are collinear. This second beam could then be used for the alignment of the DLS using the procedure indicated in the protocol [1].

Phase 2: The position of the monochromator with the input sphere and UV-PMT did not allow the second laser to be placed directly opposite the original laser in this configuration. In this configuration, for the purpose of aligning the DLS, we inserted a mirror between the shutter and aperture A1, mounted the second laser off the optical axis (at the ‘bottom’ of Figure Two), and then adjusted the position of the second laser and the position of the mirror until each laser beam was incident at the center of the output of the other laser. As above, this second beam could then be used for the alignment of the DLS using the procedure indicated in the protocol [1].

The operation of the DLS lamps was performed using the electrical power supply, monitor detector, and procedures as indicated in the protocol [1]. We occasionally had problems in igniting the DLS lamps due to breaks in the electrical connections at the DLS housing.

6.5.3 Measurement Procedure:

The basic procedure used is a sequential method: Each lamp was measured completely through the entire wavelength range before installing another lamp onto the optical axis to repeat the process. Each lamp measurement was composed of a sequence of two or more complete scans through the wavelength range.

The spectroradiometer system was calibrated by measuring various sequences of the three NRC standard lamps (section 6.3 above) at the beginning and at the end of each measurement day. A typical measurement day for the Phase 2 measurements, which used two PMTs, is summarized in Table One. The arrows between columns indicate the time sequence for the measurements. The notation (180,360,10) indicates a measurement set from 180 nm to 360 nm with measurements every 10 nm. The CCPR Measurement Number is formed from PiMj, where i=1, or 2 for the measurement Phase number, and j=1 to 4 for the measurement number in the appropriate phase.

Table 6.1 Measurement sequence for typical Phase 2 measurement day.
The numbers given in the table are the number of repeat scans performed. All scans are (180,360,10) nm.

lamp	*detector*			*CCPR measurement number*
	UV-PMT		VIS-PMT	
NBS F-176	4	→	3	
NBS YE987	3	←	3	
DLS-NRC-L#01	3	←	3	P2M1
DLS-NRC-L#02	3	→	3	P2M1
DLS-NRC-L#03	3	←	3	P2M1
DLS-NRC-L#04	3	→	3	P2M1
NIST RC0864	3	→	3	

A summary of all the measurements for this CCPR K1b comparison is given in Table 6.2. A record of the lamp burn hours for the CCPR DLS lamps is presented in the accompanying WORD document NRCLampHours2.doc (similar to Table A.6 of the protocol [1]). A record of the CCPR DLS lamp measurement summary including the monitor detector readings (similar to Table A.1 of the protocol [1]) is given in the accompanying EXCEL dataset NRCMeasSummary.xls.

Table 6.2 Summary of CCPR K1b lamp measurements.

date	*lamp measurement sequence*
Phase 1	
2003-December-23 (P1M1)	NBS YE987, NBS F-176, DLS-NRC-L02, -L03, -L04, -L01, NIST RC0864, NBS YE987, NBS F-176
2004-January-06 (P1M2)	NBS YE987, NBS F-176, DLS-NRC-L01, -L02, -L03, -L04, NIST RC0864, NBS YE987, NBS F-176
2004-January-07 (P1M3)	NIST RC0864, NBS F-176, DLS-NRC-L03, -L01, -L04, -L02, NBS YE987, NIST RC0864, NBS F-176
2004-January-08 (P1M4)	NBS YE987, DLS-NRC-L04, -L03, -L02, -L01, NIST RC0864, NBS YE987, NBS F-176
Phase 2	
2004-September-08 (P2M1)	NBS F-176, NBS YE987, DLS-NRC-L01, -L02, -L03, -L04, NIST RC0864
2004-September-09 (P2M2)	NBS F-176, NIST RC0864, DLS-NRC-L04, -L02, -L03, -L01, NBS YE987
2004-September-10 (P2M3)	NIST RC0864, DLS-NRC-L03, -L01, -L04, -L02, NBS YE987, NBS F-176

6.6 Data Analysis:

6.6.1 Calibration of the spectroradiometer:

The measurement procedure used enables the determination of a spectroradiometer calibration factor obtained from the measurements of the lamps used as standards. The units of the spectroradiometer calibration factor would be *spectral irradiance / signal voltage* for the particular spectroradiometer configuration in use.

As indicated in Section 3 above, two calibrated deuterium lamps were used during these measurements. In both Phases of the comparison, and over the several days of measurements for each Phase, it was found that the spectroradiometer calibration factors provided by these two deuterium lamps were in agreement within the calibration uncertainties of the lamps. Since the calibration for the deuterium lamp NBS YE987 was an older calibration with considerably larger uncertainties, it was decided that only the calibration provided by the deuterium lamp NIST RC0864 would be used to determine the final calibration values for the DLS comparison lamps. It was also observed that in the region where the spectral irradiance of the FEL lamp NBS F-176 and the deuterium lamps were approximately equal, the spectroradiometer calibration factors were also within the estimated uncertainties. Therefore the standard deuterium lamps were assumed to be reproducing their calibration values.

The particular spectroradiometer calibration factor used for the final determination of the spectral irradiances of the comparison DLS lamps was slightly different between the two Phases of the comparison:

Phase 1: It was observed that the spectroradiometer calibration factor for each day of the 4 days used to make measurements varied from day to day. Therefore, the spectroradiometer calibration factor used was different for each day.

Phase 2: It was observed for these three days that the spectroradiometer calibration factor remained stable enough over the three days that a 3-day average spectroradiometer calibration factor was used for the measurements of the DLS lamps.

6.6.2 Measurement Results:

The calibration values for the CCPR DLS lamps are simply determined as the product of the spectroradiometer calibration factor and the signal voltage measured for the particular DLS lamp in the appropriate measurement configuration. The resulting data for the four DLS lamps, for each of the measurements made during each Phase is presented in the accompanying Excel workbook CCPRK1bNRC.xls.

The Phase 1 measurements are for an average of the three scans of each DLS lamp made at each lighting of the lamp. The Phase 2 measurements were composed of 3 scans for each of the two detectors used. The weighted average of the resulting 6 values for the spectral irradiance was used for the final spectral irradiance value.

6.6.3 Uncertainties:

The estimated uncertainties for the measurements are also presented in the Excel workbook CCPRK1bNRC.xls. All uncertainties are given as fractional uncertainties and as one standard deviation (coverage factor k=1). The following uncertainties are presented:

Calibration of Standard Lamps:

This is the uncertainty in the calibration of the NRC lamps we used as our standards for the calibration of the spectroradiometer. As indicated in Section 6.1 above this was the one lamp NIST RC0864. The uncertainties used are taken from the calibration report [3] of this lamp.

Calibration of Spectroradiometer:

The method of determining the calibration factor for the spectroradiometer was presented above in Section 6.1. This method of determining the uncertainties for the calibration of the spectroradiometer takes account of the behaviour of the complete system: the lamp stabilities, the lamp remount/realignment variation, any monochromator drift, and the noise in the detector signals. The uncertainties presented are the standard deviation of the calibration datasets (all the repeat measurements and the re-mount measurements performed with the standard lamp), rather than the standard deviation of the mean. Since only one standard lamp was used as a sample of the primary scale, and there are several different variables accounted for (as indicated above), I have chosen to leave the uncertainties as those of the sample, rather than the mean. For Phase 1, where a daily calibration factor was used, the uncertainties given are the standard deviation (EXCEL function STDEV) of the three to six repeat scans done when the standard lamp was measured. (On one day, 2004-January-07, the standard lamp was set up twice.) For Phase 2, where a 3-day calibration factor was used, the uncertainties given are a combination of the standard deviations of the nine scans done for each of the two detectors over the three days.

DLS Lamp Stability:

The uncertainties given are the standard deviation (EXCEL function STDEV) of the three repeat scans done when the lamp was measured.

Detector Linearity:

These figures are derived from measurements in our laboratory for the detectors used in these measurements. They represent upper limits of uncertainty which can be expected.

Distance:

The method of setting the lamp positions was described above in section 6.5. A maximum uncertainty of 0.5 mm is estimated in setting the position of the lamps. Measurements performed on two deuterium lamps, the NBS YE987 and another one of similar type, indicated that the variation of the lamp irradiance with distance (at the calibrated 50 cm distance) was approximately 50% greater than the inverse square law. This result was used to calculate the uncertainty given in the dataset.

Lamp Control:

The uncertainty of all the NRC components in determining the electrical parameters for the lamp control was less than 0.01%. We estimate that at maximum this would scale up to be less than the 0.1% given on the dataset.

Wavelength:

The wavelength accuracy of the monochromator was determined to be better than 0.05 nm. The reproducibility of the monochromator wavelength settings is approximately 0.005 nm. For the calibration of similar lamps as done in this comparison, it is the wavelength reproducibility which contributes the uncertainty due to wavelength uncertainty. The uncertainty expected from the reproducibility of this monochromator is negligible compared to the uncertainties which are already presented.

Stray Light:

Due to the large range of signal sizes over the spectrum of the lamps, stray light was of considerable concern. This was the reason for the different optical configurations between Phase 1 and Phase 2, and for the use of two quite different detectors in Phase 2. However, we found that the spectral irradiances of the DLS lamps determined in all three of these situations were in good agreement. Since we suspect that there is still some stray light, the agreement in our measurements indicates that the stray light has cancelled out due to our procedure which compares lamps with similar spectral content. I have therefore concluded that the contribution of stray light to our measurements is lower than the above uncertainties, and have not included a term due to this uncertainty.

Table 6.3 Uncertainties (fractional) for the lamp calibrations.

Wavelength	**Type:**	**B**	**A**	**A**	**B**	**B**	**B**	**Quadrature Sum**	
nm	**Source:**	**Calibration of Standard lamps**	**Calibration of SpectroRadiometer**	**DLS lamp Stability**	**Detector Linearity**	**Distance**	**Lamp Control**		
200		0,0250	6,549E-03	5,369E-03	0,0020	0,0030	0,0010	0,0267	2,7%
210		0,0250	3,863E-03	3,702E-03	0,0020	0,0030	0,0010	0,0258	2,6%
220		0,0228	3,734E-03	3,100E-03	0,0020	0,0030	0,0010	0,0236	2,4%
230		0,0205	3,345E-03	3,249E-03	0,0020	0,0030	0,0010	0,0214	2,1%
240		0,0183	3,933E-03	3,343E-03	0,0020	0,0030	0,0010	0,0193	1,9%
250		0,0160	2,918E-03	3,151E-03	0,0020	0,0030	0,0010	0,0170	1,7%
260		0,0160	2,649E-03	2,756E-03	0,0020	0,0030	0,0010	0,0169	1,7%
270		0,0160	3,653E-03	2,696E-03	0,0020	0,0030	0,0010	0,0170	1,7%
280		0,0160	3,562E-03	2,563E-03	0,0020	0,0030	0,0010	0,0170	1,7%
290		0,0160	3,789E-03	3,190E-03	0,0020	0,0030	0,0010	0,0172	1,7%
300		0,0160	4,021E-03	3,010E-03	0,0020	0,0030	0,0010	0,0172	1,7%
310		0,0160	4,082E-03	4,159E-03	0,0020	0,0030	0,0010	0,0174	1,7%
320		0,0160	5,222E-03	3,786E-03	0,0020	0,0030	0,0010	0,0177	1,8%
330		0,0160	7,367E-03	5,811E-03	0,0020	0,0030	0,0010	0,0189	1,9%
340		0,0160	1,046E-02	1,033E-02	0,0020	0,0030	0,0010	0,0220	2,2%
350		0,0155	1,962E-02	1,080E-02	0,0020	0,0030	0,0010	0,0274	2,7%

6.7 References

[1] CIPM Key Comparison K1.b, Spectral Irradiance 200 nm to 350 nm, Technical Protocol, 24 October 2003.

[2] NBS Report of Calibration of One Deuterium Lamp Standard of Spectral Irradiance, NBS Test No. 534/227786, dated March 18, 1982.

[3] NIST Report of Calibration, Spectral Irradiance of Deuterium Lamp for One Hamamatsu Deuterium Lamp Model # L1627, Serial # RC0864, NBS Test No. 844/253770-94, dated August 17, 1994.

[4] NBS Report of Calibration of One Standard of Spectral Irradiance, NBS Test Number 534/235034-85-1, dated June 6, 1985.

6.8 Results

6.8.1 Deuterium Lamp systems used

The following components were used by NRC during the intercomparison:

Power supply: DLS-NRC-PS

Monitor detector: DLS-NRC-MD

Lamps: DLS-NRC-L#01, DLS-NRC-L#02, DLS-NRC-L#03, DLS-NRC-L#04

If necessary the power supply has been switched between the primary voltage settings that are common in the different countries.

6.8.2 Lamp system electrical stability

The Deuterium Lamp systems were operated at 0.2995A, the average lamp voltages measured were:

Table 6.4 Average Lamp voltages for the different NRC lamp systems

Lamp	PTB round 1	Participant round 1	PTB round 2	Participant round 2
DLS-NRC-L#01	77,52 V	77,62 V	77,71 V	77,93 V
DLS-NRC-L#02	77,12 V	77,26 V	77,34 V	77,46 V
DLS-NRC-L#03	82,71 V	82,79 V	82,87 V	82,84 V
DLS-NRC-L#03	76,57 V	76,88 V	76,96 V	77,15 V

6.8.3 Numerical results

NRC measured all four lamp systems for the intercomparison. The results for the mean of the spectral irradiance of each lamp in each measurement round are given in the following tables. λ represents the wavelength in nm, $E(\lambda)$ stands for the spectral irradiance in $W \cdot m^{-2} \cdot nm^{-1}$ and $u(E)$ is the combined relative standard uncertainty for the measurement as reported by the participant. In the case that the participant reported spectral irradiance values for each single measurement of one round, the average calculated by the pilot is shown in Table 6.5.

6.8.4 Repeatability between measurement rounds

With the results reported the repeatability of the measurements of each lamp system between each round was calculated. The difference from round 2 to round 1 as shown in Figure 6.3 might indicate outliers or a high drift of a single lamp.

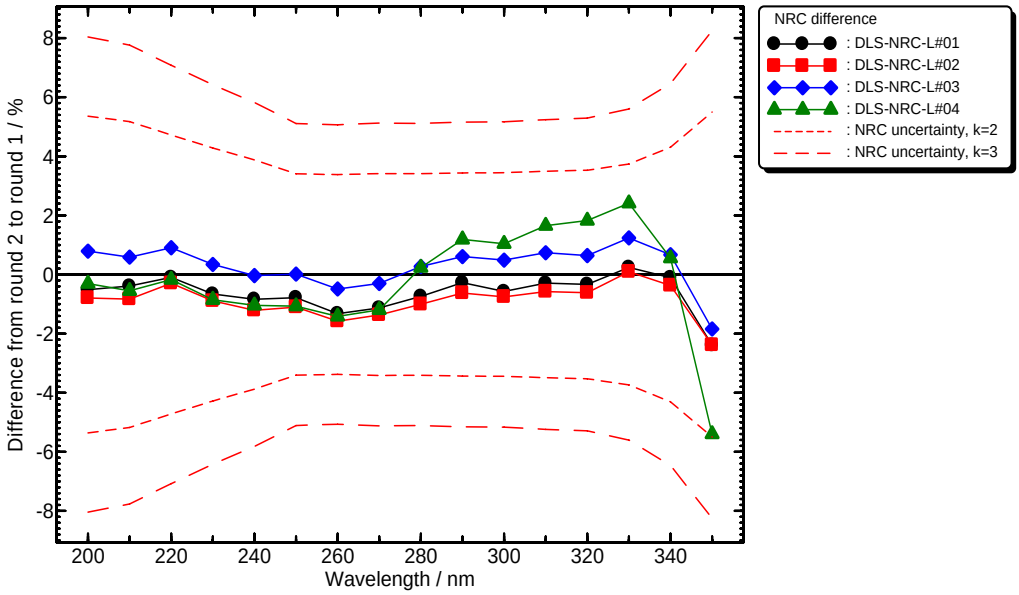

Figure 6.3 Repeatability between the measurement rounds calculated from the NRC data.
The lines indicate the expanded measurement uncertainties for k = 2 and k = 3.

All participants' lamps were calibrated in one group during the two measurement campaigns at the PTB. Therefore the PTB could assign a spectral irradiance distribution for each participant's lamps. The repeatability of these measurements is shown in Figure 6.4. In combination with the participant's outcome these results can support the indication of an exceptional drift of a lamp system. Nevertheless, the PTB calibrations are only an additional indication for the participant's lamp stabilities (see also section 9.1.2)

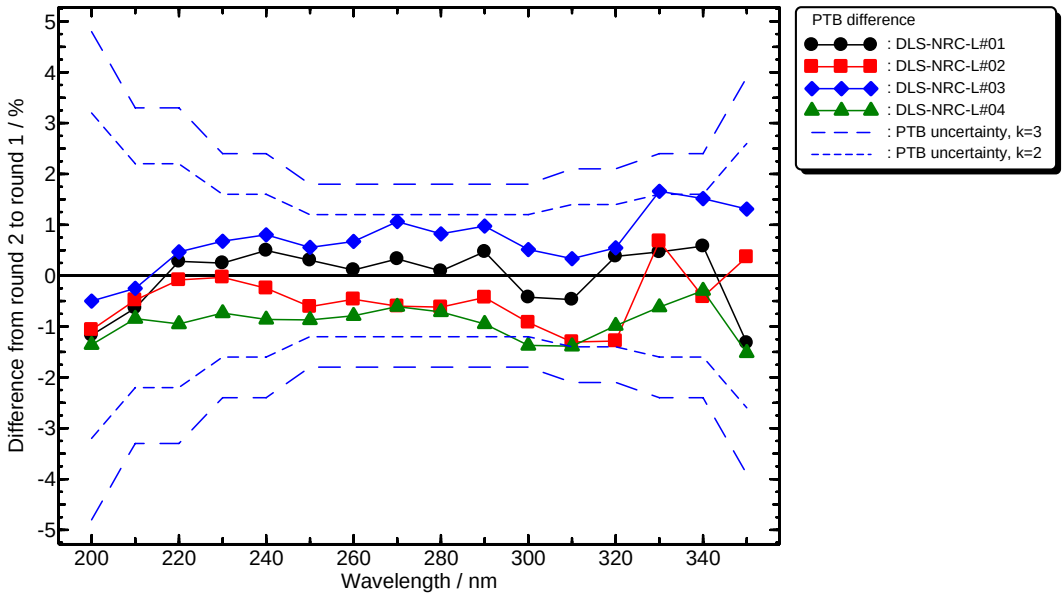

Figure 6.4 Repeatability between the measurement rounds calculated from PTB data.
The lines indicate the expanded measurement uncertainties for k = 2 and k = 3.

6.8.5 Normalized inner consistency of participants measurements

Additionally the inner consistency of the spectral irradiance calibrations of the lamps as described in section 9.1.2 was calculated (see equation (9.4)). It has to be pointed out, however, that the results presented her allow no conclusion of the absolute difference between participant and PTB.

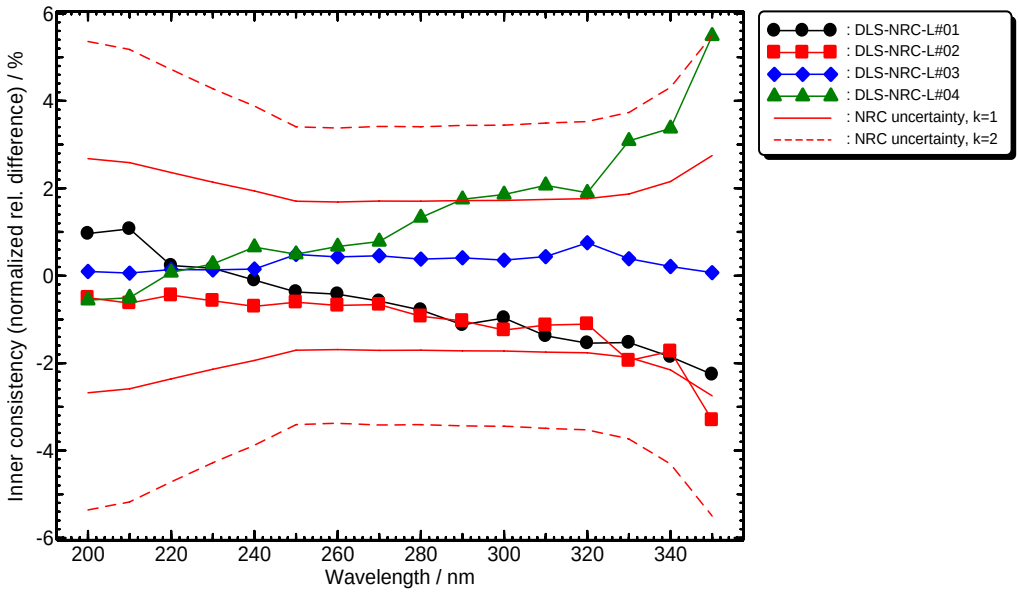

Figure 6.5 Normalized inner consistency of the NRC result compared to that of the PTB.
The lines indicate the expanded measurement uncertainties for k = 1 and k = 2.

6.8.6 Acceptance of measurements

The results presented in this section indicate that all measurement results of all lamps during both measurement rounds at the NRC can be used and that no data should be rejected.

Table 6.5 Results for the Lamp systems calibrated by NRC

	DLS-NRC-L#01		DLS-NRC-L#02		DLS-NRC-L#03		DLS-NRC-L#04		
	Round 1	Round 2	Round 1	Round 2	Round 1	Round 2	Round 1	Round 2	Uncertainty
λ	$E(\lambda)$	$E(\lambda)$	$E(\lambda)$	$E(\lambda)$	$E(\lambda)$	$E(\lambda)$	$E(\lambda)$	$E(\lambda)$	$u(E)$
[nm]	[W m^{-2}nm^{-1}]	[W m^{-2}nm^{-1}]	[W m^{-2}nm^{-1}]	[W m^{-2}nm^{-1}]	[W m^{-2}nm^{-1}]	[W m^{-2}nm^{-1}]	[W m^{-2}nm^{-1}]	[W m^{-2}nm^{-1}]	[%]
200	0,0009388	0,000934	0,000922	0,0009147	0,001011	0,001019	0,001304	0,0013	2,7
210	0,0009479	0,0009442	0,0009388	0,000931	0,001019	0,001025	0,001267	0,00126	2,6
220	0,0009141	0,0009132	0,0009129	0,0009102	0,0009826	0,0009915	0,00118	0,001178	2,4
230	0,0008477	0,0008421	0,0008515	0,0008439	0,0009092	0,0009123	0,001058	0,001049	2,1
240	0,000761	0,0007546	0,000767	0,0007577	0,0008138	0,0008135	0,0009217	0,0009121	1,9
250	0,0006641	0,0006589	0,0006718	0,0006644	0,0007084	0,0007085	0,0007847	0,0007763	1,7
260	0,0005739	0,0005663	0,0005826	0,0005734	0,0006104	0,0006074	0,0006631	0,0006537	1,7
270	0,000495	0,0004894	0,0005034	0,0004965	0,0005243	0,0005227	0,0005607	0,000554	1,7
280	0,0004201	0,000417	0,0004277	0,0004234	0,0004431	0,0004443	0,0004671	0,0004682	1,7
290	0,0003611	0,0003601	0,000368	0,0003657	0,0003797	0,000382	0,0003951	0,0003998	1,7
300	0,0003127	0,0003109	0,0003179	0,0003155	0,0003273	0,0003289	0,0003363	0,0003398	1,7
310	0,0002735	0,0002727	0,0002776	0,000276	0,0002851	0,0002872	0,0002904	0,0002952	1,7
320	0,00024	0,0002392	0,0002426	0,0002411	0,0002496	0,0002512	0,000252	0,0002566	1,8
330	0,0002096	0,0002101	0,0002114	0,0002116	0,000218	0,0002207	0,00022	0,0002253	1,9
340	0,0001874	0,0001872	0,0001886	0,0001879	0,000195	0,0001963	0,0001983	0,0001994	2,2
350	0,0001715	0,0001674	0,000172	0,0001679	0,0001789	0,0001756	0,0001871	0,000177	2,7

7 PTB

7.1 Description of the measurement facility and primary scale

7.1.1 Primary scale realization

The spectral irradiance scale at the Physikalisch-Technische Bundesanstalt (PTB) in Braunschweig is realized, maintained and disseminated [1] using a high temperature blackbody radiator of type BB3200pg [2]. The various radiometric parameters of this blackbody have been characterized in detail including modifications to improve performance as well as operating and safety conditions and it is used as a primary standard of spectral irradiance [3]-[5].

The main parameter of a blackbody, the temperature, has to be determined very accurately. At the PTB in Braunschweig, broadband-filter detectors are well established for the detector-based determination of the so-called radiometric temperature [3]. Improvements of this procedure and comparisons with other methods have been carried out and published [5],[6].

For the intercomparison the blackbody has been used at different distances around 630 mm and at different temperatures between 3020 K and 3150 K. The measuring aperture P-MB-11 with a diameter of 7.557 mm ± 3 µm was used to define the source area of the blackbody. The spectral irradiance at the reference plane of the spectroradiometer was then calculated according to Planck's law using the geometric parameters and the measured radiometric temperatures of the blackbody.

7.1.2 Measurement facility

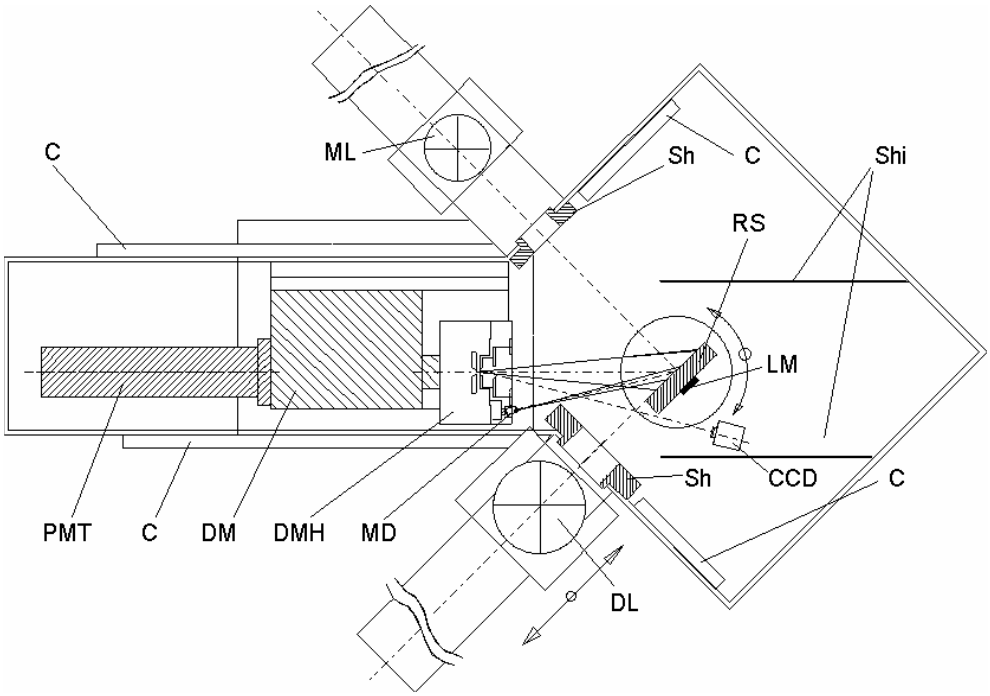

Figure 7.1 Spectroradiometer facility for spectral irradiance measurements optimized for air UV (top view). DM: double monochromator, PMT: solar-blind photomultiplier, RS: flat reflectance standard, DL: deuterium lamp, ML: monitor lamp, MD: monitor photodiode, DMH: double monochromator entrance head, Sh: shutter, CCD: CCD camera, LM: laser with vertical axis plus 45° mirror for alignment, Shi: radiation shields, C: water jackets. The flat reflectance standard RS is rotary. Its position shows the situation of the radiation measurement from the monitor lamp ML.

The PTB's spectroradiometer for spectral irradiance calibrations consists of a flat reflection standard as entrance optics, for a McPherson 275D double monochromator with single gratings and a solar blind photomultiplier-tube (PMT) to cover the spectral range from 200 nm to 350 nm. The acceptance angle of the reflectance standard is limited by a precise aperture. This aperture defines the reference plane for spectral irradiance measurements. The monochromator system has a focal length of 275 mm and a numerical aperture of f / 3.5. The monochromator gratings (1200 l/mm, size 50 mm x 50 mm) are blazed for 270 nm. All three slits are operated automatically from 0 to 2.5 mm slit width by using small DC-motors with encoders. The slit heights can be manually varied stepwise from 2 mm to 20 mm. The photomultiplier PMT is a Schlumberger type EMR 541F-09-17 with a spectral sensitivity range from 120 nm to 380 nm (solar blind). The reflectance standard is a pressed piece of fluorescence-free PTFE powder with a particle size of 0.5 µm. It is 80 mm in diameter and 10 mm thick.

7.1.3 Calibration procedure

The blackbody, working standards, or the lamps under test, were measured in the same optical path of the system in different successive measurement cycles covering each the whole recommended wavelength range. The stability of the system is verified using a deuterium monitor lamp (ML) during each measurement cycle. The signal of the blackbody source, the standard lamp, or the test lamp is compared with the signal of the monitor lamp at each wavelength position by opening two different apertures and rotating the reflection standard. The monitor lamp is a photo-current stabilized 30 W deuterium lamp similar to the lamp systems used for the intercomparison. It's stability is known to be better than $1 \cdot 10^{-3}\ h^{-1}$ in the UV spectral region and is frequently verified with self-consistency checks using different blackbody-calibrations.

During the intercomparison two measurement campaigns were carried out to calibrate the PTB deuterium lamp systems (DLS). The standards for the CCPR-K1.b intercomparison have been measured at least three times embedded by blackbody measurements. The spectral irradiance used was averaged over the blackbody calibrations for each measuring round.

7.1.4 Measurement cycle

All measurements were carried out following the same measurement procedure. The measurement started at the upper wavelength limit and at each wavelength the listed steps were carried out:

1. Go to wavelength and set according slit width
2. Turn reflection standard to test lamp and open shutter
3. Take 16 readings of photocurrent of test lamp
4. Close shutter and measure dark current
   (When operating the blackbody, measure temperature)
5. Turn reflection standard to monitor lamp and open shutter
6. Take 16 readings of photocurrent of monitor lamp
7. Close shutter
8. Measure lamp current, voltage and heater voltage
9. Start with step 1 at the next wavelength

7.2 Working standards used for the intercomparison

A set of three working standards was used for the CCPR-K1.b intercomparison. The lamps are part of the PTB-DLS. The lamps used were the lamps DLS-PTB-L#01, DLS-PTB-L#02 and DLS-PTB-L#03. The power supply for the lamps was DLS-PTB-PS#02 and as monitor-detector DLS-PTB-M#02 was used.

7.2.1 Monitor-detector measurements

To verify the temporal stability of the working standards, the monitor-detector DLS-PTB-M#02 was used before and after each spectral scan of the DLS. During one measurement campaign the measured detector signals varied less than 0.3 %. Between the two measurement rounds the signal of the monitor-detector changed by +0.4 % for DLS-PTB-L#01, +0.4 % for DLS-PTB-L#02 and +2 % for DLS-PTB-L#03.

7.2.2 Measurement of electrical parameters

The lamp current of all three lamps was set by the power supply DLS-PTB-PS#02 to a fixed value of 299.8 mA. The lamp voltages varied by 0.6 % for DLS-PTB-L#03 and by less than 0.1 % for the other two lamps during all measurements of both measurement rounds.

7.3 Measurement uncertainties

In this document the mathematical functions and the input quantities as well as their associated uncertainties are presented. Due to its complexity, the derivation and detailed description of all components of the mathematical models is not completely described in this document.

The complete measurement uncertainty budgets for the blackbody radiator temperature measurement, the spectral irradiance realization and the calibration procedure are described in detail in [5] and in the PTB quality-management system in the documents QM-AA-4.11-01 and QM-AA-4.11-02.

7.3.1 Blackbody radiator temperature measurements

The broadband-filter detectors measure the irradiance of the blackbody radiator weighted according to their spectral responsivity. Their photosignal is a measure for the temperature of the blackbody radiator.

This relationship can be described as follows

$$U_{\mathrm{FD}}(T_{\mathrm{BB}}) = \varepsilon \cdot (V_{\mathrm{iU}} + \delta V_{\mathrm{iU}}) \cdot \cos\varepsilon_1 \cdot \cos\varepsilon_2 \cdot \frac{A_{\mathrm{BB}} + \delta A_{\mathrm{BB}}}{d_{\mathrm{FD}}^2} \cdot (s_{\mathrm{abs}} + \delta s_{\mathrm{abs}}) \int s_{\mathrm{rel}}(\lambda) \frac{c_1}{n^2 \pi \lambda^5} \frac{1}{\exp\left(\frac{c_2}{n \cdot \lambda \cdot T_{\mathrm{BB}}}\right) - 1} \mathrm{d}\lambda \qquad (7.1)$$

The quantities used in this equation are

- U_{FD} photosignal of the broadband-filter detector measured in Volts
- ε effective emissivity of the blackbody radiator
- V_{iU}, δV_{iU} gain of the electrical measurements and its drift

- $\cos \varepsilon_1$, $\cos \varepsilon_2$ misalignment of filter detector to the optical axis of the blackbody
- A_{BB}, δA_{BB} size of the blackbody opening aperture and its drift
- d_{FD} distance of the filter detector to the blackbody aperture
- s_{abs}, δs_{abs} absolute spectral responsivity of the filter detector and its drift
- s_{rel} relative spectral responsivity distribution of the filter detector
- λ wavelength used for calculation
- T_{BB} radiometric temperature of the blackbody radiator
- c_1,c_2 Planck contants
- n Refractive index of air

Table 7.1 Standard measurement uncertainties for blackbody radiator temperature measurements

Quantity		**Type A Uncertainty**	**Type B Uncertainty**	**Uncertainty of Temperature / K @ 3150 K**
effective blackbody emissivity	ε		0.01 %	0.04
blackbody alignment	$\cos \varepsilon_1$		1 °	0.06
detector alignment	$\cos \varepsilon_2$		1 °	0.06
blackbody aperture	A_{BB}		3 µm	0.30
aperture contamination during operation	A_{BB}		0.06 %	0.14
distance detector to blackbody	d_{FD}		0.05 mm	0.10
absolute detector responsivity	s_{abs}		0.1 %	0.39
relative detector responsivity	s_{rel}		0.01 %	0.04
responsivity drift between calibrations	δs_{abs}		0.05 %	0.20
detector signal readings	U_{FD}	0.01 %		0.04
gain and drift of electrical measurements	V_{iU}, δV_{iU}		0.001 %	< 0.01
Total standard measurement uncertainty				0.57
Expanded uncertainty (k=2)				1.1

7.3.2 Primary spectral irradiance unit realization

With the temperature of the blackbody-radiator known, its spectral irradiance can directly be calculated as follows

$$E(\lambda,T_P) = \varepsilon \cdot \cos\varepsilon_{\mathrm{diff1}} \cdot \cos\varepsilon_{\mathrm{diff2}} \cdot \frac{A_{BB} + \delta A_{BB}}{d_{\mathrm{diff}}^2} \cdot \frac{c_1}{n^2\, \pi\, \lambda^5} \cdot \frac{1}{\exp\left(\frac{c_2}{n \cdot \lambda \cdot T_P}\right) - 1} + \delta E(\lambda,T) \qquad (7.2)$$

The quantities used in this equation are

- E_{BB} calculated spectral irradiance of the blackbody radiator
- ε emissivity of the blackbody radiator
- $\cos \varepsilon_{diff1}$, $\cos \varepsilon_{diff2}$ misalignment of the integrating sphere opening to the optical axis of the blackbody
- A_{BB}, δA_{BB} size and its drift of the blackbody opening aperture
- d_{diff} distance of the integrating sphere opening to the blackbody aperture
- λ calculated wavelength
- T_P radiometric temperature of the blackbody radiator determined by the filter detectors
- δE correction for blackbody temperature nonuniformity
- c_1,c_2 Planck contants
- n Refractive index of air

The wavelength λ has no associated uncertainty because it is used as an exact calculation parameter. The emissivity ε, the size of the blackbody opening aperture A_{BB} and its drift δA_{BB} in the mathematical model for the spectral irradiance are strongly correlated with the same input quantities that were used to determine the blackbody radiator temperature T_{BB}. The correlation slightly reduces the associated uncertainty for the temperature T_P used to calculate the spectral irradiance.

Table 7.2 Standard measurement uncertainties for primary spectral irradiance scale realization

Quantity		Uncertainty	Uncertainty in Spectral Irradiance								
			200 nm	210 nm - 220 nm	230 nm - 240 nm	250 nm - 260 nm	270 nm - 280 nm	290 nm - 300 nm	310 nm - 320 nm	330 nm - 340 nm	350 nm
blackbody alignment	$\cos \varepsilon_2$	1 °	0.02%	0.02%	0.02%	0.02%	0.02%	0.02%	0.02%	0.02%	0.02%
spectroradiometer alignment	$\cos \varepsilon_1$	1 °	0.02%	0.02%	0.02%	0.02%	0.02%	0.02%	0.02%	0.02%	0.02%
distance diffusor to blackbody	d_{diff}	0.05 mm	0.02%	0.02%	0.02%	0.02%	0.02%	0.02%	0.02%	0.02%	0.02%
effective blackbody emissivity*	ε	0.01%	0,02%	0,02%	0,01%	0,01%	0,01%	0,01%	0,01%	0,01%	0,01%
blackbody aperture (diameter)*	A_{BB}	3 µm	0,15%	0,12%	0,11%	0,09%	0,08%	0,07%	0,06%	0,05%	0,05%
aperture contamination during operation*	δA_{BB}	0.06 %	0,06%	0,05%	0,05%	0,04%	0,04%	0,03%	0,03%	0,02%	0,02%
temperature determination*	T_{P}	0.46 K	0,33%	0,30%	0,28%	0,25%	0,24%	0,22%	0,21%	0,19%	0,19%
blackbody temperature nonuniformity	δE	0.15 K	0,07%	0,07%	0,06%	0,06%	0,05%	0,05%	0,05%	0,04%	0,04%
Total standard measurement uncertainty			**0,38%**	**0,34%**	**0,31%**	**0,28%**	**0,26%**	**0,24%**	**0,22%**	**0,21%**	**0,20%**

* The uncertainty values for blackbody emissivity, aperture and aperture contermination are strongly correlated with the temperature determination. Therefore the uncertainty for the temperature determination is slighty reduced by these parts and the correlation is taken into account in this uncertainty budget. For details see [5].

7.3.3 Calibration procedure

The mathematical model of the calibration procedure considers that separate measurements of the monitor lamp against the working standard B (at the time t_1) and the transfer standard S (at the time t_2) have to be combined. Several correction factors κ have to be implemented under varying conditions to allow simplifications of the complex physical model and to account for variations of system parameters. The determination of the spectral irradiance of the transfer standard S can then be expressed as follows

$$E_S(\lambda,t_2,T_S) = \frac{v_S(\lambda_2,b,t_2)}{v_M(\lambda_2,b,t_2)} \cdot \kappa_{\lambda,S,M}(\lambda,\lambda_2,t_2) \cdot \kappa_{b,S,M}(\lambda,b) \cdot \kappa_{L,S,M}(t_2) \cdot \kappa_{\varepsilon,S}(t_2) \cdot \kappa_{d,S}(t_2) \cdot \frac{\kappa_{I,S}(t_2)}{\kappa_{I,M}(t_2)} \cdot \frac{1}{\kappa_{t,M}(\lambda,t_2,t_1)} \cdot$$

$$\frac{v_M(\lambda_1,b,t_1)}{v_B(\lambda_1,b,t_1)} \cdot \kappa_{\lambda,M,B}(\lambda,\lambda_1,t_1) \cdot \kappa_{b,M,B}(\lambda,b) \cdot \kappa_{L,M,B}(t_1) \cdot \frac{1}{\kappa_{\varepsilon,B}(t_1) \cdot \kappa_{d,B}(t_1)} \cdot \frac{\kappa_{I,M}(t_1)}{\kappa_{I,B}(t_1)} \cdot \frac{1}{\kappa_{t,B}(\lambda,t_1,t_0)}$$

$$\cdot E_B(\lambda,t_0) \qquad (7.3)$$

The quantities used in this equation are

- E_S calibrated spectral irradiance of the transfer standard
- t_0, t_1, t_2 times of measurements/calibrations
- λ calculated wavelength
- λ_1, λ_2 wavelengths set at the spectroradiometer at times t_1 and t_2
- b spectral bandwidth of the spectroradiometer
- v_S, v_B, v_M photosignals of the lamps
- $\kappa_{d,S}$, $\kappa_{d,B}$ correction factor for distance settings of the transfer standard and the working standard
- $\kappa_{\varepsilon,S}$, $\kappa_{\varepsilon,B}$ correction factor for alignment of the transfer standard and the working standard, also considering irradiance nonuniformities
- $\kappa_{L,S,M}$, $\kappa_{L,M,B}$ combined correction factor for nonlinearity of the measurement electronics settings at times t_1 and t_2
- $\kappa_{\lambda,S,M}$, $\kappa_{\lambda,M,B}$ combined correction factor for wavelength settings at times t_1 and t_2
- $\kappa_{b,S,M}$, $\kappa_{b,M,B}$ combined correction factor for spectroradiometer bandwidth
- $\kappa_{I,S}$, $\kappa_{I,B}$, $\kappa_{I,M}$ correction factor for electrical current settings of the lamps
- $\kappa_{t,B}$, $\kappa_{t,M}$ correction factor for the drift of the working standard and the monitor lamp / measurement facility since the last measurement or calibration
- E_B spectral irradiance of the working standard

All correction factors are selected to be exactly one under ideal conditions of the defined calibration procedures. Their associated uncertainties are considered for these conditions.

The combined correction factors take into account, that maladjustment of a quantity (e.g. the wavelength λ) has the same effect on the monitor lamp and on the other lamp measured at the same time.[3]

[3] If for instance the spectral distribution of the two lamps is similar (same lamp txpe), a maladjustment of the wavelength has a negligible effect on the ratio of the photosignals measured at the same time.

Therefore the associated measurement uncertainty of this quantity for the spectral irradiance calibration can be significantly lower than usually assumed.

Times of measurements t_0, t_1, t_2

The parameters t_0, t_1, t_2 are the points in measurement time when the measurement were taken. t_0 is the time when the working standard has been calibrated the last time. The working standard then is measured at the time t_1 again. The difference t_1-t_0 equals the burning time of the working standard since the last calibration. When using the blackbody, t_1-t_0 = 0 because the spectral irradiance is calculated instantaneously during the measurements. The time t_2 is when the transfer standard is calibrated. The difference t_2-t_1 equals the burning time of the monitorlamp since the last measurements with the working standard.

Photosignals v_S, v_B, v_M of the lamps

The photosignals of the lamps are linked to the readout of the measurement electronics. They are averaged over at least 16 readouts and substracted by the corresponding dark-signal. The photosignal v_M of the monitorlamp is taken directly after the photosignals of the standard lamp v_S or the blackbody v_B have been measured. Therefore the measurements can be handled as synchronous readouts to compensate short-term instabilities of the system. The assigned measurement uncertainty of the photosignals is the standard deviation of the mean of the readout.

Distance of the standard lamps (correction factor $\kappa_{d,S}$)

The distance of 300 mm between the lamp opening and the reference plane of the spectroradiometer has to be extended by approx. 80 mm to consider the distance from the lamp opening to the lamp center itself. The distance is set with a caliper gauge with an uncertainty of 0.05 mm (rectangular distributed). The correction factor results in $\kappa_{d,S}$ = 1 ± 0.0003.

Alignment of the standard lamps and irradiance nonuniformity (correction factor κ_ε)

The deuterium lamps are operated at a very narrow distance to the irradiated reference plane. Deuterium lamps also have a nonuniform irradiance distribution. The lamps for the DLS are selected in that way, that their irradiance at a distance of 300 mm (calibration distance) varies less than ±0.4 % over a diameter of 32 mm around their optical axis. When carefully angular and lateral aligning the lamps the correction results in κ_ε = 1 ± 0.002 (assuming a rectangular distribution of the nonuniformity combined with the alignment).

Linearity correction $\kappa_{L,S,M}$, $\kappa_{L,M,B}$:

The solar-blind photomultiplier tube shows a slight nonlinearity at higher photocurrent levels. Usually this level of photocurrents should be avoided and the photomultiplier should be operated within the linear range. When comparing the spectral irradiance of the blackbody radiator with that of deuterium lamps, a dynamic signal range of 10^4 has to be covered. To achieve sufficient signal-to-noise ratios, the PMT had to be operated in the nonlinear range for higher irradiances. Using the beam conjoiner method, the nonlinearity has been measured and the photocurrent could be corrected by correction factors.

Therefore the measured photocurrent v_x has to be devided by the (photocurrent-dependend) correction factor $f(v_x)$. The correction for high photocurrents is up to 1.015 and is 1.0000 for the lower range. The correction has to be applied for both, the standard lamp and the monitor lamp. Therefore, the combined linearity correction factors $\kappa_{L,S,M}$ and $\kappa_{L,B,M}$ are defined as ratios of the correction factors:

$$\kappa_{L,S,M} = \frac{f(v_M)}{f(v_S)} \text{ and } \kappa_{L,M,B} = \frac{f(v_B)}{f(v_M)}.$$

For similar irradiances of the standard lamp and the (deuterium) monitor lamp $\kappa_{L,S,M} = \kappa_{L,M,B} = 1 \pm 0.001$. When operating the blackbody, $\kappa_{L,M,B}$ can rise up to 1.015 ± 0.007 for wavelengths below 250 nm. Above 250 nm the correction factor is smaller than 1.006 ± 0.003.

Wavelength correction factor $\kappa_{\lambda,S,M}$, $\kappa_{\lambda,M,B}$

Due to the strong slope and the different gradients of the spectral irradiances of the blackbody radiator and deuteriums lamps, the wavelength of the spectroradiometer has to be set very accurately to the recommended wavelengths. Both, the photocurrent of the standard lamp (or blackbody) and the monitor lamp are measured at the same wavelength setting at the same time t (within one minute). Therefore only the ratio of the photocurrents would have to be corrected for a potentially wrong wavelength setting. Assuming a correct wavelength setting, the wavelength correction factor for both photocurrent ratios is $\kappa_{\lambda,S,M} = \kappa_{\lambda,M,B} = 1$. The uncertainty for this assumption can be calculated from the 1st derivative of the photocurrent ratios:

$$u^2(\kappa_{\lambda,S,M}) = \left(u(\lambda) \cdot \frac{\mathrm{d}\left(\frac{v_S(\lambda)}{v_M(\lambda)}\right) \Big/ \mathrm{d}\lambda}{\frac{v_S(\lambda)}{v_M(\lambda)}} \right)^2 \quad \text{and} \quad u^2(\kappa_{\lambda,M,B}) = \left(u(\lambda) \cdot \frac{\mathrm{d}\left(\frac{v_M(\lambda)}{v_B(\lambda)}\right) \Big/ \mathrm{d}\lambda}{\frac{v_M(\lambda)}{v_B(\lambda)}} \right)^2$$

The relative change of the photocurrent ratios is shown in Figure 7.2. For the transfer standard S as well as for the monitor lamp M deuterium lamps are used, so that their photocurrent ratio does not vary remarkably with the wavelength. Nevertheless, at 200 nm the ratios changes by 4 %/nm. This effect is due to different lamp bulb materials. When using the blackbody radiator, the relative change rises up to 8 %/nm at 200 nm. The wavelength of the spectroradiometer can be set to the recommended wavelengths with an uncertainty of $u(\lambda) = 0{,}05$ nm. For the deuterium lamps then, the resulting uncertainty $u(\kappa_{\lambda,S,M})$ is < 0.02 % for the wavelength region from 210 to 350 nm and is estimated to 0.2 % at 200 nm. For the blackbody versus the deuterium monitor lamp, the uncertainty for the combined wavelength correction varies from 0.4 % at 200 nm to 0.2 % at 350 nm.

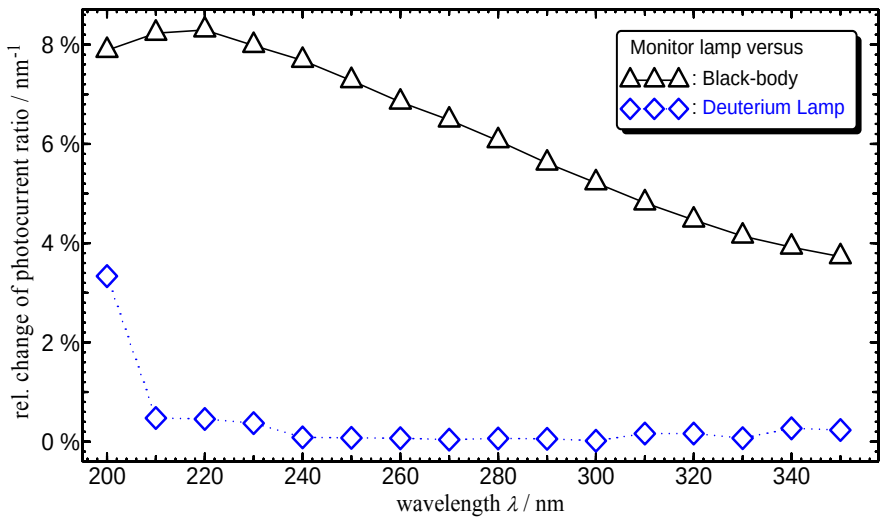

Figure 7.2 The relative spectral change of the photocurrent ratio between the monitorlamp and the blackbody (triangles) or the deuterium lamps (rhombs) respectively.

Combined correction factor for spectroradiometer bandwidth ($\kappa_{b,S,M}$, $\kappa_{b,M,B}$)

Several assumptions and simplification lead to equation (7.3). The most comprehensive assumption is that the spectroradiometer is an instrument that separates only radiation of the wavelength λ_x it is set to. This simplification can be valid for very narrow-banded instruments and/or where their

spectral sensitivity and the measured spectra vary only slightly or linear with wavelength. In a real monochromator system, however, the bandpass-slit function N_{mon}, the relative instrument responsivity r_{mon} and the spectral irradiance E_S of the measured standard lamp have to be considered to calculate the (true) photo-signal:

$$v_S(\lambda_x,b) = v_0(\lambda_x) \cdot \int_0^\infty N_{mon}(\lambda,\lambda_x,b) \cdot r_{mon}(\lambda,\lambda_x) \cdot E_S(\lambda)\, d\lambda \quad (7.4)$$

This equation can usually not be solved to directly get the spectral irradiance $E_S(\lambda_x)$ at the wavelength λ_x. Some ancillary conditions and measurements allow simplifying equation (7.4). The bandwidth and the slit-function of the monochromator system were measured using narrow-banded single lines of a low pressure mercury lamp. The slit-function was found to be symmetric and approximate triangular with the full width $2 \cdot b$ where b represents the bandwidth of the monochromator system. Therefore according to [7] the measured photo-signals have to be corrected by the relative change of the second derivative. This correction has to be applied to both the photo-signal assigned to the monitor-lamp and the photo-signal of the standard lamp or the working standard, respectively. It results in the correction factors

$$\kappa_{b,S,M} = \frac{1 - \frac{b^2}{12}\frac{v_S''(\lambda_x)}{v_S(\lambda_x)}}{1 - \frac{b^2}{12}\frac{v_M''(\lambda_x)}{v_M(\lambda_x)}}, \quad \kappa_{b,M,B} = \frac{1 - \frac{b^2}{12}\frac{v_M''(\lambda_x)}{v_M(\lambda_x)}}{1 - \frac{b^2}{12}\frac{v_B''(\lambda_x)}{v_B(\lambda_x)}}$$

where v_S'', v_M'' and v_B'' are the second derivatives of the photo-signals.

If the transfer standard S is of the same type as the monitor lamp M (e.g. deuterium lamp), the correction factor $\kappa_{b,S,M}$ is one. For the working standard B being a blackbody radiator, $\kappa_{b,M,B}$ can vary significantly from one. In Figure 7.3 the combined correction factors for the used bandwidths of 2.9 nm (in the spectral range from 200 nm to 320 nm) and 5 nm (330 nm to 350 nm) are shown. The corrections to be applied are less than 0,7 % in the spectral range from 200 nm to 320 nm and rise up to -3 % at 350 nm.

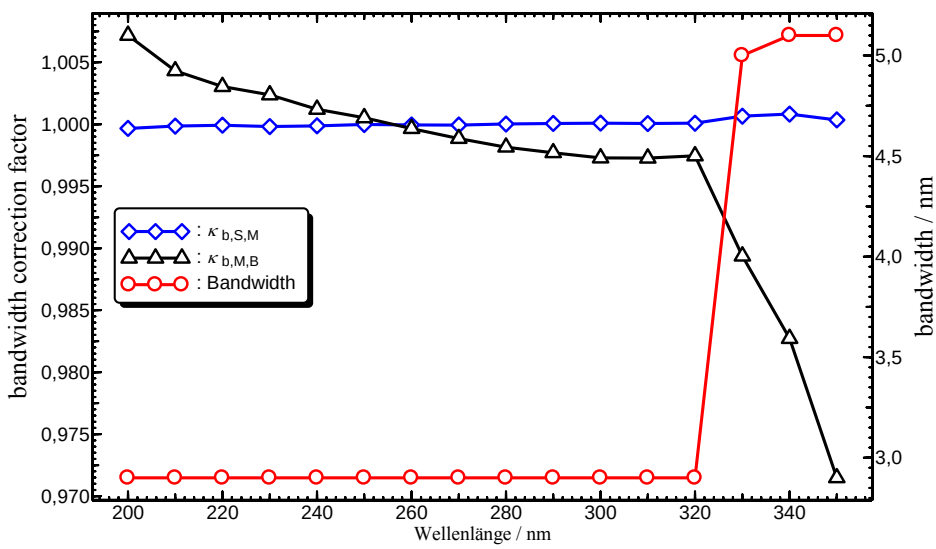

Figure 7.3 The combined bandwidth correction factors.

Correction factor for the temporal drift of the working standard or the monitor lamp $\kappa_{t,B}, \kappa_{t,M}$

Working standard and transfer standard were calibrated at the same place but could not be calibrated at the same time. The short term temporal drift of the standards and of the measurement facility have to be considered. With the blackbody radiator as the working standard, the spectral irradiance E_B was assigned online during the measurements and $\kappa_{t,B} = 1$. The monitor lamp was used to keep the spectral irradiance and to transfer it to the transfer standard S. Although it was photocurrent stabilized, the comparison of several measurements with the blackbody radiator showed a linear drift of $\delta \approx 10^{-4}\ h^{-1}$. The small correction

$$\kappa_{t,M}(\lambda,t_2,t_1) = (1 + \delta(\lambda))\cdot(t_2 - t_1)$$

was applied to compare measurements that where separated more than 100 hrs in monitor lamp burning time. The uncertainty for this correction is in the range of 0,1 %.

Correction factor for electrical current settings of the lamps $\kappa_{I,S}$, $\kappa_{I,B}$, $\kappa_{I,M}$

The spectral irradiance of a lamp is strongly dependent on the electrical parameters assigned to it. Therefore it is important to set and keep the lamp current at its defined value. The DLS are equipped with a constant current power supply with a fixed lamp current of about 300 mA. The exact value might slightly vary between different power supplies and a single lamp should consequently always be operated with the same power supply. The lamp current was monitored during the measurements and turned out to change less than 3 µA for all lamps during all measurements. Thus, the correction factors for the electrical current are set to unity with a negligible uncertainty.

Table 7.3 Standard measurement uncertainties for spectral irradiance calibrations

Parameter		Type A Uncertainty	Type B Uncertainty	Uncertainty in Spectral Irradiance								
				200 nm	210 nm - 220 nm	230 nm - 240 nm	250 nm - 260 nm	270 nm - 280 nm	290 nm - 300 nm	310 nm - 320 nm	330 nm - 340 nm	350 nm
primary blackbody scale realisation	E_B		0.57 K	0,38%	0,34%	0,31%	0,28%	0,26%	0,24%	0,22%	0,21%	0,20%
distance of transfer standard	$\kappa_{d,S}$		0,05 mm	0,03%	0,03%	0,03%	0,03%	0,03%	0,03%	0,03%	0,03%	0,03%
distance of working standard	$\kappa_{d,B}$		0,05 mm	0,02%	0,02%	0,02%	0,02%	0,04%	0,02%	0,02%	0,02%	0,02%
alignment of transfer standard	$\kappa_{\varepsilon,S}$		0,2%	0,2%	0,2%	0,2%	0,2%	0,2%	0,2%	0,2%	0,2%	0,2%
alignment of working standard	$\kappa_{\varepsilon,B}$		0,03%	0,03%	0,03%	0,03%	0,03%	0,03%	0,03%	0,03%	0,03%	0,03%
bandwidth correction factor	$\kappa_{b,S,M}$		0,05% - 0,1%	0,1%	0,05%	0,05%	0,05%	0,05%	0,05%	0,05%	0,05%	0,3%
bandwidth correction factor	$\kappa_{b,M,B}$		0,05% - 0,1%	0,1%	0,05%	0,05%	0,05%	0,05%	0,05%	0,05%	0,05%	0,3%
wavelength for transfer standard	$\kappa_{\lambda,S,M}$		0.05 nm	0,17%	0,02%	0,02%	0,01%	0,01%	0,01%	0,01%	0,01%	0,01%
wavelength for working standard	$\kappa_{\lambda,B,M}$		0.05 nm	0,39%	0,41%	0,40%	0,36%	0,32%	0,28%	0,24%	0,21%	0,19%
stability of facility and monitorlamp	$\kappa_{t,M}$	0,1%		0,10%	0,10%	0,10%	0,10%	0,10%	0,10%	0,10%	0,10%	0,10%
standard deviation of working standard	v_B	0,2 – 1,4%		1,4%	0,8%	0,4%	0,2%	0,2%	0,2%	0,2%	0,2%	0,3%
standard deviation of transfer standard	v_S	0,1% - 1%		0,1%	0,1%	0,1%	0,1%	0,2%	0,3%	0,4%	0,5%	1%
reproducibility of transfer standard	E_S	0,2% - 0,7%		0,5%	0,4%	0,30%	0,20%	0,2%	0,3%	0,3%	0,5%	0,7%
total standard measurement uncertainty				1,6%	1,1%	0,8%	0,6%	0,6%	0,6%	0,7%	0,8%	1,3%
Expanded uncertainty (k=2)				3,2%	2,2%	1,5%	1,2%	1,2%	1,2%	1,4%	1,6%	2,6%

7.4 References

[1] Metzdorf J., Metrologia, 1993, 30, 403-408.

[2] Sapritsky V. I., Khlevnoy B. B., Khromchenko V. B., Lisiansky B. E., Mekhontsev S. N., Melenevsky U. A., Morozova S. P., Prokhorov A. V., Samoilov L. N., Shapoval V. I., Sudarev K. A., Zelener M. F., Appl. Opt., 1997, 36, 5403-5408.

[3] Sperfeld P., Metzdorf J., Galal Yousef S., Stock K. D., Möller W., Metrologia, 1998, 35, 267-271. [4]

[4] Sperfeld P., Metzdorf J., Harrison N. J., Fox N. P., Khlevnoy B. B., Khromchenko V. B., Mekhontsev S. N., Shapoval V. I., Zelener M. F., Sapritsky V. I., Metrologia, 1998, 35, 419-422.

[5] Sperfeld P., Entwicklung einer empfängergestützten spektralen Bestrahlungs-stärkeskala, Braunschweig, 1999. http://www.biblio.tu-bs.de/ediss/data/19990628a/19990628a.html

[6] Khlevnoy B.B., Harrison N.J., Rogers L.J., Pollard D.F., Fox N.P., Sperfeld P., Fischer J., Friedrich R., Metzdorf J., Seidel J., Samoylov M.L., Stolyarevskaya R.I., Khromchenko V.B., Ogarev S.A., Sapritsky V.I., Metrologia, 2003, 40, S39–S44

[7] Cox M.G., Harris P.M., Kenward P.D., Woolliams E.R., "Spectral characteristic modelling", NPL Report CMSC 27/03. Available at: http://www.npl.co.uk/ssfm/download/

7.5 Results

7.5.1 Deuterium Lamp systems used

The following components were used by PTB during the intercomparison:

Power supply: DLS-PTB-PS

Monitor detector: DLS-PTB-MD (detector failed during first round)

Lamps: DLS-PTB-L#01, DLS-PTB-L#02, DLS-PTB-L#03

If necessary the power supply has been switched between the primary voltage settings that are common in the different countries.

7.5.2 Lamp system electrical stability

The Deuterium Lamp systems were operated at 0.2996 A, the average lamp voltages measured were:

Table 7.4 Average Lamp voltages for the different PTB lamp systems

Lamp	PTB round 1	Participant round 1	PTB round 2	Participant round 2
DLS-PTB-L#01	79,73 V		79.82 V	
DLS-PTB-L#02	78,74 V		78,82 V	
DLS-PTB-L#03	82,54 V		82,80 V	

7.5.3 Numerical results

The participant measured all three lamp systems for the intercomparison. The results for the mean of the spectral irradiance of each lamp in each measurement round are given in the following tables. λ represents the wavelength in nm, $E(\lambda)$ stands for the spectral irradiance in $W \cdot m^{-2} \cdot nm^{-1}$ and $u(E)$ is the combined relative standard uncertainty for the measurement as reported by the participant. In the case that the participant reported spectral irradiance values for each single measurement of one round, the average calculated by the pilot is shown in Table 7.5.

7.5.4 Repeatability between measurement rounds

With the results reported the repeatability of the measurements of each lamp system between each round was calculated. The difference from round 2 to round 1 as shown in Figure 7.4 might indicate outliers or a high drift of a single lamp.

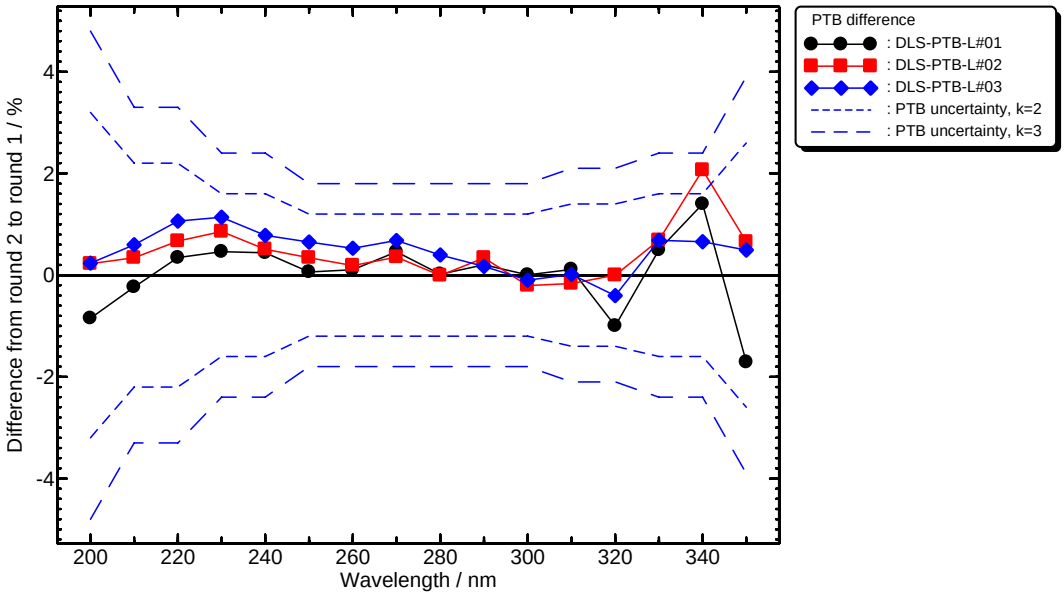

Figure 7.4 Repeatability between the measurement rounds calculated from the PTB data. The lines indicate the expanded measurement uncertainties for k = 2 and k = 3.

7.5.5 Acceptance of measurements

The results presented in this section indicate that all measurement results of all lamps during both measurement rounds at the participant can be used and that no data should be rejected.

Table 7.5 Results for the Lamp systems calibrated by PTB

	DLS-PTB-L#01		DLS-PTB-L#02		DLS-PTB-L#03		
	Round 1	Round 2	Round 1	Round 2	Round 1	Round 2	Uncertainty
λ	$E(\lambda)$	$E(\lambda)$	$E(\lambda)$	$E(\lambda)$	$E(\lambda)$	$E(\lambda)$	$u(E)$
[nm]	[W m^{-2}nm^{-1}]	[W m^{-2}nm^{-1}]	[W m^{-2}nm^{-1}]	[W m^{-2}nm^{-1}]	[W m^{-2}nm^{-1}]	[W m^{-2}nm^{-1}]	[%]
200	0,000885	0,0008775	0,0008489	0,0008508	0,001085	0,001087	1,6
210	0,0008932	0,0008911	0,0008887	0,0008918	0,001108	0,001115	1,1
220	0,0008374	0,0008403	0,0008541	0,0008599	0,001038	0,001049	1,1
230	0,0007646	0,0007681	0,0007955	0,0008023	0,0009476	0,0009583	0,8
240	0,000673	0,000676	0,0007121	0,0007157	0,0008368	0,0008433	0,8
250	0,0005861	0,0005865	0,0006247	0,0006268	0,000728	0,0007327	0,6
260	0,000502	0,0005025	0,0005396	0,0005406	0,0006216	0,0006249	0,6
270	0,0004274	0,0004293	0,0004612	0,0004629	0,0005269	0,0005305	0,6
280	0,0003638	0,0003638	0,0003936	0,0003936	0,0004473	0,0004491	0,6
290	0,0003112	0,0003118	0,0003364	0,0003375	0,0003804	0,000381	0,6
300	0,0002677	0,0002677	0,0002897	0,0002891	0,0003272	0,0003269	0,6
310	0,0002337	0,000234	0,0002523	0,0002519	0,0002823	0,0002823	0,7
320	0,0002074	0,0002053	0,0002213	0,0002213	0,0002468	0,0002458	0,7
330	0,0001851	0,000186	0,0001967	0,000198	0,0002189	0,0002204	0,8
340	0,0001621	0,0001643	0,000174	0,0001776	0,000192	0,0001933	0,8
350	0,0001431	0,0001407	0,0001545	0,0001555	0,000168	0,0001688	1,3

8 Pilot

8.1 Description of the measurement facility

The measurements of the pilot where carried out at the PTB measurement facility as described in section 7.1.2. The deuterium lamps where directly compared in successive measurements using again the monitor deuterium lamp to provide stability of the system and comparability even over longer time periods.

8.1.1 Measurement cycle and calibration procedure

For each deuterium lamp and each single wavelength the measurement cycle as described in section 7.1.4 was used. This ensures to measure the monitor lamp and the deuterium lamp systems under identical system settings. As the monitor lamp comes with a very similar spectral shape to that of the DLS, boundary conditions and effects such as wavelength setting and bandwidth corrections are extensively eliminated.

The calibration procedure was carried out in alternate measurements of participant's lamps and pilot's lamps. A group of lamps of different participants was always measured in conjunction with one of the pilot's lamps. Using the stability of the monitor lamp, each of the pilot's lamp can be calibrated by each of the participant's lamps. All lamps of the comparison were measured at least three times during a measurement campaign. Finally the pilot's lamps were calibrated by each lamp of the participants by calculating the average of the corresponding measurements and using the spectral irradiance values assigned by the participants to their lamps.

8.2 Reference standards used as pilot's lamps for the intercomparison

A set of three comparison reference standards were used as pilot's lamps for the CCPR-K1.b intercomparison. The lamps are part of the PTB-DLS. The lamps used where the lamps DLS-PTB-L#04, DLS-PTB-L#05 and DLS-PTB-L#06. The power supply for the lamps was DLS-PTB-PS#03 and as monitor-detector DLS-PTB-M#03 was used.

8.2.1 Monitor-detector measurements

To verify the temporal stability of the comparison reference standards, the monitor-detector DLS-PTB-M#03 was used before and after each spectral scan of the DLS. During the measurement campaign for the intercomparison the measured detector signals varied less than 0.3 %.

8.2.2 Measurement of electrical parameters

The lamp current of all three lamps was set by the power supply DLS-PTB-PS#03 to a fixed value of 299.8 mA. The lamp voltages varied by less than 0.16 % for the lamps during all measurements of both measurement rounds.

8.3 Measurement uncertainties

As the calibration procedure is similar to that described in section 7.3.3, a similar measurement equation can be used. The facts that the monitor lamp is similar to the deuterium lamp systems and that identical lamp systems are compared, however eliminates several correction factors. Thus, equation (7.3) can be reduced to

$$E_S(\lambda,t_2,T_S) = \frac{v_S(\lambda_2,b,t_2)}{v_M(\lambda_2,b,t_2)} \cdot \kappa_{\varepsilon,S}(t_2) \cdot \kappa_{d,S}(t_2) \cdot \frac{1}{\kappa_{t,M}(\lambda,t_2,t_1)} \cdot \frac{v_M(\lambda_1,b,t_1)}{v_P(\lambda_1,b,t_1)} \cdot \frac{1}{\kappa_{\varepsilon,P}(t_1) \cdot \kappa_{d,P}(t_1)} \cdot \frac{1}{\kappa_{t,P}(\lambda,t_1,t_0)} \cdot E_P(\lambda) \quad (8.1)$$

The quantities used in this equation are

- E_S calibrated spectral irradiance of the comparison reference standard
- t_0, t_1, t_2 times of measurements/calibrations
- λ calculated wavelength
- λ_1, λ_2 wavelengths set at the spectroradiometer at times t_1 and t_2
- b spectral bandwidth of the spectroradiometer
- v_S, v_P, v_M photosignals of the lamps
- $\kappa_{d,S}$, $\kappa_{d,P}$ correction factor for distance settings of the comparison reference standard and the transfer standard
- $\kappa_{\varepsilon,S}$, $\kappa_{\varepsilon,P}$ correction factor for alignment of the comparison reference standard and the transfer standard, also considering irradiance nonuniformities
- $\kappa_{t,P}$, $\kappa_{t,M}$ correction factor for the drift of the comparison reference standard and the monitor lamp / measurement facility since the last measurement or calibration
- E_P spectral irradiance of the transfer standard assigned by the participant

The correction factors are analog to that described in section 7.3.3. The correction factor for the drift of the working standard $\kappa_{t,P}$ can again be considered to be unity. The spectral irradiance assigned to the participant's transfer standard lamp is the average of the participant's calibrations before and after the measurements at the pilot's laboratory. Assuming a linear drift of the transfer standards this leads to $\kappa_{t,P}$ = 1. The uncertainty for the correction factor can be individually determined for each participant's lamp using the repeated results of the measurements at the participant's and the pilot's laboratories. A relative uncertainty of 0.1 % however is a reliable result for the majority of all working standards. The uncertainties for the other correction factors and quantities can directly be taken from Table 7.3. This leads to the relative transfer uncertainty $u_{Ts,rel}(E_s)$ for comparing the pilot's lamps with the participant's lamps as shown in table Table 8.1. This uncertainty budget does not include the uncertainties $u(E_P)$ for the spectral irradiance E_P of the transfer standard which is provided by the participant.

Table 8.1 Standard measurement uncertainties of the pilot measurements
(not included: spectral irradiance uncertainty of the participant's /working standard)

Parameter		Type A Uncertainty	Type B Uncertainty	Uncertainty in Spectral Irradiance								
				200 nm	210 nm - 220 nm	230 nm - 240 nm	250 nm - 260 nm	270 nm - 280 nm	290 nm - 300 nm	310 nm - 320 nm	330 nm - 340 nm	350 nm
distance of comparison reference standard	$\kappa_{d,S}$		0,05 mm	0,03%	0,03%	0,03%	0,03%	0,03%	0,03%	0,03%	0,03%	0,03%
distance of transfer standard	$\kappa_{d,P}$		0,05 mm	0,03%	0,03%	0,03%	0,03%	0,03%	0,03%	0,03%	0,03%	0,03%
alignment of comparison reference standard	$\kappa_{\varepsilon,S}$		0,2%	0,2%	0,2%	0,2%	0,2%	0,2%	0,2%	0,2%	0,2%	0,2%
alignment of transfer standard	$\kappa_{\varepsilon,P}$		0,2%	0,2%	0,2%	0,2%	0,2%	0,2%	0,2%	0,2%	0,2%	0,2%
stability of facility and monitorlamp	$\kappa_{t,M}$	0,1%		0,10%	0,10%	0,10%	0,10%	0,10%	0,10%	0,10%	0,10%	0,10%
stability of transfer standard	$\kappa_{t,P}$	0,1%		0,10%	0,10%	0,10%	0,10%	0,10%	0,10%	0,10%	0,10%	0,10%
standard deviation of transfer standard	v_P	0,1% - 1%		0,1%	0,1%	0,1%	0,1%	0,2%	0,3%	0,4%	0,5%	1%
Standard deviation of comparison reference standard	v_S	0,1% - 1%		0,1%	0,1%	0,1%	0,1%	0,2%	0,3%	0,4%	0,5%	1%
total standard measurement uncertainty				0,35 %	0,35 %	0,35 %	0,35 %	0,43%	0,53%	0,65%	0,78 %	1,04%
Expanded uncertainty (k=2)				0,7 %	0,7 %	0,7 %	0,7 %	0,85 %	1,1 %	1,3 %	1,6 %	2,1%

9 Analysis of data

This key comparison consists of a set of 16 individual comparisons of spectral irradiance, each comparison corresponding to a separate wavelength. Therefore, for the purposes of this analysis, the results at each comparison wavelength will be treated and analysed independently. Although for practical presentational purposes, only one final report will be produced containing all the data.

It should be noted that due to the nature of this intercomparison, in particular the non-ideal performance of the transfer standard lamps and differences in the number of independent measurements made by each participant, the analysis of the data is relatively complex. The following procedure will be followed to ensure that an appropriate representative value and associated uncertainty are obtained for each participant.

To simplify the analysis, measurements and calibrations are taken as separate comparisons for each wavelength. The same analysis will apply to the results at all wavelengths. However, relations or correlations between different wavelengths that are present will not be considered or discussed in this analysis.

Although it represents a slightly different approach, the following analysis closely follows the analysis method described in appendix C of the CCPR-K1.a intercomparison report and follows the Guidelines for CCPR Comparison Report Preparation.

9.1 Establishing the NMI (National Metrology Institute) representative value

The main purpose of the analysis is to create (at each wavelength) a single quantity and associated uncertainty to determine the best estimate of the difference between each participant and the Key Comparison reference scale, as held by the group of deuterium lamp systems at the pilot laboratory (unilateral deviation). This value will combine the results from all the deuterium lamps measured by the participants. A distinctive method to establish the spectral irradiance of the pilot's lamp systems (comparison reference standards) is intended to receive a direct comparability between the participants and to assign a weighted mean spectral irradiadiance to the group of comparison reference lamp systems to incorporate the key comparison reference value (KCRV). This relative comparison method is extensively independend from the absolute spectral irradiance unit realization of the NMI that is acting as pilot and allows especially to distinguish between *pilot* PTB and *participant* PTB.

Six main procedures are carried out:

1. For each of the participants' lamp systems the mean of the spectral irradiances assigned in round 1 and round 2 is calculated.
2. Stability and consistency checks are carried out to verify the acceptability of the participants' lamp systems.
3. Each of the participants' lamp systems and the mean of their spectral irradiances assigned by the participants will be used to calibrate each of the comparison reference lamp systems.
4. The average of all calibrations of the pilot lamp systems is taken for each participant to establish the NMI representative value.
5. The weigthed mean of all NMI representative values is caculated to form the Key Comparison Reference Value (KCRV)
6. The Degrees of Equivalence (DoE) are calculated to compare the NMIs results to the KCRV and to that of other participants.

9.1.1 Determination of the mean of each participants lamp systems

The participant *i* reported spectral irradiance values $E_{i,j,r}$ for each of their lamp systems *j* and for each of the two rounds *r*. For the comparison, the mean of the reported values of each round was then calculated for each lamp system:

$$E_{i,j} = \frac{E_{i,j,1} + E_{i,j,2}}{2} \qquad (9.1).$$

If no further details are mentioned, it is assumed that the measurements of the two rounds are nearly fully correlated for each lamp and thus the resulting relative uncertainty is approximated by

$$u_{rel}(E_{i,j}) = \frac{1}{2}\sum_{r=1}^{2} u_{rel}(E_{i,j,r}) \ . \qquad (9.2)$$

If the uncertainties for the measurements are separated by the participants in the uncertainty for the scale realization $u_{S,rel}(E_i)$ and for the scale transfer in each round $u_{T,rel}(E_{i,j,r})$ the resulting relative uncertainty for the average of two rounds is given by

$$u_{rel}(E_{i,j}) = \sqrt{u^2{}_{S,rel}(E_i) + \frac{1}{2}\sum_{r=1}^{2} u^2{}_{T,rel}(E_{i,j,r})} \qquad (9.3)$$

The results for equations (9.2) and (9.3) are identical, if the relative uncertainties specified for each round are identical or if the uncertainty of the transfer measurements (usually random components) is much smaller than the uncertainty for the scale.

9.1.2 Establishing the acceptability of a lamp system

Measurements were made in the sequence: PTB – participant – PTB – participant. The repeatability of the PTB's measurements and the repeatability of the participant's measurements will be used to determine if the lamp has been stable for the entire comparison or at least for the set participant – pilot – participant. If none of these situations is met, the lamp will be rejected from the analysis.

It has to be pointed out that for this stability check the spectral irradiance values and assigned standard measurement uncertainties of the *participant* PTB had to be used, as the spectral irradiances calculated for the pilot as described below will not directly lead to any information about the stabilities of the participants' lamp systems. Therefore the stability examinations are strongly dependent on the repeatability of the PTB measurements between the two rounds.

The stability was determined by comparing the repeatability of the lamp to the standard measurement uncertainties of the participants' or PTB's uncertainty budgets, as appropriate. It was anticipated that a coverage factor of 3 has been used to determine acceptability.

In addition an inner consistency check for all lamps of a participant was carried out. The averaged results $E_{i,j}$ were compared to the spectral irradiances $E_{PTB,i,j}$ assigned by the PTB to the participants' lamps *j* during round 2 of the pilot's measurements. This operation eliminates a possible linear drift

of the lamps between the measurement rounds. The consistency check took place at the stage of Pre-Draft A where no absolute deviations must be presented. Therefore the average or normalized difference for each lamp was calculated:

$$\delta_{i,j} = \left(\frac{\dfrac{E_{i,j}}{E_{PTB,i,j}}}{\dfrac{1}{N}\sum_{j=1}^{N} \dfrac{E_{i,j}}{E_{PTB,i,j}}} - 1 \right) \cdot 100\ \%\} \qquad (9.4)$$

Here N is the number of lamps of participant *i* and $\delta_{i,j}$ represents the inner consistency of each lamp *j* for the results of the participant compared to that of the PTB.

The results of the stability checks and the inner consisteny checks are given in the according participants' sections. For the given intercomparison none of the 20 lamps and the corresponding 80 measurement rounds had to be rejected.

9.1.3 Establishing the spectral irradiance for the pilot's deuterium lamp systems and the deviation for each participant's lamp

The pilot's measurement facility and the set of lamp systems assigned to be the pilot's comparison reference standards were used to compare the spectral irradiance realizations of the participants. Therefore the pilot's lamp systems DLS-PTB-L#04, DLS-PTB-L#05 and DLS-PTB-L#06 have been calibrated using the participant's transfer standards and their assigned spectral irradiances. This calibration was physically carried out using the measurements at the pilot institute between the two calibration rounds of the participants (see section 8). With each lamp *j* of a participant *i* and its assigned spectral irradiance $E_{i,j}$ each comparison reference lamp *s* of the pilot is calibrated by direct comparison at the pilot's measurement facility. The spectral irradiance $E_{s,i,j}$ of each pilot's lamp assigned by each participant's transfer standard is the mean of all measurements with this according pair of lamps at the pilot lab. It is calculated using equation (8.1) in section 8.3. The resulting uncertainty of each calibration is a combination of the participants uncertainty $u_{rel}(E_{i,j})$ and the transfer uncertainty $u_{Ts,rel}(E_{s,i,j})$ of the calibration at the pilot lab

$$u_{rel}(E_{s,i,j}) = \sqrt{u^2_{rel}(E_{i,j}) + u^2_{Ts,rel}(E_{s,i,j})} \qquad (9.5)$$

The mean of all calibrations of the three pilot comparison reference lamps *s* by one participant's transfer standard *j* is the representative value for the participant's lamp and is a virtual spectral irradiance

$$\hat{E}_{i,j} = \frac{1}{3}\sum_{s=1}^{3} E_{s,i,j} \qquad (9.6)$$

which is not physically assigned to one artefact but to the group of the three artifacts of the comparison reference standards *s*.

The related relative uncertainty

$$u_{\mathrm{rel}}(\hat{E}_{\mathrm{i,j}}) = \frac{1}{3}\sum_{\mathrm{s}=1}^{3} u_{\mathrm{rel}}(E_{\mathrm{s,i,j}}) \qquad (9.\ 7)$$

is a reasonable approximation that takes into account the strong correlation of all measurements.

These virtual spectral irradiances $\hat{E}_{\mathrm{i,j}}$ allow to additionally compare the internal consistency of the participants' calibrations

$$\hat{\delta}_{\mathrm{i,j}} = \left(\frac{\hat{E}_{\mathrm{i,j}}}{\frac{1}{\mathrm{N}}\sum_{\mathrm{j}=1}^{\mathrm{N}} \hat{E}_{\mathrm{i,j}}} - 1 \right) \cdot 100\ \% \qquad (9.8)$$

where $\hat{\delta}_{\mathrm{i,j}}$ is the deviation of the virtual spectral irradiance $\hat{E}_{\mathrm{i,j}}$ assigned by the participant's lamp j to the mean of the virtual spectral irradiances.

9.1.4 Establishing the NMI representative value

For each participant i the mean of all virtual spectral irradiance values $\hat{E}_{\mathrm{i,j}}$ is used to get the participating NMI's representative virtual spectral irradiance values

$$\hat{E}_{\mathrm{i}} = \frac{1}{\mathrm{N}}\sum_{\mathrm{j}=1}^{\mathrm{N}} \hat{E}_{\mathrm{i,j}} \qquad (9.9)$$

with the relative uncertainty

$$u_{\mathrm{rel}}(\hat{E}_{\mathrm{i}}) = \frac{1}{N}\sum_{\mathrm{j}=1}^{N} u_{\mathrm{rel}}(\hat{E}_{\mathrm{i,j}}) = \frac{1}{3N}\sum_{\mathrm{j}=1}^{N}\sum_{\mathrm{s}=1}^{3} u_{\mathrm{rel}}(E_{\mathrm{s,i,j}}) \qquad (9.10)$$

which again takes into account the strong correlations between the N lamps of the participant i. These results can then be used to calculate the Key Comparison Reference Value or to directly compare different participants with each other.

9.2 Establishing the Key Comparison Reference Value (KCRV) and the deviations of the NMI

The weigthed mean of the virtual spectral irradiance values of all NMIs represent the KCRV. Following the the Guidelines for CCPR Comparison Report Preparation the weight is calculated with cut-off which is calculated as the average of the NMIs uncertainties which are less than or equal to the median of the uncertainties of all NMIs. For this comparison with five participants the cutt-off uncertainty $u_{\text{cut-off}}$ is the average of the three institutes stating the lowest uncertainties

$$u_{\text{cut-off}} = \frac{1}{3}\sum_{\mathrm{i}=1}^{3} u_{\mathrm{rel}}(E_{\mathrm{i}}) \qquad \text{for } u_{\mathrm{rel}}(E_{\mathrm{i}}) \leq \text{median}\{u_{\mathrm{rel}}(E_{\mathrm{k}})\}_{\mathrm{k}\,=\,1\text{ to }5} \qquad (9.11)$$

where $u_{\mathrm{rel}}(E_{\mathrm{i}})$ is the mean relative uncertainty stated by the participant *i*. The relative uncertainties are shown graphically, along with the cut-off in Figure 9.1.

For each participant the uncertainty for the NMI representative value $u_{\mathrm{rel}}(\hat{E}_{\mathrm{i}})$ is then adjusted by the cut-off:

$$u_{\mathrm{adj}}(\hat{E}_{\mathrm{i}}) = \begin{cases} u_{\mathrm{rel}}(\hat{E}_{\mathrm{i}}) & \text{for } u_{\mathrm{rel}}(\hat{E}_{\mathrm{i}}) \geq u_{\text{cut-off}} \\ u_{\text{cut-off}} & \text{for } u_{\mathrm{rel}}(\hat{E}_{\mathrm{i}}) < u_{\text{cut-off}} \end{cases} \tag{9.12}$$

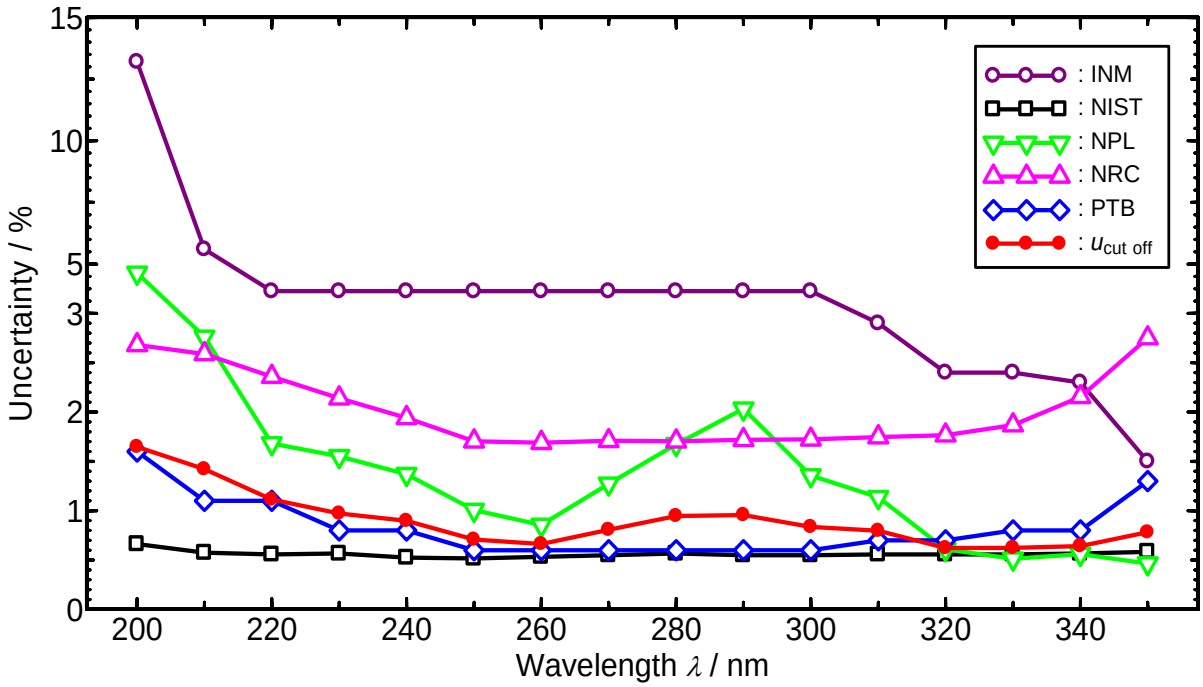

Figure 9.1 Combined standard uncertainties $u_{\mathrm{rel}}(E_{\mathrm{i}})$ of the participants and resulting cut-off $u_{\text{cut off}}$

The weight w_{i} for the participant *i* is then calculated as

$$w_{\mathrm{i}} = \frac{u_{\mathrm{adj}}^{-2}(\hat{E}_{\mathrm{i}})}{\sum_{\mathrm{i}=1}^{5} u_{\mathrm{adj}}^{-2}(\hat{E}_{\mathrm{i}})} \tag{9.13}$$

and the KCRV for five participants is calculated as

$$\hat{E}_{\mathrm{KCRV}} = \sum_{\mathrm{i}=1}^{5} w_{\mathrm{i}}\, \hat{E}_{\mathrm{i}} \tag{9.14}$$

with the relative standard uncertainty

$$u_{\mathrm{rel}}(\hat{E}_{\mathrm{KCRV}}) = \sqrt{\frac{1}{\sum_{\mathrm{i}=1}^{5} u_{\mathrm{adj}}^{-2}(\hat{E}_{\mathrm{i}})}} \tag{9.15}$$

These results directly lead to the unilateral and bilateral Degrees of Equivalence (DoE). The unilateral DoE of NMI *i* is given by

$$D_{\mathrm{i}} = \frac{\hat{E}_{\mathrm{i}} - \hat{E}_{\mathrm{KCRV}}}{\hat{E}_{\mathrm{KCRV}}} \tag{9.16}$$

with its expanded uncertainty

$$U_{\mathrm{i}} = k\sqrt{u_{\mathrm{rel}}^2(\hat{E}_{\mathrm{KCRV}}) + u_{\mathrm{rel}}^2(\hat{E}_{\mathrm{i}})} \quad ; \quad k = 2. \tag{9.17}$$

In the same way the bilateral DoE of NMI *i* to NMI *m* is calculated as

$$D_{\mathrm{i,m}} = D_{\mathrm{i}} - D_{\mathrm{m}} = \frac{\hat{E}_{\mathrm{i}} - \hat{E}_{m}}{\hat{E}_{\mathrm{KCRV}}} \tag{9.18}$$

with

$$U_{\mathrm{i,m}} = k\sqrt{u_{\mathrm{rel}}^2(\hat{E}_{\mathrm{i}}) + u_{\mathrm{rel}}^2(\hat{E}_{\mathrm{m}}) + u_{\mathrm{rel}}^2(\hat{E}_{\mathrm{KCRV}})} \quad ; \quad k = 2. \tag{9.19}$$

This definition follows the convention for the analysis of Key Comparisons and provides bilateral DoEs that are symmetrical and consistent with the unilateral DoEs.

The simple data analysis presented here and the resulting parameters give satisfactory informations to compare the participants' abilities in calibrating deuterium lamps in terms of spectral irradiance.

10 Results: KCRV and DOE for the CCPR-K1.b intercomparison

In this section the NMI representative spectral irradiances $\hat{E}_i$ as well as the resulting KCRV are listed, following the analysis method as described in section 9. The unilateral DoEs as well as the bilateral DoEs are presented and tabulated.

10.1 NMIs representative spectral irradiances and the KCRV

The NMI representative spectral irradiances $\hat{E}_i$ were calculated accorting to equation (9.9) in section 9.1.4. The virtual spectral irradiance $\hat{E}_{KCRV}$ which forms the KCRV could then be calculated as the weighted mean of all representative spectral irradiances using equation (9.14) in section 9.2. Therefore the KCRV for different wavelengths represent the spectral irradiance of a typical 30W deuterium lamp system (DLS). The calculated virtual spectral irradiances for all wavelengths are summarized in Figure 10.1 together with the expanded absolute standard uncertainties $u_{rel}(\hat{E}_i)\cdot\hat{E}_i$ and $u_{rel}(\hat{E}_{KCRV})\cdot\hat{E}_{KCRV}$ (k=2).

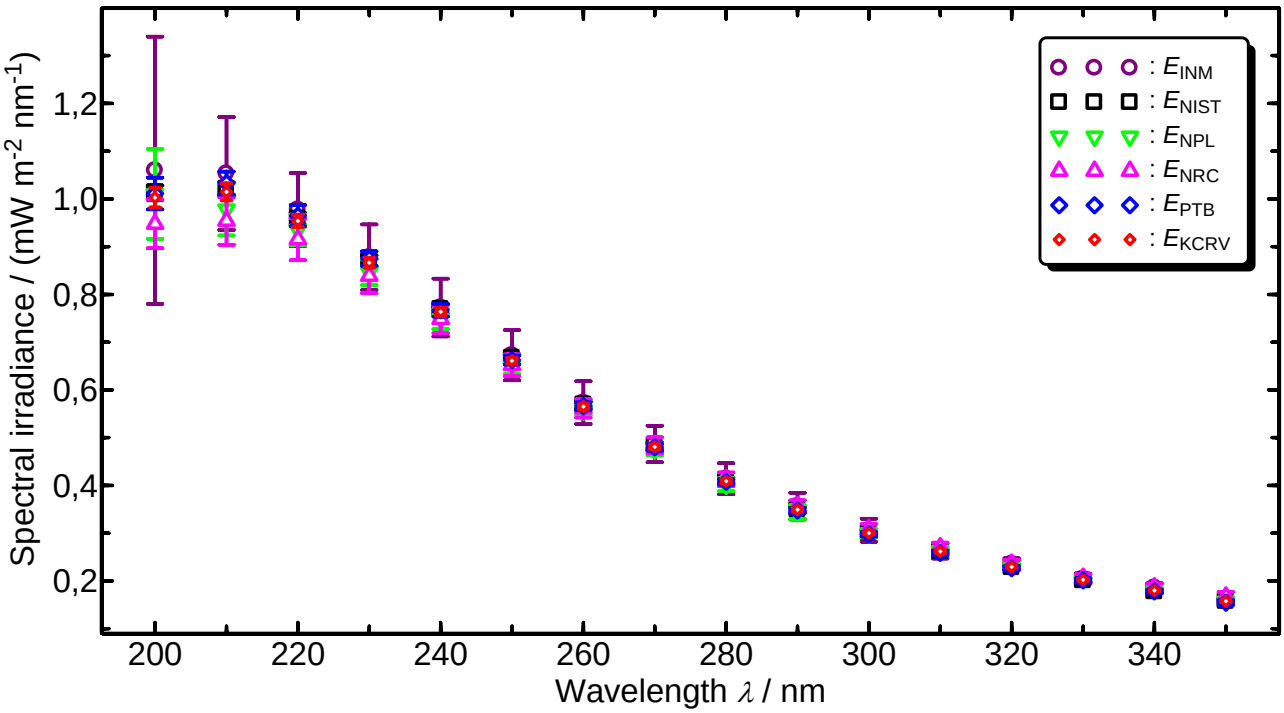

Figure 10.1 The NMI representative virtual irradiances and the resulting KCRV summarized for all wavelengths.
The error bars indicate the expanded uncertainties (k=2) for the calculated spectral irradiances.

10.2 Unilateral DoE

The deviations of the NMI representative values to the KCRV directly result in the unilateral DoE for each participant. A summary for all participants is given in Figure 10.2. The lines between the data points are only used to indicate the group of DoEs at different wavelengths that belong to one NMI. As stated earlier in section 9, a possible spectral interrelation is not taken into account.

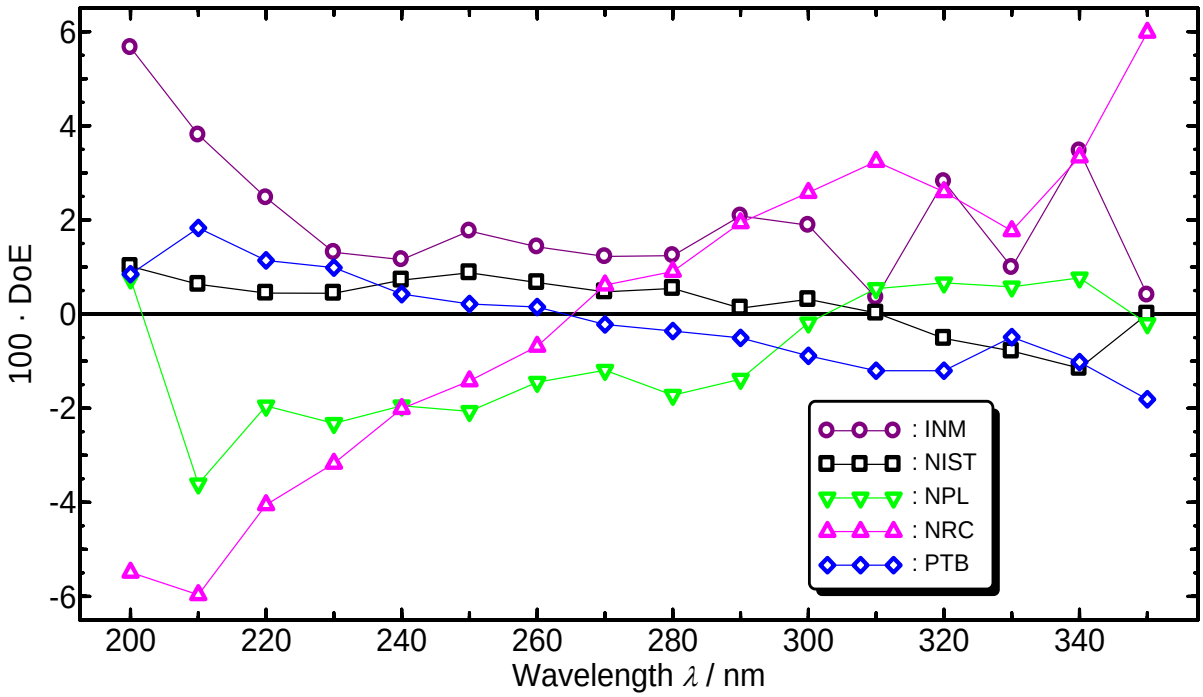

Figure 10.2 Summary of the unilateral DoE for the participants.

10.2.1 Unilateral DoE for Each participant

In the following graphs the DoEs for each participant at each wavelength are summarized. The closed lines represent the uncertainty for the unilateral DoE U_i as given by equation (9.17) as the 95 % level of confidence as required by the Mutual Recognition Arrangement ("2 sigma"). The dotted lines stand for $0.5 \cdot U_i$ ("1 sigma") and for $1{,}5 \cdot U_i$ ("3 sigma").

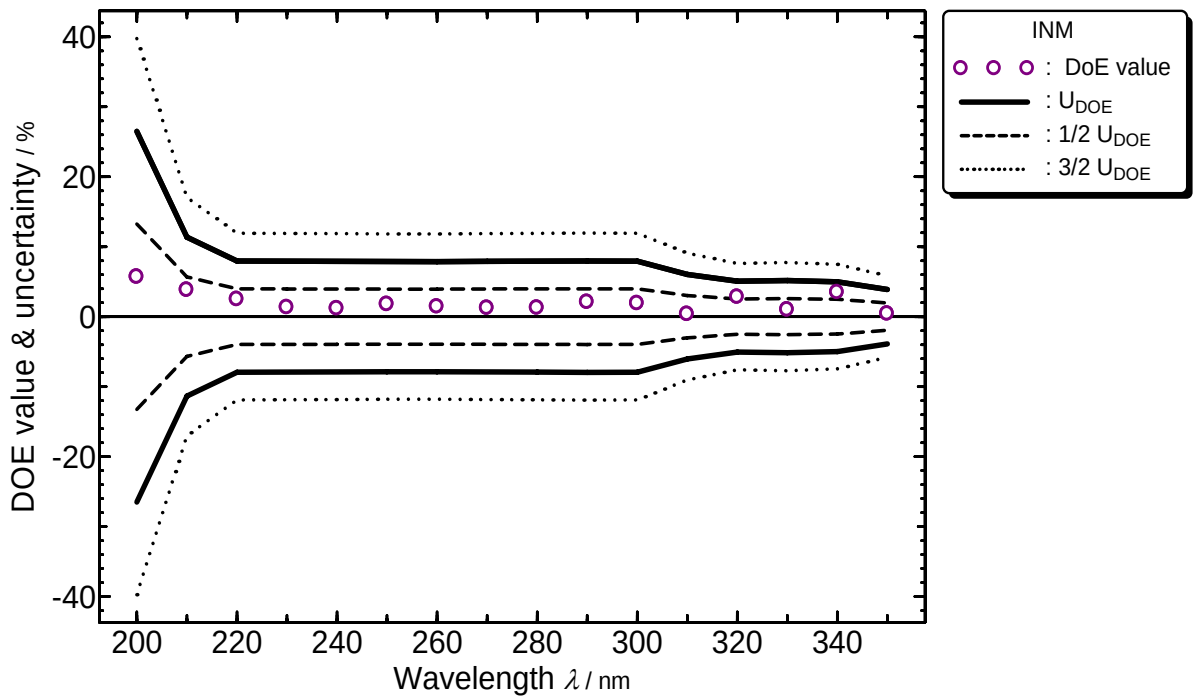

Figure 10.3 Unilateral DoE for INM.

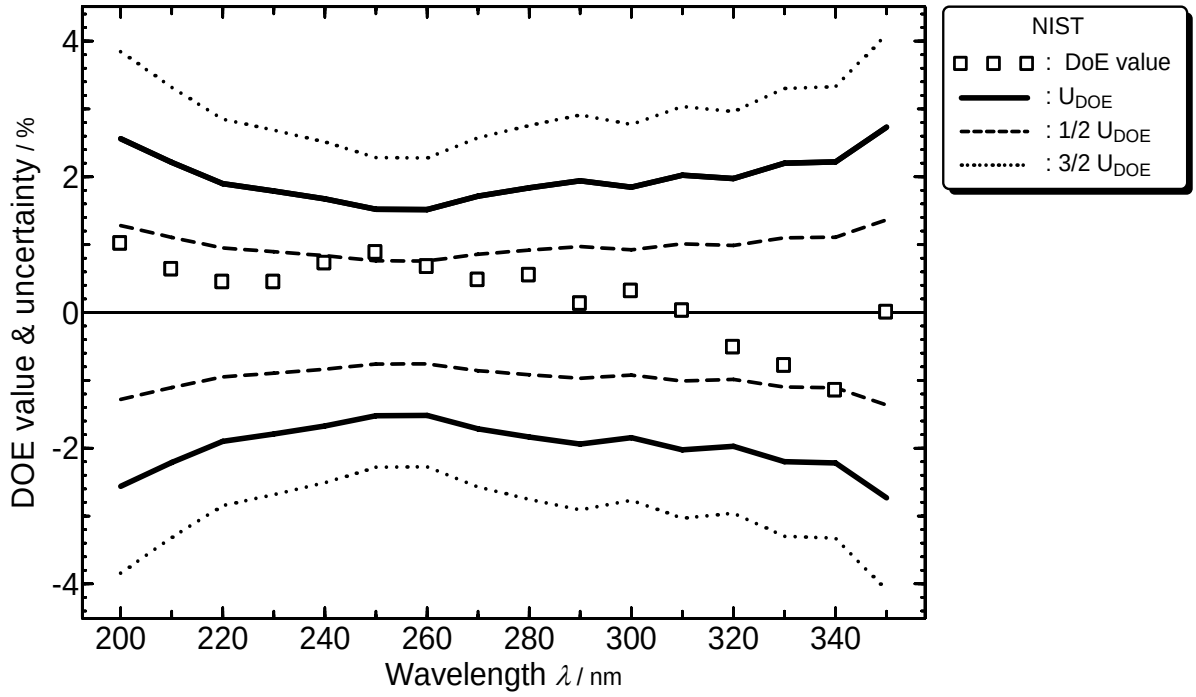

Figure 10.4 Unilateral DoE for NIST.

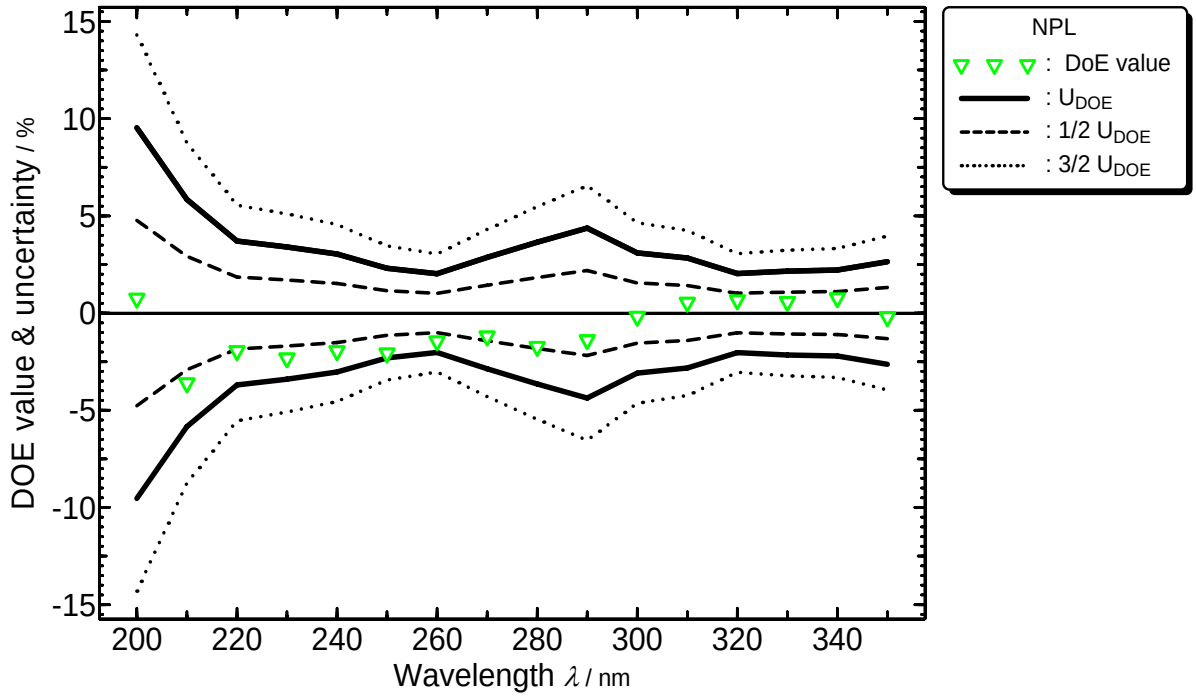

Figure 10.5 Unilateral DoE for NPL.

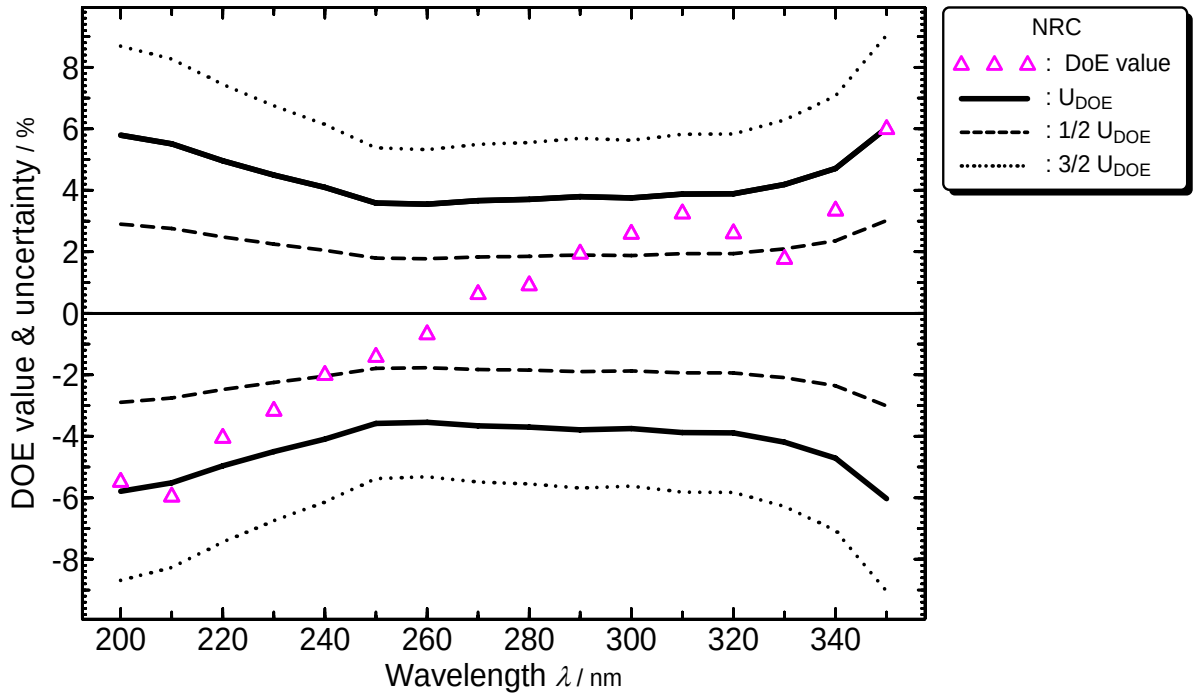

Figure 10.6 Unilateral DoE for NRC.

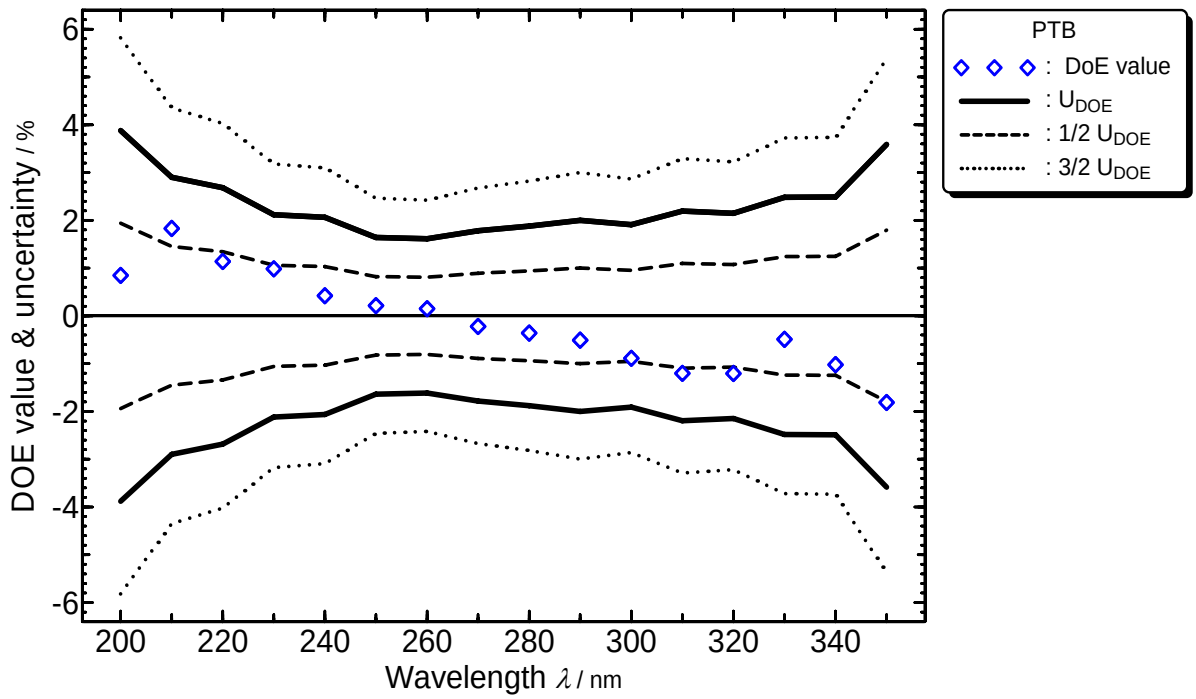

Figure 10.7 Unilateral DoE for PTB.

10.2.2 Unilateral DoE by wavelength – all participants

The following graphs show the results separately for every wavelength. The uncertainty 'bars' represent the uncertainty of the DoEs U_i for the participant i.

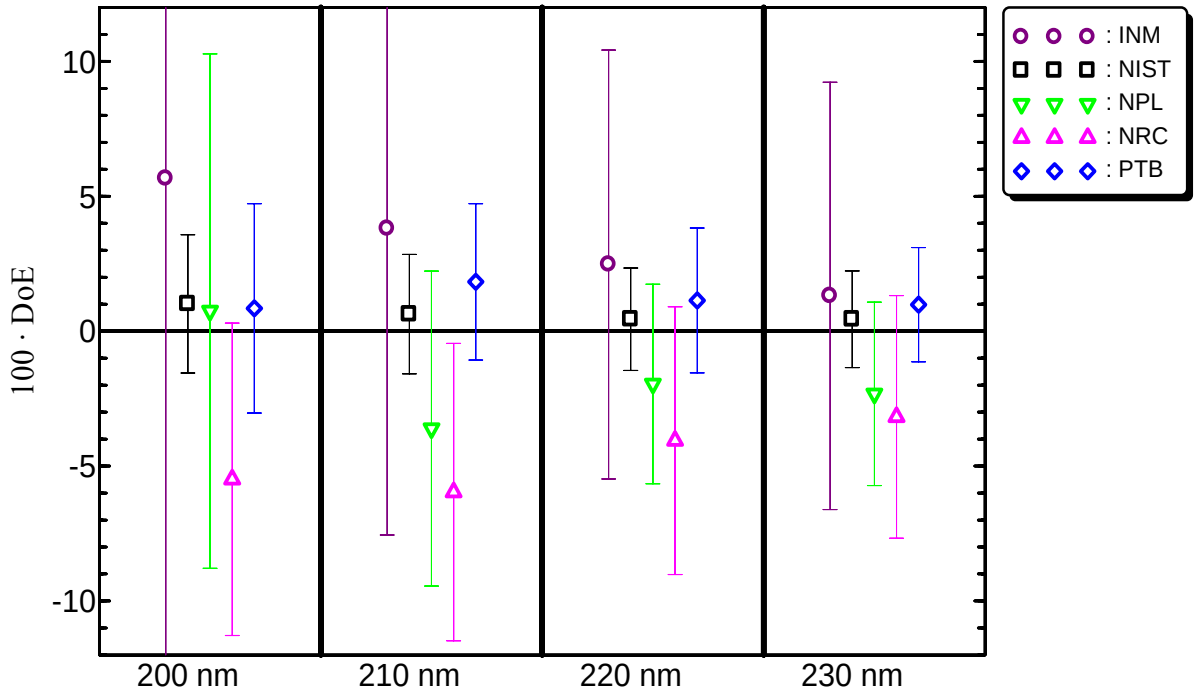

Figure 10.8 Unilateral DoE for the wavelengths 200 nm, 210 nm, 220 nm and 230 nm.

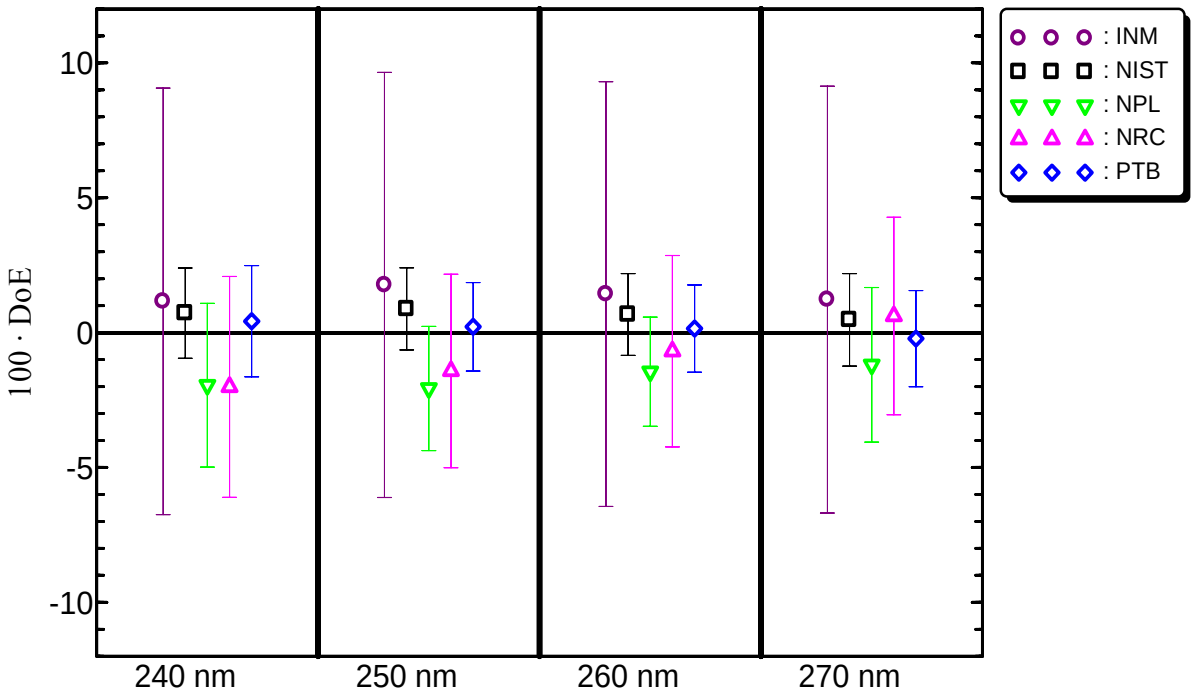

Figure 10.9 Unilateral DoE for the wavelengths 240 nm, 250 nm, 260 nm and 270 nm.

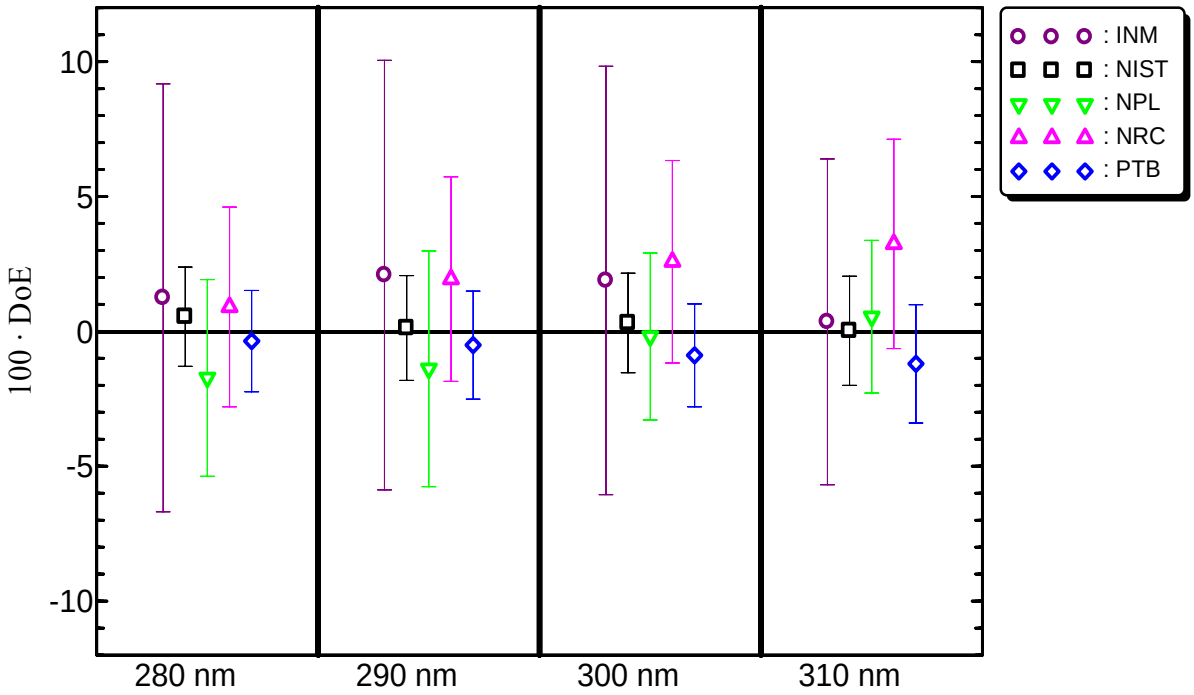

Figure 10.10 Unilateral DoE for the wavelengths 280 nm, 290 nm, 300 nm and 310 nm.

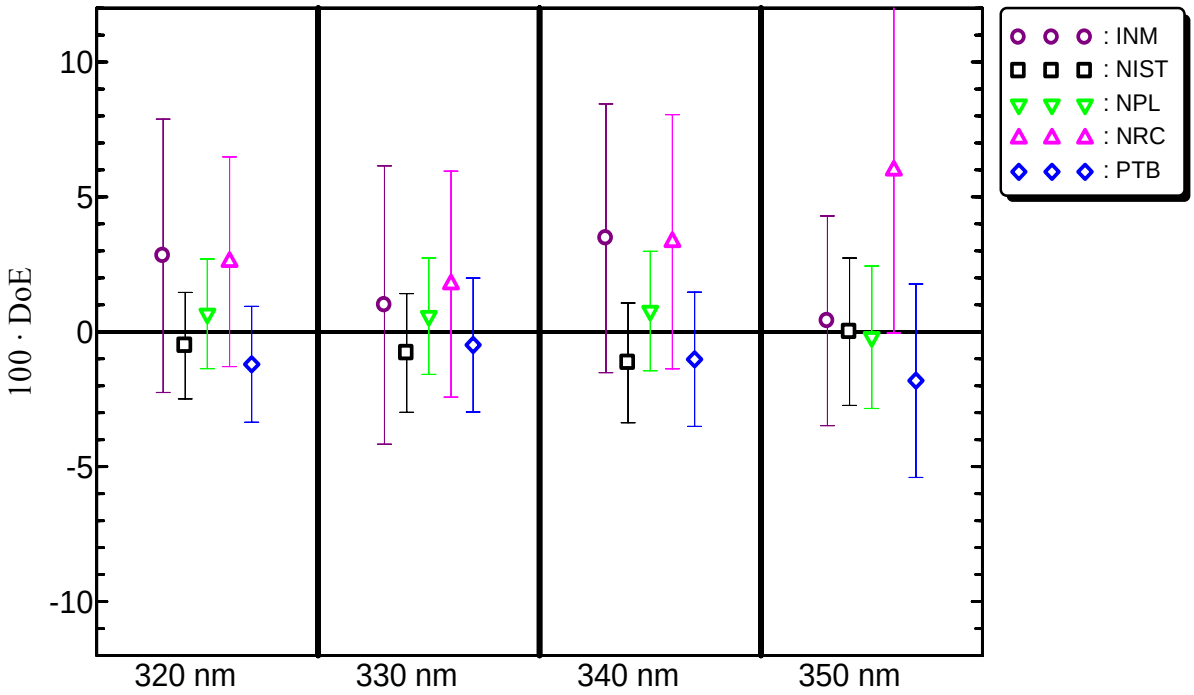

Figure 10.11 Unilateral DoE for the wavelengths 320 nm, 330 nm, 340 nm and 350 nm.

10.3 Bilateral DoE

The bilateral DoE of one participant *i* stand for the deviation to the other participants *m* as given by equation (9.18). The following graphs show these bilateral DoE for each participant together with the resulting uncertainty $U_{i,m}$ for the bilateral DoE (dotted lines, 95 % level of confidence).

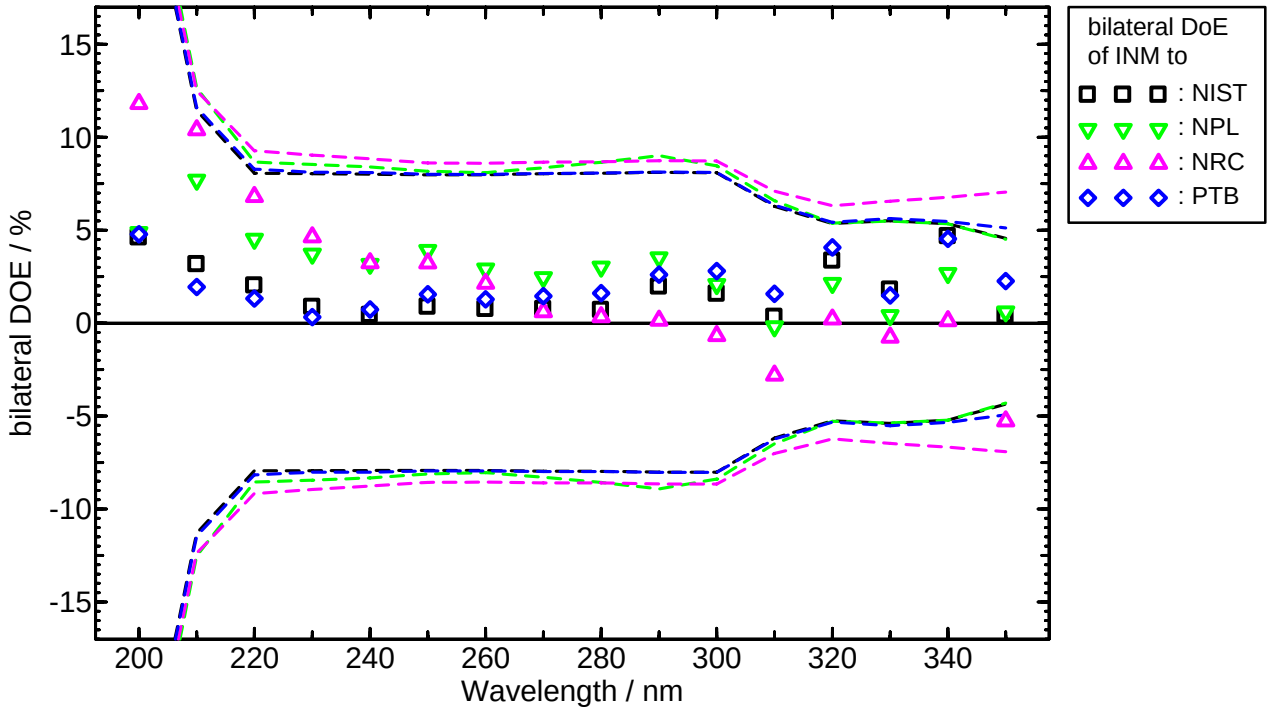

Figure 10.12 Bilateral DoEs for INM.

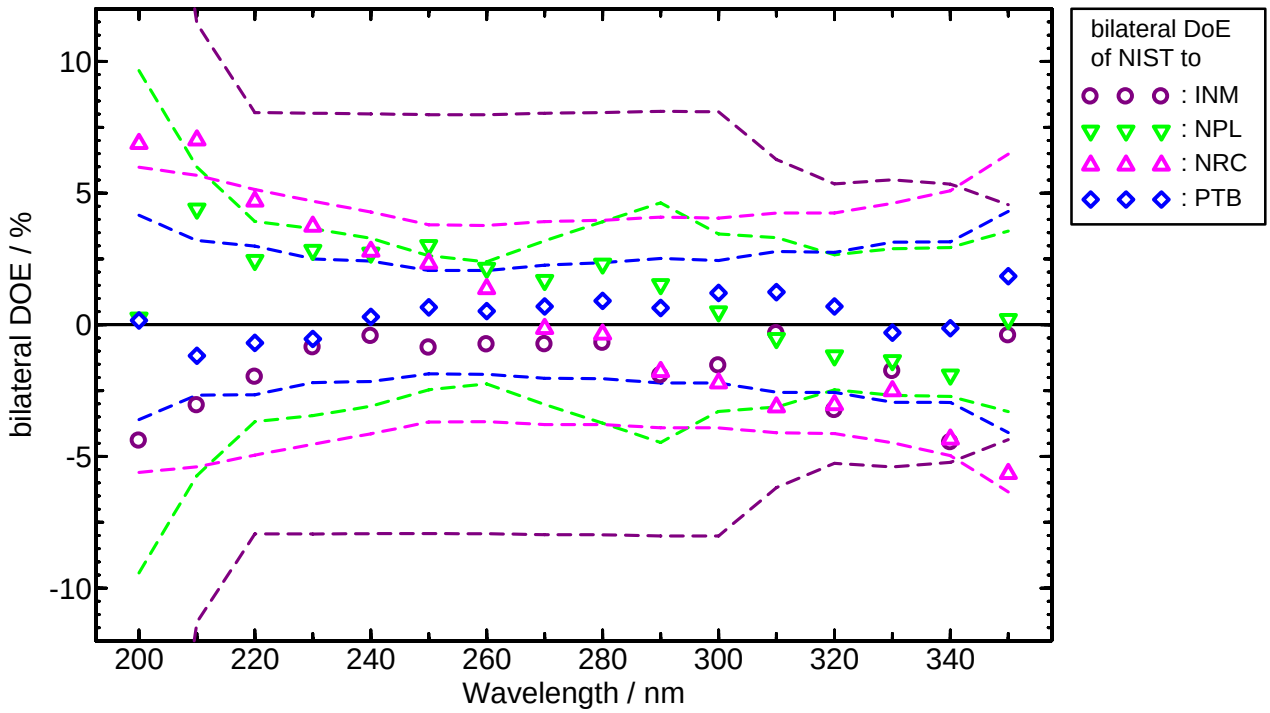

Figure 10.13 Bilateral DoEs for NIST.

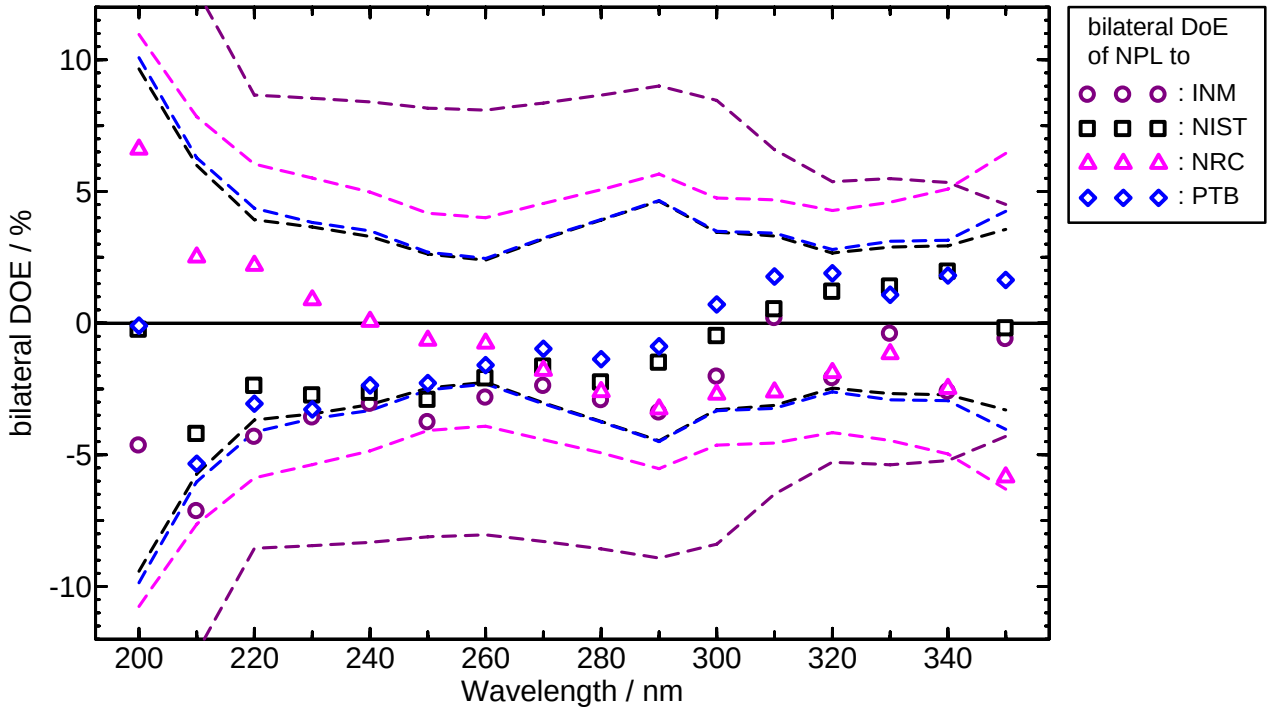

Figure 10.14 Bilateral DoEs for NPL.

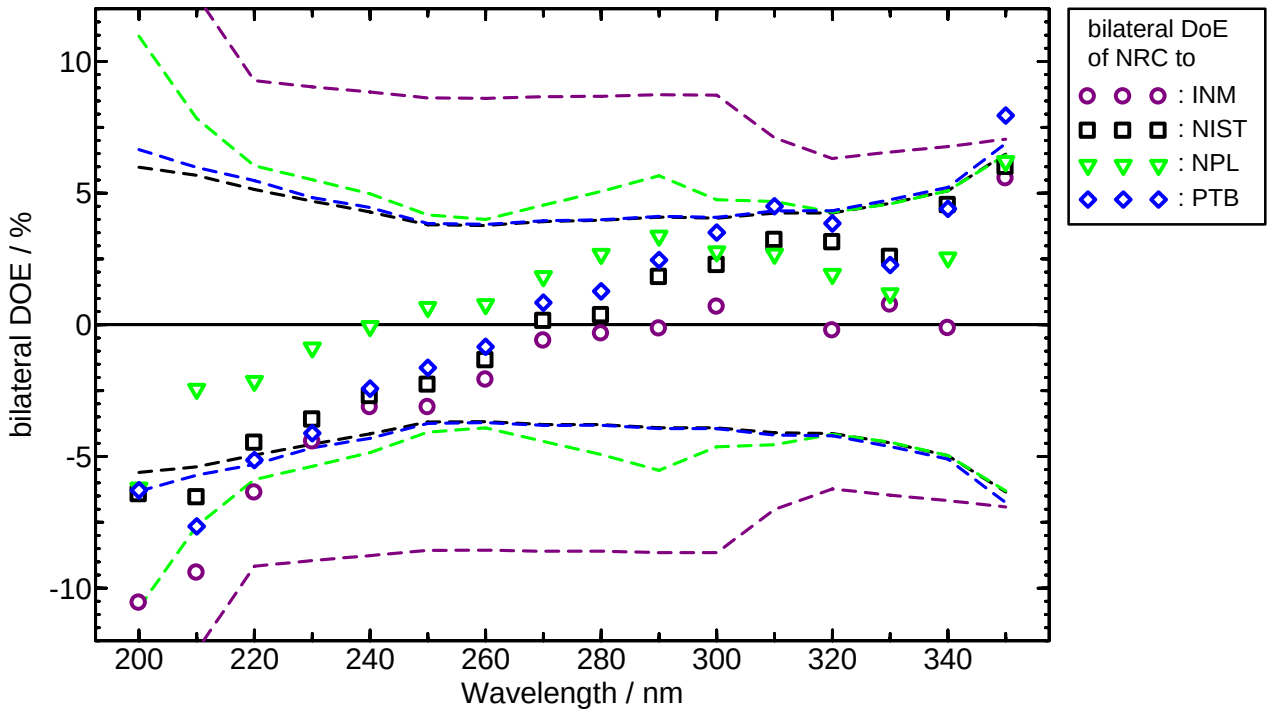

Figure 10.15 Bilateral DoEs for NRC.

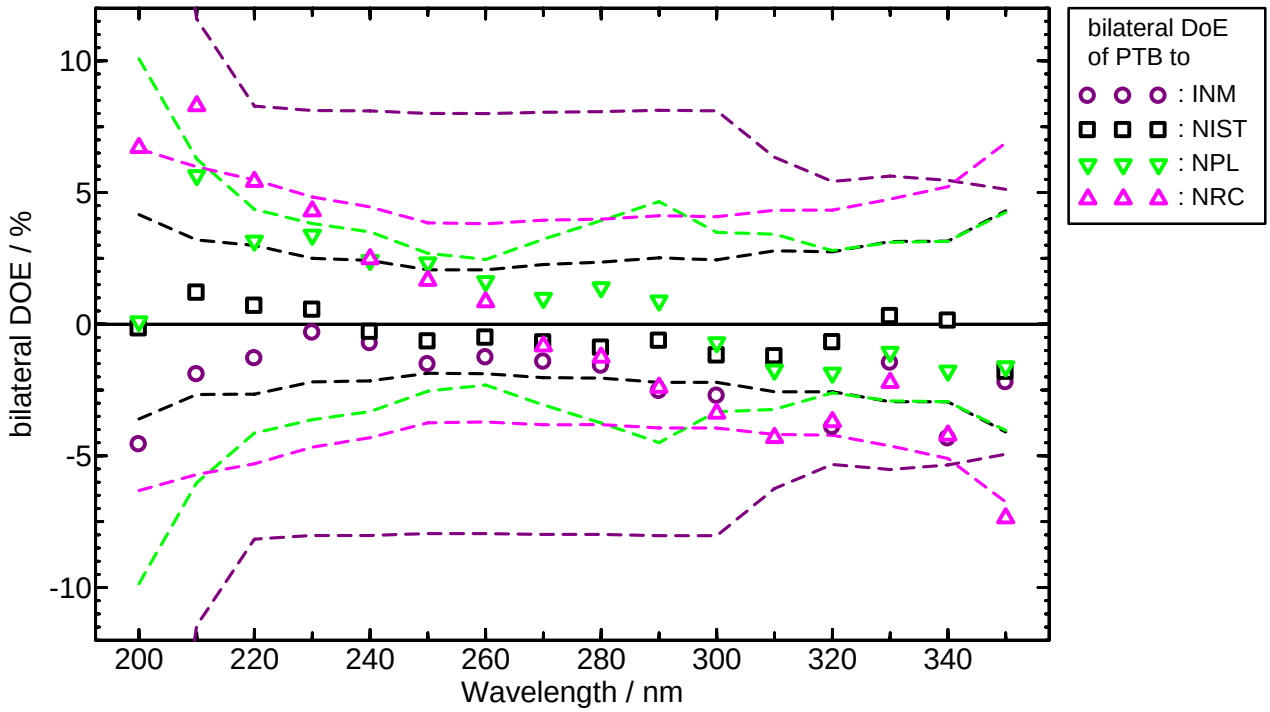

Figure 10.16 Bilateral DoEs for PTB.

10.4 Tabulated results

All relevant results are listed in the following tables, starting with the Key Comparison reference values $\hat{E}_{\mathrm{KCRV}}$ and the NMI representative spectral irradiances $\hat{E}_{\mathrm{i}}$. The uncertainties given are at the 95 % level of confidence.

Table 10.1 Key comparison reference values $\hat{E}_{\mathrm{KCRV}}$ and the NMI representative spectral irradiances $\hat{E}_{\mathrm{i}}$.

	KCRV		**INM**		**NIST**		**NPL**		**NRC**		**PTB**	
λ [nm]	$\hat{E}_{\mathrm{KCRV}}$ $\left[\frac{\mathrm{mW}}{\mathrm{m^2\ nm}}\right]$	$u_{\mathrm{rel}}(\hat{E}_{\mathrm{KCRV}})$ [%]	$\hat{E}_{\mathrm{i}}$ $\left[\frac{\mathrm{mW}}{\mathrm{m^2\ nm}}\right]$	$u_{\mathrm{rel}}(\hat{E}_{\mathrm{i}})$ [%]	$\hat{E}_{\mathrm{i}}$ $\left[\frac{\mathrm{mW}}{\mathrm{m^2\ nm}}\right]$	$u_{\mathrm{rel}}(\hat{E}_{\mathrm{i}})$ [%]	$\hat{E}_{\mathrm{i}}$ $\left[\frac{\mathrm{mW}}{\mathrm{m^2\ nm}}\right]$	$u_{\mathrm{rel}}(\hat{E}_{\mathrm{i}})$ [%]	$\hat{E}_{\mathrm{i}}$ $\left[\frac{\mathrm{mW}}{\mathrm{m^2\ nm}}\right]$	$u_{\mathrm{rel}}(\hat{E}_{\mathrm{i}})$ [%]	$\hat{E}_{\mathrm{i}}$ $\left[\frac{\mathrm{mW}}{\mathrm{m^2\ nm}}\right]$	$u_{\mathrm{rel}}(\hat{E}_{\mathrm{i}})$ [%]
200	1.0029	2.1	1.0597	26.4	1.0130	1.5	1.0104	9.3	0.9478	5.4	1.0114	3.3
210	1.0146	1.8	1.0532	11.2	1.0210	1.3	0.9780	5.6	0.9540	5.2	1.0331	2.3
220	0.9540	1.4	0.9776	7.8	0.9582	1.3	0.9353	3.4	0.9153	4.8	0.9648	2.3
230	0.8664	1.2	0.8777	7.8	0.8702	1.3	0.8462	3.2	0.8389	4.3	0.8749	1.7
240	0.7636	1.1	0.7724	7.8	0.7691	1.3	0.7487	2.8	0.7482	3.9	0.7668	1.7
250	0.6611	0.9	0.6728	7.8	0.6669	1.2	0.6474	2.1	0.6517	3.5	0.6625	1.4
260	0.5652	0.8	0.5733	7.8	0.5690	1.3	0.5571	1.8	0.5614	3.5	0.5661	1.4
270	0.4809	1.0	0.4868	7.8	0.4832	1.4	0.4751	2.7	0.4838	3.5	0.4798	1.5
280	0.4089	1.2	0.4140	7.8	0.4112	1.4	0.4019	3.5	0.4126	3.5	0.4075	1.5
290	0.3493	1.2	0.3566	7.9	0.3497	1.5	0.3444	4.2	0.3560	3.6	0.3475	1.6
300	0.3003	1.0	0.3060	7.9	0.3012	1.5	0.2998	2.9	0.3081	3.6	0.2976	1.6
310	0.2617	1.1	0.2626	5.9	0.2617	1.7	0.2631	2.6	0.2701	3.7	0.2585	1.9
320	0.2294	1.0	0.2359	5.0	0.2282	1.7	0.2309	1.8	0.2354	3.8	0.2267	1.9
330	0.2024	1.1	0.2044	5.0	0.2008	1.9	0.2036	1.9	0.2060	4.0	0.2014	2.2
340	0.1799	1.1	0.1861	4.9	0.1778	1.9	0.1813	1.9	0.1859	4.6	0.1781	2.2
350	0.1575	1.3	0.1581	3.7	0.1575	2.4	0.1571	2.3	0.1669	5.9	0.1546	3.3

Table 10.2 The unilateral degrees of equivalence D_i and their uncertainties U_i

	KCRV		INM		NIST		NPL		NRC		PTB	
λ [nm]	$\hat{E}_{KCRV}$ $\left[\frac{mW}{m^2\,nm}\right]$	$u_{rel}(\hat{E}_{KCRV})$ [%]	$100 \cdot D_i$	U_i [%]	$100 \cdot D_i$	U_i [%]	$100 \cdot D_i$	U_i [%]	$100 \cdot D_i$	U_i [%]	$100 \cdot D_i$	U_i [%]
200	1.0029	2.1	5.7	26.5	1.0	2.6	0.7	9.5	-5.5	5.8	0.8	3.9
210	1.0146	1.8	3.8	11.4	0.6	2.2	-3.6	5.8	-6.0	5.5	1.8	2.9
220	0.9540	1.4	2.5	7.9	0.4	1.9	-2.0	3.7	-4.1	5.0	1.1	2.7
230	0.8664	1.2	1.3	7.9	0.4	1.8	-2.3	3.4	-3.2	4.5	1.0	2.1
240	0.7636	1.1	1.2	7.9	0.7	1.7	-2.0	3.0	-2.0	4.1	0.4	2.1
250	0.6611	0.9	1.8	7.9	0.9	1.5	-2.1	2.3	-1.4	3.6	0.2	1.6
260	0.5652	0.8	1.4	7.9	0.7	1.5	-1.4	2.0	-0.7	3.5	0.1	1.6
270	0.4809	1.0	1.2	7.9	0.5	1.7	-1.2	2.9	0.6	3.7	-0.2	1.8
280	0.4089	1.2	1.2	7.9	0.5	1.8	-1.7	3.6	0.9	3.7	-0.4	1.9
290	0.3493	1.2	2.1	8.0	0.1	1.9	-1.4	4.4	1.9	3.8	-0.5	2.0
300	0.3003	1.0	1.9	7.9	0.3	1.8	-0.2	3.1	2.6	3.8	-0.9	1.9
310	0.2617	1.1	0.4	6.0	0.0	2.0	0.5	2.8	3.2	3.9	-1.2	2.2
320	0.2294	1.0	2.8	5.1	-0.5	2.0	0.7	2.0	2.6	3.9	-1.2	2.1
330	0.2024	1.1	1.0	5.2	-0.8	2.2	0.6	2.2	1.8	4.2	-0.5	2.5
340	0.1799	1.1	3.5	5.0	-1.2	2.2	0.8	2.2	3.3	4.7	-1.0	2.5
350	0.1575	1.3	0.4	3.9	-0.0	2.7	-0.2	2.6	6.0	6.0	-1.8	3.6

Table 10.3 The bilateral degrees of equivalence $D_{i,m}$ and their uncertainties $U_{i,m}$ for INM

	INM		**NIST**		**NPL**		**NRC**		**PTB**	
λ [nm]	$100 \cdot D_{i,m}$	$U_{i,m}$ [%]	$100 \cdot D_{i,m}$	$U_{i,m}$ [%]	$100 \cdot D_{i,m}$	$U_{i,m}$ [%]	$100 \cdot D_{i,m}$	$U_{i,m}$ [%]	$100 \cdot D_{i,m}$	$U_{i,m}$ [%]
200	-	-	4.7	26.5	4.9	28.1	11.2	27.0	4.8	26.7
210	-	-	3.2	11.4	7.4	12.6	9.8	12.5	2.0	11.6
220	-	-	2.0	8.1	4.4	8.7	6.5	9.3	1.3	8.3
230	-	-	0.9	8.0	3.6	8.5	4.5	9.0	0.3	8.1
240	-	-	0.4	8.0	3.1	8.4	3.2	8.8	0.7	8.1
250	-	-	0.9	8.0	3.8	8.2	3.2	8.6	1.6	8.0
260	-	-	0.8	8.0	2.9	8.1	2.1	8.6	1.3	8.0
270	-	-	0.8	8.0	2.4	8.4	0.6	8.7	1.4	8.0
280	-	-	0.7	8.1	3.0	8.7	0.3	8.7	1.6	8.1
290	-	-	2.0	8.1	3.5	9.0	0.1	8.7	2.6	8.1
300	-	-	1.6	8.1	2.1	8.5	-0.7	8.7	2.8	8.1
310	-	-	0.3	6.3	-0.2	6.6	-2.9	7.1	1.6	6.3
320	-	-	3.3	5.4	2.2	5.4	0.2	6.3	4.0	5.4
330	-	-	1.8	5.5	0.4	5.5	-0.8	6.6	1.5	5.6
340	-	-	4.6	5.3	2.7	5.3	0.1	6.8	4.5	5.5
350	-	-	0.4	4.6	0.6	4.5	-5.6	7.0	2.2	5.1

Table 10.4 The bilateral degrees of equivalence $D_{i,m}$ and their uncertainties $U_{i,m}$ for NIST

	INM		**NIST**		**NPL**		**NRC**		**PTB**	
λ [nm]	$100 \cdot D_{i,m}$	$U_{i,m}$ [%]	$100 \cdot D_{i,m}$	$U_{i,m}$ [%]	$100 \cdot D_{i,m}$	$U_{i,m}$ [%]	$100 \cdot D_{i,m}$	$U_{i,m}$ [%]	$100 \cdot D_{i,m}$	$U_{i,m}$ [%]
200	-4.7	26.5	-	-	0.3	9.7	6.5	6.0	0.2	4.2
210	-3.2	11.4	-	-	4.2	6.0	6.6	5.7	-1.2	3.2
220	-2.0	8.1	-	-	2.4	3.9	4.5	5.1	-0.7	3.0
230	-0.9	8.0	-	-	2.8	3.6	3.6	4.7	-0.5	2.5
240	-0.4	8.0	-	-	2.7	3.3	2.7	4.3	0.3	2.4
250	-0.9	8.0	-	-	2.9	2.6	2.3	3.8	0.7	2.1
260	-0.8	8.0	-	-	2.1	2.4	1.4	3.8	0.5	2.1
270	-0.8	8.0	-	-	1.7	3.2	-0.1	3.9	0.7	2.3
280	-0.7	8.1	-	-	2.3	3.9	-0.4	4.0	0.9	2.4
290	-2.0	8.1	-	-	1.5	4.6	-1.8	4.1	0.6	2.5
300	-1.6	8.1	-	-	0.5	3.4	-2.3	4.0	1.2	2.4
310	-0.3	6.3	-	-	-0.5	3.3	-3.2	4.2	1.2	2.8
320	-3.3	5.4	-	-	-1.2	2.7	-3.1	4.2	0.7	2.7
330	-1.8	5.5	-	-	-1.4	2.9	-2.6	4.6	-0.3	3.1
340	-4.6	5.3	-	-	-1.9	2.9	-4.5	5.1	-0.1	3.1
350	-0.4	4.6	-	-	0.2	3.6	-6.0	6.5	1.8	4.3

Table 10.5 The bilateral degrees of equivalence $D_{i,m}$ and their uncertainties $U_{i,m}$ for NPL

	INM		**NIST**		**NPL**		**NRC**		**PTB**	
λ [nm]	$100 \cdot D_{i,m}$	$U_{i,m}$ [%]	$100 \cdot D_{i,m}$	$U_{i,m}$ [%]	$100 \cdot D_{i,m}$	$U_{i,m}$ [%]	$100 \cdot D_{i,m}$	$U_{i,m}$ [%]	$100 \cdot D_{i,m}$	$U_{i,m}$ [%]
200	-4.9	28.1	-0.3	9.7	-	-	6.2	11.0	-0.1	10.1
210	-7.4	12.6	-4.2	6.0	-	-	2.4	7.8	-5.4	6.3
220	-4.4	8.7	-2.4	3.9	-	-	2.1	6.0	-3.1	4.4
230	-3.6	8.5	-2.8	3.6	-	-	0.9	5.5	-3.3	3.8
240	-3.1	8.4	-2.7	3.3	-	-	0.1	5.0	-2.4	3.5
250	-3.8	8.2	-2.9	2.6	-	-	-0.6	4.2	-2.3	2.7
260	-2.9	8.1	-2.1	2.4	-	-	-0.8	4.0	-1.6	2.5
270	-2.4	8.4	-1.7	3.2	-	-	-1.8	4.5	-1.0	3.2
280	-3.0	8.7	-2.3	3.9	-	-	-2.6	5.1	-1.4	3.9
290	-3.5	9.0	-1.5	4.6	-	-	-3.3	5.7	-0.9	4.7
300	-2.1	8.5	-0.5	3.4	-	-	-2.8	4.7	0.7	3.5
310	0.2	6.6	0.5	3.3	-	-	-2.7	4.7	1.7	3.4
320	-2.2	5.4	1.2	2.7	-	-	-1.9	4.3	1.9	2.8
330	-0.4	5.5	1.4	2.9	-	-	-1.2	4.6	1.1	3.1
340	-2.7	5.3	1.9	2.9	-	-	-2.6	5.1	1.8	3.1
350	-0.6	4.5	-0.2	3.6	-	-	-6.2	6.4	1.6	4.2

Table 10.6 The bilateral degrees of equivalence $D_{i,m}$ and their uncertainties $U_{i,m}$ for NRC

	INM		**NIST**		**NPL**		**NRC**		**PTB**	
λ [nm]	$100 \cdot D_{i,m}$	$U_{i,m}$ [%]	$100 \cdot D_{i,m}$	$U_{i,m}$ [%]	$100 \cdot D_{i,m}$	$U_{i,m}$ [%]	$100 \cdot D_{i,m}$	$U_{i,m}$ [%]	$100 \cdot D_{i,m}$	$U_{i,m}$ [%]
200	-11.2	27.0	-6.5	6.0	-6.2	11.0	-	-	-6.3	6.7
210	-9.8	12.5	-6.6	5.7	-2.4	7.8	-	-	-7.8	6.0
220	-6.5	9.3	-4.5	5.1	-2.1	6.0	-	-	-5.2	5.5
230	-4.5	9.0	-3.6	4.7	-0.9	5.5	-	-	-4.2	4.8
240	-3.2	8.8	-2.7	4.3	-0.1	5.0	-	-	-2.4	4.5
250	-3.2	8.6	-2.3	3.8	0.6	4.2	-	-	-1.6	3.8
260	-2.1	8.6	-1.4	3.8	0.8	4.0	-	-	-0.8	3.8
270	-0.6	8.7	0.1	3.9	1.8	4.5	-	-	0.8	3.9
280	-0.3	8.7	0.4	4.0	2.6	5.1	-	-	1.3	4.0
290	-0.1	8.7	1.8	4.1	3.3	5.7	-	-	2.4	4.1
300	0.7	8.7	2.3	4.0	2.8	4.7	-	-	3.5	4.1
310	2.9	7.1	3.2	4.2	2.7	4.7	-	-	4.4	4.3
320	-0.2	6.3	3.1	4.2	1.9	4.3	-	-	3.8	4.3
330	0.8	6.6	2.6	4.6	1.2	4.6	-	-	2.3	4.7
340	-0.1	6.8	4.5	5.1	2.6	5.1	-	-	4.4	5.2
350	5.6	7.0	6.0	6.5	6.2	6.4	-	-	7.8	6.9

Table 10.7 The bilateral degrees of equivalence $D_{i,m}$ and their uncertainties $U_{i,m}$ for PTB

	INM		**NIST**		**NPL**		**NRC**		**PTB**	
λ [nm]	$100 \cdot D_{i,m}$	$U_{i,m}$ [%]	$100 \cdot D_{i,m}$	$U_{i,m}$ [%]	$100 \cdot D_{i,m}$	$U_{i,m}$ [%]	$100 \cdot D_{i,m}$	$U_{i,m}$ [%]	$100 \cdot D_{i,m}$	$U_{i,m}$ [%]
200	-4.8	26.7	-0.2	4.2	0.1	10.1	6.3	6.7	-	-
210	-2.0	11.6	1.2	3.2	5.4	6.3	7.8	6.0	-	-
220	-1.3	8.3	0.7	3.0	3.1	4.4	5.2	5.5	-	-
230	-0.3	8.1	0.5	2.5	3.3	3.8	4.2	4.8	-	-
240	-0.7	8.1	-0.3	2.4	2.4	3.5	2.4	4.5	-	-
250	-1.6	8.0	-0.7	2.1	2.3	2.7	1.6	3.8	-	-
260	-1.3	8.0	-0.5	2.1	1.6	2.5	0.8	3.8	-	-
270	-1.4	8.0	-0.7	2.3	1.0	3.2	-0.8	3.9	-	-
280	-1.6	8.1	-0.9	2.4	1.4	3.9	-1.3	4.0	-	-
290	-2.6	8.1	-0.6	2.5	0.9	4.7	-2.4	4.1	-	-
300	-2.8	8.1	-1.2	2.4	-0.7	3.5	-3.5	4.1	-	-
310	-1.6	6.3	-1.2	2.8	-1.7	3.4	-4.4	4.3	-	-
320	-4.0	5.4	-0.7	2.7	-1.9	2.8	-3.8	4.3	-	-
330	-1.5	5.6	0.3	3.1	-1.1	3.1	-2.3	4.7	-	-
340	-4.5	5.5	0.1	3.1	-1.8	3.1	-4.4	5.2	-	-
350	-2.2	5.1	-1.8	4.3	-1.6	4.2	-7.8	6.9	-	-

11 Conclusions

The CCPR-K1.b intercomparison of Spectral Irradiance in the spectral range from 200 nm to 250 nm involved repeatet measurements by five participants with 20 deuterium lamp systems (DLS) in total within the time period from 2003 to 2005.

All participants supplied detailed reports of their measurements including full uncertainty statements. All measurement results reported by the participants could be used for the intercomparison and no measurement was subject of rejection. The analysis method introduced in section 9 follows the Guidelines for CCPR Comparison Report Preparation and has been accepted by the participants. For the calculation of the key comparison reference value no participant had to be excluded and the used weighted mean with cut-off has been supported by all participants. The unilateral degrees of equivalence (DoE) calculated for each participant are in 96 % consistent with their uncertainties at the k = 2 level and fully consistent within k = 3.

These results impressively demonstrate the substantial improvements in UV-radiometry during the last years and the excellent calibration capabilities of all participants. The outstanding quality of the results was greatly supported by the availability of high quality transfer standards. For the first time the stability and reproducibility of the DLS allowed a reasonable direct comparison of UV spectral irradiance calibrations.

Appendix A The Deuterium Lamp System (DLS)

The measurement artefacts (transfer standards) used for the intercomparison are specially developed transfer standard lamp systems, consisting of a set of deuterium lamps in special housings, an associated power supply and a monitor detector. This deuterium lamp system (DLS) is a result of extended investigations on several deuterium lamp types from different manufacturers[4].

Each deuterium lamp system consists of a lamp power supply (PS), a monitor detector (MD, with its own power supply unit MP) and a set of three or four lamps mounted in a housing (L#01, L#02 etc) with an accompanying alignment jig (J#01, J#02 etc). Each DLS has its own notation marking their correlation. The nomenclature is of the type "DLS-nnn-ttt" where "nnn" is the system notation (typically the institute name) and "ttt" is the name for the part of the system. For example the full name of one lamp of the PTB system would then be "DLS-PTB-L#01" with its alignment jig "DLS-PTB-J#01".

Power supply:
The deuterium lamp power supply used is a DLV300 type from Leistungselektronik Jena GmbH, Germany, especially designed for the 30 W deuterium lamp type. The nominal output current after the lamp ignition is (300 ± 3) mA. The relative reproducibility and stability of the power supplies have been found to be better than 10^{-4} under normal laboratory conditions. Each power supply has its own assigned operating current which is independent of the lamp operated. However, each lamp is equipped with its own resistor to measure the lamp current. The corresponding current values for each lamp-power-supply combination are given in the accompanying technical documents. Each power supply also includes a (pre-) heater for the deuterium lamp cathode. A pre-heating time of 20 s and a heating value of 10 V for pre-heating and 6 V for heating under operation has to be selected (see Figure A.1). A power supply should only be used with the set of lamps that is assigned to it by the system notation. The power supplies can be set to 115 V, where necessary.

Figure A.1 Power supply DLV300
The settings for preheating time (20 s) and heating level (10V/6V) have to be set as shown on the picture. These settings and the notation of the power supply are printed on a label on top of the power supply.

Lamps:
The deuterium lamp type Cathodeon J64 has been thoroughly investigated by PTB and an optimum selection, characterisation and operational procedure have been determined.
Each lamp is operated at a current of (300.0 ± 3) mA. The lamps are working at a nominal DC voltage of 72 - 80 volts and are operated in constant current mode. Each lamp is assigned to its own special power supply and must only be operated with this power supply and must be aligned using its correlated jig.

[4] Sperfeld P., Stock K.D., Raatz K.-H., Nawo B. and Metzdorf J., " Characterization and use of deuterium lamps as transfer standards of spectral irradiance", Metrologia, 40 (2003) S111–S114

The lamps must be allowed to warm up at least 45 min before starting spectral measurements.

Figure A.2 The lamp housing
It includes a connector for electrical measurements at the back (not shown), a base plate to be placed on a flat surface and a specially designed opening that allows the lamp jig and the monitor detector to be connected reproducibly to the housing.

Lamp housing:
Each deuterium lamp is set up in its own housing, which protects the lamps from environmental conditions. The housing together wit the alignment jig is defining the optical measurement axis which is perpendicular to the centre of the jig marked with a target. The base plate of the housing allows it be placed on a table or to be mounted on a measurement system.

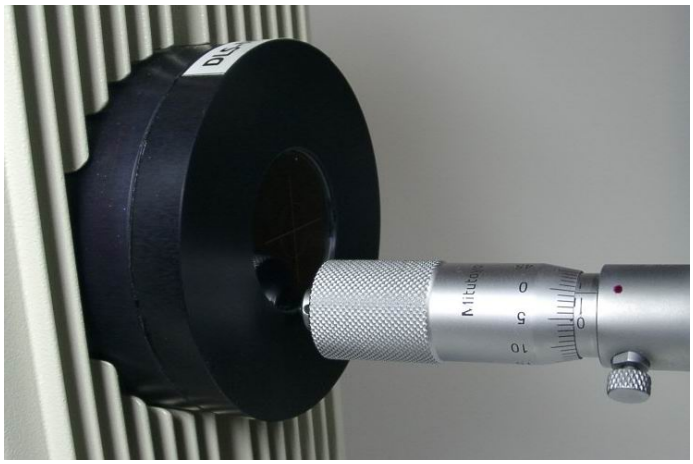

Figure A.3 The alignment jig in front of the lamp.
Each jig is assigned to one lamp and has to be connected so that the sign on it shows upwards.
The reference point for distance measurements is below the window.

Alignment jig:
Each lamp has its own alignment jig with a glass window and a target in its centre. The jig has to be connected to the lamp housing in that way that the sign on it shows upwards. It is save to leave the jig at the housing during the lamp is operating but it is necessary to remove it for spectral calibrations. The front of the jig below the glass target is used as the reference plane for the distance measurement.

Figure A.4 Lamp pre-alignment
The UV-irradiance distribution of the lamps are aligned to the centre of the optical axis using the lamp housing alignment capabilities. A SiC-detector was used to scan the lateral irradiance distribution at a distance of 300 mm to the lamp jig front.

Lamp pre-alignment:
The lamp mounting inside the lamp housing allows the lamp to be aligned to the optical measurement axis which is defined by the housing and the jig. The operating Lamp has been aligned so that its UV-irradiance is at its maximum on the optical axis. Therefore, the irradiance distribution of the lamp at a distance of 300 mm from the front jig has been measured using a SiC photodiode. The lamp has been turned and tilted until the centre of the irradiance distribution is on the optical axis. For this alignment the lamp may be tilted and turned up to 2°. The irradiance uniformity on a 32 mm diameter area around the optical axis was documented in the accompanying technical documents. The centre of the UV irradiance is dependent on the electrode ignition. It is shown that its position is reproducible even after several re-ignitions of the lamps. But it may not be coinciding to the distribution of the visible light. Therefore, it is possible that the visible light spot is not centred to the optical axis. This should be ignored. The lamp pre-alignment must not be changed and the accompanying screws are secured (!) to avoid accidental misalignment during transportation or use of the lamp systems.

Lamp holder:
The lamp housing can directly be placed on an optical table. To allow the lamp system to be mounted on a mechanical alignment facility, an adapter has been delivered with the system. The dimensions of that adapter are 165 mm x 48 mm x 12 mm. It has a 6 mm tapped hole in the centre and the optical axis is at app. 139 mm above the bottom of the adapter (127 mm + 12 mm).

Figure A.5 Holder for the lamp systems.

The lamps can easily be replaced and fixed on that adapter.

Measuring connector:
The lamps are equipped with a connector to measure the electrical parameters of the lamps. The pin occupancy of the connector is shown on the back of each lamp housing (Figure A.6). The lamp current is determined measuring the voltage drop over a 1 Ω resistor inside each lamp. The lamp voltage and the voltage of the heater are measured to monitor sudden changes of the lamps. The ignition voltage pulse of the lamps can be up to 600 V so that the measuring instruments should be capable to stand such voltage pulses.

Figure A.6 Connector at the lamps back to measure the electrical parameters of the lamp

Lamp characterisation:
The initial ageing of the lamps took 100 h at minimum. During that time the lamps have been switched on and off several times and their re-ignition reproducibility and the temporal (spectral) irradiance drift has been monitored. The characteristic drift of each lamp could be used to correct for changes during the calibration process (usually not necessary).

Monitor detector:

Each set of lamp systems comes with a monitor detector equipped with a SiC photodiode. This detector can be connected to the front of the lamp housing before and after each spectral measurement to monitor the drift of the lamps during calibration. Each monitor detector is assigned to the set of lamps of each participant and has also been circulated during the intercomparison. A power supply for each detector was also part of the circulating equipment. The photocurrent-equivalent voltage (< 0,2 V) can be measured at a LEMOSA connector.

System availability:

The deuterium lamp system has been developed and investigated at PTB in preparation of the key comparison. A limited number of 20 DLS have been produced and distributed to the participants. Provided an increased additional interest in further DLS, the deuterium lamp system could be ordered at www.schreder-cms.com .

Appendix B List of figures

Figure 3.1 Traceability scheme for BNM-INM 11
Figure 3.2 Schematic of the entrance optics 13
Figure 3.3 Repeatibility between the measurement rounds calculated from the INM data. 19
Figure 3.4 Repeatibility between the measurement rounds calculated from PTB data. 19
Figure 3.5 Normalized inner consistencies of the INM results compared to that of the PTB. 20
Figure 4.1 Schematic of the measurement setup showing the placement of the synchrotron with the deuterium lamp at the side of the beamline. 22
Figure 4.2 Repeatibility between the measurement rounds calculated from the NIST data. 27
Figure 4.3 Repeatibility between the measurement rounds calculated from PTB data. 27
Figure 4.4 Normalized inner consistency of the NIST result compared to that of the PTB. 28
Figure 5.1 Traceability chain for the primary spectral irradiance scale at NPL 29
Figure 5.2 SRIPS Facility diagram 30
Figure 5.3 Irradiance of the UHTBB and deuterium lamps 34
Figure 5.4 Bandwidth correction applied. 35
Figure 5.5 Absorption effect: Correction applied. 36
Figure 5.6 Raw calculation of deuterium irradiance, showing as “error bars” the blackbody repeatability during these measurements 37
Figure 5.7 Standard uncertainty associated with blackbody radiance and a percentage of spectral radiance and as a function of wavelength 43
Figure 5.8 Repeatability of SRIPS. 44
Figure 5.9 Uncertainty due to bandwidth correction (the correction itself is Figure 5.4) 46
Figure 5.10 Overall k=1 uncertainty for a single measurement of a comparison lamp 48
Figure 5.11 Repeatibility between the measurement rounds calculated from the NPL data. 54
Figure 5.12 Repeatibility between the measurement rounds calculated from PTB data. 55
Figure 5.13 Normalized inner consistency of the NPL result compared to that of the PTB. 55
Figure 6.1 Schematic of the NRC Spectroradiometer (Phase 1) 60
Figure 6.2 Schematic of the NRC Spectroradiometer (Phase 2) 61
Figure 6.3 Repeatibility between the measurement rounds calculated from the NRC data. 69
Figure 6.4 Repeatibility between the measurement rounds calculated from PTB data. 69
Figure 6.5 Normalized inner consistency of the NRC result compared to that of the PTB. 70
Figure 7.1 Spectroradiometer facility for spectral irradiance measurements optimized for air UV (top view). 72
Figure 7.2 The relative spectral change of the photocurrent ratio between the monitorlamp and the blackbody (triangles) or the deuterium lamps (rhombs) respectively. 80
Figure 7.3 The combined bandwidth correction factors. 81

Figure 7.4 Repeatibility between the measurement rounds calculated from the PTB data. 85
Figure 9.1 Combined standard uncertainties $u_{rel}(E_i)$ of the participants and resulting cut-off $u_{cut\ off}$ 94
Figure 10.1 The NMI representative virtual irradiances and the resulting KCRV summarized for all wavelengths. 96
Figure 10.2 Summary of the unilateral DoE for the participants. 97
Figure 10.3 Unilateral DoE for the INM. 97
Figure 10.4 Unilateral DoE for NIST. 98
Figure 10.5 Unilateral DoE for NPL. 98
Figure 10.6 Unilateral DoE for NRC. 99
Figure 10.7 Unilateral DoE for PTB. 99
Figure 10.8 Unilateral DoE for the wavelengths 200 nm, 210 nm, 220 nm and 230 nm. 100
Figure 10.9 Unilateral DoE for the wavelengths 240 nm, 250 nm, 260 nm and 270 nm. 100
Figure 10.10 Unilateral DoE for the wavelengths 280 nm, 290 nm, 300 nm and 310 nm. 101
Figure 10.11 Unilateral DoE for the wavelengths 320 nm, 330 nm, 340 nm and 350 nm. 101
Figure 10.12 Bilateral DoEs for INM. 102
Figure 10.13 Bilateral DoEs for NIST. 102
Figure 10.14 Bilateral DoEs for NPL. 103
Figure 10.15 Bilateral DoEs for NRC. 103
Figure 10.16 Bilateral DoEs for PTB. 104
Figure A.1 Power supply DLV300 113
Figure A.2 The lamp housing 114
Figure A.3 The alignment jig in front of the lamp. 114
Figure A.4 Lamp pre-alignment. 115
Figure A.5 Holder for the lamp systems. 115
Figure A.6 Connector at the lamps back to measure the electrical parameters of the lamp 116

Appendix C List of tables

Table 2.1Contact details for the participants of the CCPR-K1.b intercomparison 7
Table 3.1 Lower spectral range measurement uncertainty 15
Table 3.2 Higher spectral range measurement uncertainty 16
Table 3.3 Average Lamp voltages for the different INM lamp systems 17
Table 3.4 Results for the Lamp systems calibrated by BNM-INM 18
Table 4.1 Dates and location of the measurements 21
Table 4.2 Components of the relative uncertainties (*k*=2) of spectral irradiance of synchrotron radiation. 23
Table 4.3 Components of the relative uncertainty (k=2) of spectral irradiance of deuterium lamp calibration 24
Table 4.4 Average Lamp voltages for the different NIST lamp systems 25
Table 4.5 Results for the Lamp systems calibrated by NIST 26
Table 5.1 Description of the UV grating 30
Table 5.2 Wavelengths measured at NPL for the CCPR-K1.b comparison 32
Table 5.3 Uncertainty components and overall uncertainty associated with the blackbody temperature measurement. All are standard uncertainties (k = 1) 42
Table 5.4 Uncertainty components split between correlated and uncorrelated 49
Table 5.5 Overall uncertainty components that make up the submitted uncertainties. 50
Table 5.6 Overall uncertainty components that make up the submitted uncertainties, round 1. 51
Table 5.7 Overall uncertainty components that make up the submitted uncertainties, round 2. 51
Table 5.8 Uncertainties combined for three measurements of the lamp 52
Table 5.9 Average Lamp voltages for the different NPL lamp systems 54
Table 5.10 Results for the lamp systems calibrated by NPL 56
Table 6.1 Measurement sequence for typical Phase 2 measurement day. 63
Table 6.2 Summary of CCPR K1b lamp measurements. 64
Table 6.3 Uncertainties (fractional) for the lamp calibrations. 67
Table 6.4 Average Lamp voltages for the different NRC lamp systems 68
Table 6.5 Results for the Lamp systems calibrated by NRC 71
Table 7.1 Standard measurement uncertainties for blackbody radiator temperature measurements. 75
Table 7.2 Standard measurement uncertainties for primary spectral irradiance scale realization 77
Table 7.3 Standard measurement uncertainties for spectral irradiance calibrations 83
Table 7.4 Average Lamp voltages for the different PTB lamp systems 84
Table 7.5 Results for the Lamp systems calibrated by PTB 86
Table 8.1 Standard measurement uncertainties of the pilot measurements 89

Table 10.1 Key comparison reference values $\hat{E}_{\mathrm{KCRV}}$ and the NMI representative spectral irradiances $\hat{E}_{\mathrm{i}}$ 105

Table 10.2 The unilateral degrees of equivalence D_{i} and their uncertainties U_{i} 106

Table 10.3 The bilateral degrees of equivalence $D_{\mathrm{i,m}}$ and their uncertainties $U_{\mathrm{i,m}}$ for INM 107

Table 10.4 The bilateral degrees of equivalence $D_{\mathrm{i,m}}$ and their uncertainties $U_{\mathrm{i,m}}$ for NIST 108

Table 10.5 The bilateral degrees of equivalence $D_{\mathrm{i,m}}$ and their uncertainties $U_{\mathrm{i,m}}$ for NPL 109

Table 10.6 The bilateral degrees of equivalence $D_{\mathrm{i,m}}$ and their uncertainties $U_{\mathrm{i,m}}$ for NRC 110

Table 10.7 The bilateral degrees of equivalence $D_{\mathrm{i,m}}$ and their uncertainties $U_{\mathrm{i,m}}$ for PTB 111